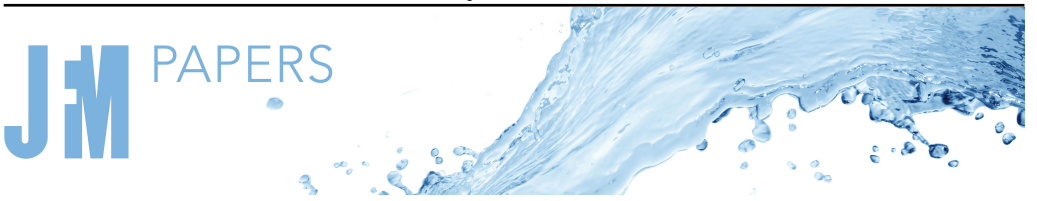
J. Fluid Mech. (2026), *vol.* 1032, A25, doi:10.1017/jfm.2026.11366



Compressible N-phase fluid mixture models

Marco F.P. ten Eikelder[1], **E. Harald van Brummelen**[2] **and Dominik Schillinger**[1]

[1]Institute for Mechanics, Computational Mechanics Group, Technical University of Darmstadt, Franziska-Braun-Str, 7, 64287, Darmstadt Germany

[2]Department of Mechanical Engineering, Eindhoven University of Technology, Eindhoven 5600MB, The Netherlands

Corresponding author: Marco F.P. ten Eikelder, marco.eikelder@tu-darmstadt.de

(Received 17 March 2025; revised 20 December 2025; accepted 19 February 2026)

Fluid mixture models are essential for describing a wide range of physical phenomena, including wave dynamics and spinodal decomposition. However, there is a lack of consensus in the modelling of compressible mixtures, with limited connections between different classes of models. On the one hand, existing compressible two-phase flow models accurately describe wave dynamics, but do not incorporate phase separation mechanisms. On the other hand, phase-field technology in fluid dynamics consists of models incorporating spinodal decomposition; however, a general phase-field theory for compressible mixtures remains largely undeveloped. In this paper we take an initial step toward bridging the gap between compressible two-phase flow models and phase-field models by developing a theory for compressible, isothermal N-phase mixtures. Our theory establishes a system of reduced complexity by formulating N mass balance laws alongside a single momentum balance law, thereby naturally extending the Navier–Stokes Korteweg model to N phases and providing the Navier–Stokes Cahn–Hilliard/Allen–Cahn model for compressible mixtures. Key aspects of the framework include its grounding in continuum mixture theory and its preservation of thermodynamic consistency despite its reduced complexity.

Key words: shock waves, interfacial flows (free surface), Navier-Stokes equations

1. Introduction

1.1. *Background*

The modelling of compressible multiphase fluid mixtures is fundamental to a wide range of scientific and engineering applications, including geophysical flows, aerospace

© The Author(s), 2026. Published by Cambridge University Press. This is an Open Access article, distributed under the terms of the Creative Commons Attribution licence (https://creativecommons.org/licenses/by/4.0/), which permits unrestricted re-use, distribution and reproduction, provided the original article is properly cited.

https://doi.org/10.1017/jfm.2026.11366 Published online by Cambridge University Press

engineering and industrial processes. A key challenge in describing such systems lies in formulating a mathematical framework that consistently captures the interactions between phases while accounting for compressibility effects, diffusion and interfacial dynamics. (We utilise 'phase' to denote different fluid constituents (e.g. air and water).) A widely used class of partial differential equation (PDE)-based models for multiphase flows consists of sharp-interface models, which either explicitly track the phase boundaries and prescribe conditions at the interface (Ghias, Mittal & Dong 2007; Shen, Ren & Ding 2020) or are approximated by smooth interface (level-set) approximations (Sussman, Smereka & Osher 1994; Sethian 1999; ten Eikelder & Akkerman 2021). These models have been successfully applied to problems where the interface between phases remains well defined. Complex mixture problems, however, where phases are dispersed throughout the domain and interpenetrate one another, or emerge from phase separation, do not belong to the class of sharp-interface problems. As a consequence, these problems demand an alternative modelling approach. Below we discuss two classes of models that describe these complex mixtures: compressible two-phase models and phase-field models.

Compressible two-phase flow models play a fundamental role in describing mixture flows, where compressibility and interfacial dynamics are essential. Among these models, the Baer-Nunziato model is often regarded as one of the most comprehensive frameworks for describing two-phase flows (Baer & Nunziato 1986). This diffuse-interface, non-equilibrium model consists of separate mass, momentum and energy balance equations for each phase, along with an additional equation governing the topology of the two-fluid interface. Over time, significant extensions have been proposed, including generalisations to N-component mixtures (see, e.g. Müller *et al.* 2016), broadening the applicability to more complex multiphase systems. We refer for details on the analysis and derivation of the Baer-Nunziato model to Hillairet (2019), Perrier & Gutiérrez (2021) and, for numerical methods, to Andrianov & Warnecke (2004), Tokareva & Toro (2010), Crouzet *et al.* (2013), Coquel, Hérard & Saleh (2017), Sirianni, Re & Abgrall (2025).

Despite their generality, Baer-Nunziato-type models introduce considerable computational complexity due to their large number of equations and wave families. To address this, reduced models with fewer equations have been developed (Kapila *et al.* 2001; Murrone & Guillard 2005). These reduced formulations are often derived through relaxation procedures that assume velocity, pressure or temperature equilibrium between phases (Saurel & Abgrall 1999). However, such simplifications come at a cost: reduced models may fail to strictly conserve energy, suffer from an ill-posed mixture speed of sound (Saurel, Petitpas & Berry 2009) or lose asymptotic consistency with the full nonlinear system (Saleh & Seguin 2020). These limitations motivate the exploration of alternative modelling approaches for compressible mixtures, particularly those that incorporate interfacial dynamics and phase transition effects in a thermodynamically consistent manner.

Over the past decades, phase-field modelling has become a valuable tool for moving boundary problems in computational fluid mechanics (Anderson, McFadden & Wheeler 1998; Gomez & van der Zee 2018). It addresses two key challenges: geometrical representation and physical modelling. The phase-field variable naturally captures topological changes, providing advantages over traditional interface-tracking methods for complex flows. Additionally, phase-field models offer a thermodynamically consistent framework for capillary effects, phase transitions and material composition. They also provide an effective description of wetting, making them well suited for complex wetting phenomena (Aland & Mokbel 2021; Bhopalam, Bueno & Gomez 2022; Demont *et al.* 2024).

https://doi.org/10.1017/jfm.2026.11366 Published online by Cambridge University Press

The state-of-the art phase-field models for fluids may roughly be classified into two categories. The first category describes single-fluid flow with phase change (Gomez *et al.* 2010; Bresch, Gisclon & Lacroix-Violet 2019) through the Navier–Stokes Korteweg (NSK) model. The two phases correspond to the liquid and gaseous states of the same component. In the NSK model the density field itself acts as a phase-field variable. Areas with low density identify as vapour and high-density regions as liquid. Liquid–vapour transitions are often incorporated in the NSK model by means of the van der Waals capillarity model, named after the 1910 Nobel Laureate in physics (Van der Waals 1894).

The second category consists of models that describes viscous (incompressible) mixture flow through the Navier–Stokes Cahn–Hilliard (Allen–Cahn) (NSCHAC) model. The origin of NSCHAC models may be traced back to 1977 when Hohenberg and Halperin proposed a NSCHAC model via the coupling between the Navier–Stokes equations, describing viscous fluid flow, and the Cahn–Hilliard equation, describing spinoidal decomposition (Hohenberg & Halperin 1977). The most important limitation of this model is that the density of the fluids are assumed equal. This precludes the applicability of the model to a large number of practical problems such as ink-droplet dynamics. Since the end of the last century, a number of efforts of extending the model to the case of non-matching densities have been made, e.g. Lowengrub & Truskinovsky (1998), Boyer (2002), Ding, Spelt & Shu (2007), Abels, Garcke & Grün (2012), Shen, Yang & Wang (2013), Aki *et al.* (2014). Each of these works aims to describe the same physics, yet the proposed models are different. The occurrence of a many NSCH(AC) models shows that consensus in the realm of single-phase multicomponent flows has been missing. Note that this is in contrast to single-fluid flow with phase change, where the NSK model is the widely adopted model. In two recent articles we have proposed a unified mixture-theory framework of NSCHAC models as a resolution to this open problem (see ten Eikelder *et al.* (2023), ten Eikelder (2025) for the theoretical framework and ten Eikelder & Schillinger (2024), Brunk & ten Eikelder (2025) for supporting benchmark computations). The framework indicates a single NSCHAC model that is invariant to the choice of fundamental variables.

1.2. *Objective and main results*

Although significant progress has been made in modelling multiphase flows, a general phase-field theory for compressible mixtures remains largely undeveloped, despite some important contributions (see, e.g. Málek & Rajagopal (2008); Freistühler & Kotschote (2017); Huang & Johnsen (2023, 2024); Mukherjee & Gomez (2024) and the references therein). While compressible two-phase flow models exist and provide a well-established framework for describing compressible mixtures, they differ fundamentally from phase-field models in both structure and formulation. Phase-field models, on the other hand, have been extensively used for capturing interfacial dynamics in incompressible fluid mixtures but have not been systematically extended to fully compressible regimes. As a result, the connection between compressible two-phase flow models and phase-field approaches is largely unresolved. Although both modelling strategies aim to describe similar physical processes, their underlying formulations remain distinct. This disconnect has hindered the development of a unified theoretical framework that accommodates both compressibility effects and the diffuse-interface nature of phase-field models.

In this paper we take an initial step toward expanding the theoretical foundation of compressible mixture modelling by developing a thermodynamically consistent theory for compressible, isothermal N-phase mixtures. As part of this development, we draw connections to both phase-field models and compressible two-phase flow models, outlining key points of overlap and distinction. Our approach introduces a set of N mass

https://doi.org/10.1017/jfm.2026.11366 Published online by Cambridge University Press

balance equations coupled with a single momentum balance law. In particular, we derive the following multiphase-field model for constituents $\alpha = 1, \dots, N$:

$$\partial_t(\rho \boldsymbol{v}) + \operatorname{div}(\rho \boldsymbol{v} \otimes \boldsymbol{v}) + \sum_\beta \tilde{\rho}_\beta \nabla \mu_\beta - \operatorname{div}(\nu(2\boldsymbol{D} + \lambda(\operatorname{div}\boldsymbol{v})\boldsymbol{I})) - \rho \boldsymbol{g} = 0, \tag{1.1a}$$

$$\partial_t \tilde{\rho}_\alpha + \operatorname{div}(\tilde{\rho}_\alpha \boldsymbol{v}) - \operatorname{div}\left(\sum_\beta \boldsymbol{M}_{\alpha\beta} \nabla \mu_\beta\right) + \sum_\beta m_{\alpha\beta} \mu_\beta = 0, \tag{1.1b}$$

$$\mu_\alpha - \frac{\partial \Psi}{\partial \tilde{\rho}_\alpha} + \operatorname{div}\left(\frac{\partial \Psi}{\partial \nabla \tilde{\rho}_\alpha}\right) = 0. \tag{1.1c}$$

Here $\boldsymbol{v}$ is the fluid velocity, $\tilde{\rho}_\alpha$ are the partial densities, $\rho = \sum_\beta \tilde{\rho}_\beta$ is the mixture density, $\boldsymbol{g}$ is the force vector, ν is the dynamical viscosity, $\nu\lambda$ is the second viscosity coefficient and $\boldsymbol{D}$ is the symmetric velocity gradient. Furthermore, Ψ is the free energy, μ_α are constituent chemical potentials, and $\boldsymbol{M}_{\alpha\beta}$ and $m_{\alpha\beta}$ are mobility parameters. Equation (1.1*a*) describes the mixture momentum equation, (1.1*b*) are the constituent mass balance laws and (1.1*c*) define the chemical potentials.

A distinguishing feature of the model, in contrast to compressible two-phase flow models, is its preservation of thermodynamic consistency despite its reduced complexity (i.e. the combination of N mass balance laws with just a single momentum balance law). Furthermore, the model connects to phase-field models and distinguishes itself from compressible two-phase flow models as follows. For specific closure models, it extends the NSK framework to multiple fluids, where the last two terms in (1.1*b*) vanish in the single-fluid case. Additionally, under particular closure choices, these terms take the form of Cahn–Hilliard and Allen–Cahn-type contributions, establishing a direct link to NSCH(AC) models. Key distinctions from existing compressible two-phase flow models lie in (i) the absence of an explicit evolution equation for the volume fraction, and (ii) the formulation of the equation of state, as given in (1.1*c*).

We note that the proposed model offers the description of compressible spinodal-decomposition phenomena, which may occur in phase-transforming mixtures with significant density changes. A representative case is a water–air system undergoing vapour–liquid transformation, covering both condensation and evaporation (e.g. fog formation, evaporating droplets). A single mixture Helmholtz free energy encodes a van der Waals-type equation of state for the vapour–liquid transition and a demixing/mixing effect between the water and air components. The resulting thermodynamic quantities (pressure, chemical potentials, Gibbs free energy) determine whether phase change and separation/mixing occur. This contrasts with compressible two-phase flow models (e.g. Baer–Nunziato (BN)), where phase change is introduced via mass-transfer source terms proportional to chemical-potential differences. In the proposed model, mass-transfer source terms occur via Allen–Cahn contributions representing a chemical reaction.

Beyond the above example, a central advantage of the proposed framework in comparison with compressible two-phase flow models is that all thermodynamic driving forces are derived from a single Helmholtz free energy. As a consequence, pressure(s), chemical potentials, capillarity/Korteweg-type stresses, Cahn–Hilliard diffusive fluxes and Allen–Cahn-type mass-transfer contributions are mutually consistent and satisfy the same equilibrium conditions, which reduces ambiguity in closure choices and avoids internal inconsistencies that can arise when these ingredients are specified independently. This unified structure is particularly beneficial in the compressible multiphase setting, where constituent interactions influence both phase separation and mixture-acoustic response. A practical implication is that it facilitates the design of robust discretisations that respect

https://doi.org/10.1017/jfm.2026.11366 Published online by Cambridge University Press

the underlying energy structure, thereby reducing spurious interfacial forces. At the same time, the present framework is isothermal and adopts a single-velocity mixture description; therefore, it is not intended for regimes with significant slip or detailed thermal/latent-heat effects. In addition, the diffuse-interface approach implies an interfacial thickness set by the Helmholtz free energy. As such, reliable simulations must resolve this length scale to obtain accurate capillary forces and grid-independent results.

1.3. *Plan of the paper*

The remainder of the paper is structured as follows. In § 2 we present the continuum theory of rational mechanics for compressible isothermal fluid mixtures. Next, in § 3 we perform constitutive modelling via the Coleman–Noll procedure. Then, in § 4 we discuss some properties of the model. In § 5 we study the associated first-order system. Next, in § 6 we discuss the case of binary mixtures. Subsequently, in § 7 we discuss connections to existing models. Finally, in § 8 we conclude and provide further research directions.

2. Continuum mixture theory

This section outlines the continuum theory for mixtures of compressible, isothermal constituents, serving as a foundational framework. While the theory is well known, its inclusion here is essential, particularly as it differs from the starting point for the design of compressible two-phase flow models. The outlined mixture-theory description is closely aligned with ten Eikelder, Van Der Zee & Schillinger (2024), ten Eikelder (2025), underscoring its suitability as a first-principles basis for the development for a wide range of models.

Continuum mixture theory is based on the following three general principles outlined in the groundbreaking work of Truesdell & Toupin (1960), Truesdell (1984).

(i) All properties of the mixture must be mathematical consequences of properties of the constituents.
(ii) So as to describe the motion of a constituent, we may in imagination isolate it from the rest of the mixture, provided we allow properly for the actions of the other constituents upon it.
(iii) The motion of the mixture is governed by the same equations as is a single body.

The first principle explains that the mixture is formed by its individual constituents. The second principle describes that the components of the physical model are interconnected through interaction terms. Lastly, the third principle states that the movement of the mixture cannot be distinguished from that of a single fluid.

In § 2.1 we provide the groundwork for the continuum theory of mixtures, covering essential kinematics. Following this, § 2.2 presents the evolution laws for individual constituents and mixtures.

2.1. *Preliminaries and kinematics*

The central concept of the continuum theory of mixtures posits that the material body consists of N constituent bodies $\mathscr{B}_\alpha$, where α ranges from 1 to N. These constituent bodies $\mathscr{B}_\alpha$ can simultaneously occupy the same region in space. Let $\boldsymbol{X}_\alpha$ represent the spatial position of a particle of $\mathscr{B}_\alpha$ in the Lagrangian (reference) configuration. The spatial position of a particle is described by the invertible deformation map:

$$\boldsymbol{x} := \boldsymbol{\chi}_\alpha(\boldsymbol{X}_\alpha, t). \tag{2.1}$$

https://doi.org/10.1017/jfm.2026.11366 Published online by Cambridge University Press

The constituent partial mass density $\tilde{\rho}_\alpha$ and specific mass density $\tilde{\rho}_\alpha > 0$ are respectively defined as

$$\tilde{\rho}_\alpha(\boldsymbol{x}, t) := \lim_{|V|\to 0} \frac{M_\alpha(V)}{|V|}, \tag{2.2a}$$

$$\rho_\alpha(\boldsymbol{x}, t) := \lim_{|V_\alpha|\to 0} \frac{M_\alpha(V)}{|V_\alpha|}, \tag{2.2b}$$

where $V \subset \Omega$ (measure $|V|$) is an arbitrary control volume around $\boldsymbol{x}$, $V_\alpha \subset V$ (measure $|V_\alpha|$) is the volume of constituent α so that $V = \cup_\alpha V_\alpha$. Furthermore, the constituents masses are $M_\alpha = M_\alpha(V)$, and the total mass in V is $M = M(V) = \sum_\alpha M_\alpha(V)$. The mixture density is the superposition of the partial mass densities:

$$\rho(\boldsymbol{x}, t) := \lim_{|V|\to 0} \frac{M(V)}{|V|} = \sum_\alpha \tilde{\rho}_\alpha(\boldsymbol{x}, t). \tag{2.3}$$

We introduce the mass fractions and volume fractions respectively as

$$Y_\alpha(\boldsymbol{x}, t) := \lim_{|V|\to 0} \frac{M_\alpha(V)}{M(V)} = \frac{\tilde{\rho}_\alpha}{\rho}, \tag{2.4a}$$

$$\phi_\alpha(\boldsymbol{x}, t) := \lim_{|V|\to 0} \frac{|V_\alpha|}{|V|} = \frac{\tilde{\rho}_\alpha}{\rho_\alpha}, \tag{2.4b}$$

which satisfy

$$\sum_\alpha Y_\alpha(\boldsymbol{x}, t) = 1, \tag{2.5a}$$

$$\sum_\alpha \phi_\alpha(\boldsymbol{x}, t) = 1. \tag{2.5b}$$

Next, we introduce the material time derivative $\dot{\psi}_\alpha$ of the differentiable constituent function ψ_α:

$$\dot{\psi}_\alpha = \partial_t \psi_\alpha(\boldsymbol{X}_\alpha, t)|_{\boldsymbol{X}_\alpha}. \tag{2.6}$$

Here the notation $|_{\boldsymbol{X}_\alpha}$ is used to emphasise that $\boldsymbol{X}_\alpha$ is held fixed. The constituent velocity is a constituent material derivative of the deformation map:

$$\boldsymbol{v}_\alpha(\boldsymbol{x}, t) = \partial_t \boldsymbol{\chi}_\alpha(\boldsymbol{X}_\alpha, t)|_{X_\alpha} = \dot{\boldsymbol{\chi}}_\alpha. \tag{2.7}$$

The mass-averaged mixture velocity $\boldsymbol{v}$ (also called barycentric velocity) is defined via the following identification:

$$\rho(\boldsymbol{x}, t)\boldsymbol{v}(\boldsymbol{x}, t) = \sum_\alpha \tilde{\rho}_\alpha(\boldsymbol{x}, t)\boldsymbol{v}_\alpha(\boldsymbol{x}, t). \tag{2.8}$$

Furthermore, the (constituent) peculiar velocity is defined as

$$\boldsymbol{w}_\alpha(\boldsymbol{x}, t) := \boldsymbol{v}_\alpha(\boldsymbol{x}, t) - \boldsymbol{v}(\boldsymbol{x}, t) \tag{2.9}$$

and specifies the constituent velocity relative to the mixture's general motion. Introducing the (scaled) peculiar velocity

$$\boldsymbol{J}_\alpha(\boldsymbol{x}, t) := \tilde{\rho}_\alpha(\boldsymbol{x}, t)\boldsymbol{w}_\alpha(\boldsymbol{x}, t), \tag{2.10}$$

we have the identity

$$\sum_\alpha \boldsymbol{J}_\alpha(\boldsymbol{x}, t) = 0. \tag{2.11}$$

https://doi.org/10.1017/jfm.2026.11366 Published online by Cambridge University Press

Finally, we introduce the material derivative of the mixture as

$$\dot{\psi}(\boldsymbol{x}, t) = \partial_t \psi(\boldsymbol{x}, t) + \boldsymbol{v}(\boldsymbol{x}, t) \cdot \nabla \psi(\boldsymbol{x}, t). \tag{2.12}$$

2.2. *Constituent balance laws*

The motion of each constituent in the continuum theory of mixtures is expressed by an individualised set of balance laws, as outlined in the second general principle. These laws incorporate interaction terms that depict how the different constituents interact. The motion of each constituent $\alpha = 1, \ldots, N$ is governed by the following set of local balance laws for all $\boldsymbol{x} \in \Omega$ and $t > 0$:

$$\partial_t \tilde{\rho}_\alpha + \operatorname{div}(\tilde{\rho}_\alpha \boldsymbol{v}_\alpha) = \gamma_\alpha, \tag{2.13a}$$

$$\partial_t (\tilde{\rho}_\alpha \boldsymbol{v}_\alpha) + \operatorname{div} (\tilde{\rho}_\alpha \boldsymbol{v}_\alpha \otimes \boldsymbol{v}_\alpha) - \operatorname{div} \boldsymbol{T}_\alpha - \tilde{\rho}_\alpha \boldsymbol{b}_\alpha = \boldsymbol{\pi}_\alpha, \tag{2.13b}$$

$$\boldsymbol{T}_\alpha - \boldsymbol{T}_\alpha^T = \boldsymbol{N}_\alpha. \tag{2.13c}$$

Here Ω is the spatial domain. Equation (2.13*a*) describes the local constituent mass balance law, (2.13*b*) the local constituent linear momentum balance law and (2.13*c*) the local constituent angular momentum balance. The interaction terms are γ_α, $\boldsymbol{\pi}_\alpha$ and $\boldsymbol{N}_\alpha$. These denote respectively the mass supply of constituent α due to chemical reactions with the other constituents, the momentum exchange rate of constituent α and the intrinsic moment of momentum of constituent α. Furthermore, $\boldsymbol{T}_\alpha$ is the Cauchy stress tensor of constituent α, $\boldsymbol{b}_\alpha$ the constituent external body force. In this paper we assume equal body forces ($\boldsymbol{b}_\alpha = \boldsymbol{b}$ for $\alpha = 1, \ldots, N$) and restrict to body forces of gravitational type $\boldsymbol{b} = -b\boldsymbol{\jmath} = -b\nabla y$, with y the vertical coordinate, $\boldsymbol{\jmath}$ the vertical unit vector and b a constant.

In addition, one can infer that the constituent mass balance law can be written as

$$\partial_t \tilde{\rho}_\alpha + \operatorname{div}(\tilde{\rho}_\alpha \boldsymbol{v}) + \operatorname{div} \boldsymbol{J}_\alpha = \gamma_\alpha. \tag{2.14}$$

We denote the kinetic and gravitational energies of the constituents respectively as

$$\mathscr{K}_\alpha = \tilde{\rho}_\alpha \|\boldsymbol{v}_\alpha\|^2/2, \tag{2.15a}$$

$$\mathscr{G}_\alpha = \tilde{\rho}_\alpha b y, \tag{2.15b}$$

where $\|\boldsymbol{v}_\alpha\| = (\boldsymbol{v}_\alpha \cdot \boldsymbol{v}_\alpha)^{1/2}$ is the Euclidean norm of the velocity $\boldsymbol{v}_\alpha$.

REMARK 2.1 *(Volume-averaged mixture velocity). Alternative to the mass-averaged mixture velocity (2.8), another commonly adopted mixture velocity is the volume-averaged velocity* $\boldsymbol{u}$ *defined as* $\boldsymbol{u} = \sum_\alpha \phi_\alpha \boldsymbol{v}_\alpha$. *In the case of incompressible flow* ($\rho_\alpha(\boldsymbol{x}, t) = \rho_\alpha$) *without mass transfer* ($\gamma_\alpha = 0$) *one may deduce from (2.5b) and (2.13a) that it is divergence free, i.e.* $\operatorname{div}\boldsymbol{u} = 0$.

2.3. *Mixture balance laws*

Next, we proceed to the continuum balance laws of the mixtures. In agreement with the first general principle, the motion of the mixture results from that of the individual constituents. Summing the individual balance laws (2.13) across all constituents yields

$$\partial_t \rho + \operatorname{div}(\rho \boldsymbol{v}) = 0, \tag{2.16a}$$

$$\partial_t (\rho \boldsymbol{v}) + \operatorname{div} (\rho \boldsymbol{v} \otimes \boldsymbol{v}) - \operatorname{div} \boldsymbol{T} - \rho \boldsymbol{b} = 0, \tag{2.16b}$$

$$\boldsymbol{T} - \boldsymbol{T}^T = 0, \tag{2.16c}$$

https://doi.org/10.1017/jfm.2026.11366 Published online by Cambridge University Press

where

$$\boldsymbol{T} := \sum_\alpha \boldsymbol{T}_\alpha - \tilde{\rho}_\alpha \boldsymbol{w}_\alpha \otimes \boldsymbol{w}_\alpha, \tag{2.17a}$$

$$\boldsymbol{b} := \frac{1}{\rho} \sum_\alpha \tilde{\rho}_\alpha \boldsymbol{b}_\alpha. \tag{2.17b}$$

In agreement with the third general principle, we have postulated the following balance conditions:

$$\sum_\alpha \gamma_\alpha = 0, \tag{2.18a}$$

$$\sum_\alpha \boldsymbol{\pi}_\alpha = 0, \tag{2.18b}$$

$$\sum_\alpha \boldsymbol{N}_\alpha = 0. \tag{2.18c}$$

The first general principle of mixture theory additionally implies that the kinetic and gravitational energy of the mixture are the superposition of the constituent energies:

$$\mathscr{K} = \sum_\alpha \mathscr{K}_\alpha, \tag{2.19a}$$

$$\mathscr{G} = \sum_\alpha \mathscr{G}_\alpha. \tag{2.19b}$$

REMARK 2.2 *(Kinetic energy). The kinetic energy of the mixture can be decomposed as*

$$\mathscr{K} = \overline{\mathscr{K}} + \sum_\alpha \frac{1}{2} \tilde{\rho}_\alpha \|\boldsymbol{w}_\alpha\|^2, \tag{2.20a}$$

$$\overline{\mathscr{K}} = \frac{1}{2} \rho \|\boldsymbol{v}\|^2, \tag{2.20b}$$

where $\overline{\mathscr{K}}$ is a kinetic energy quantity expressed in pure mixture variables, and where the second member is comprised of kinetic energies based on peculiar velocities.

3. Constitutive modelling

This section is devoted to the construction of constitutive models, employing a structured approach akin to ten Eikelder *et al.* (2024), ten Eikelder (2025). First, § 3.1 provides assumptions and details on the Coleman–Noll modelling procedure (Coleman & Noll 1974). Following this, in § 3.2 we determine the constitutive modelling restriction following from § 3.1. Finally, in § 3.3 we identify specific constitutive models that align with these restrictions.

3.1. *Assumptions and modelling choices*

Instead of working with the full set of balance laws (2.13*a*)–(2.13*c*), we restrict to the reduced set

$$\partial_t \tilde{\rho}_\alpha + \operatorname{div}(\tilde{\rho}_\alpha \boldsymbol{v}) + \operatorname{div} \boldsymbol{H}_\alpha = \zeta_\alpha, \tag{3.1a}$$

$$\partial_t (\rho \boldsymbol{v}) + \operatorname{div} (\rho \boldsymbol{v} \otimes \boldsymbol{v}) - \operatorname{div} \boldsymbol{T} - \rho \boldsymbol{b} = 0, \tag{3.1b}$$

$$\boldsymbol{T} - \boldsymbol{T}^T = 0, \tag{3.1c}$$

https://doi.org/10.1017/jfm.2026.11366 Published online by Cambridge University Press

and where $\alpha = 1, \ldots, N$ in (3.1*a*). We have decomposed the mass-transfer terms into conservative and possible non-conservative parts via $\gamma_\alpha = \zeta_\alpha - \operatorname{div} \boldsymbol{j}_\alpha$ with $\boldsymbol{H}_\alpha := \boldsymbol{J}_\alpha + \boldsymbol{j}_\alpha$. The state variables in the system (3.1) are $\tilde{\rho}_\alpha$ ($\alpha = 1, \ldots, N$) and $\boldsymbol{v}$. We seek constitutive models for $\boldsymbol{T}$, $\boldsymbol{H}_\alpha$ and ζ_α ($\alpha = 1, \ldots, N$). Hereby we discard the definition (2.10), but enforce the balance condition (2.11).

REMARK 3.1 *(Decomposition mass transfer). Rather than modelling $\boldsymbol{H}_\alpha$ and ζ_α, one may work directly with the original terms $\boldsymbol{J}_\alpha$ and γ_α, as both approaches yield equivalent closure models. The decomposition $\gamma_\alpha = \zeta_\alpha - \operatorname{div} \boldsymbol{j}_\alpha$ is introduced solely for interpretative purposes. For example, assuming identical constituent velocities, $\boldsymbol{v}_\alpha = \boldsymbol{v}$, does not conflict with the constitutive model for $\boldsymbol{H}_\alpha$.*

We postulate the energy-dissipation law

$$\frac{\mathrm{d}}{\mathrm{d}t}\mathscr{E} = \mathscr{W} - \mathscr{D} \tag{3.2}$$

as a design principle for constructing closure models for $\boldsymbol{T}$, $\boldsymbol{H}_\alpha$ and ζ_α ($\alpha = 1, \ldots, N$). The total energy is composed of the Helmholtz free energy, the kinetic energy and the gravitational energy:

$$\mathscr{E} = \int_{\mathcal{R}(t)} (\Psi + \overline{\mathscr{K}} + \mathscr{G})\, \mathrm{d}v. \tag{3.3}$$

In this formulation, $\mathcal{R}(t) \subset \Omega$ is an arbitrary, time-dependent control volume with volume element $\mathrm{d}v$ and unit outward normal $\boldsymbol{\nu}$, transported by the velocity field $\boldsymbol{v}$. Moreover, $\mathscr{W}$ denotes the work rate applied on the boundary $\partial\mathcal{R}(t)$, while $\mathscr{D}$ represents the internal dissipation, which is required to satisfy $\mathscr{D} \geqslant 0$.

REMARK 3.2 *(Energy-dissipation statement). In the energy-dissipation law (3.2), the kinetic energy term is taken as $\overline{\mathscr{K}}$, rather than the full kinetic energy of the mixture $\mathscr{K}$ (see Remark 2.2). Consequently, (3.2) can be seen as a simplified formulation of the second law of thermodynamics for mixtures (see, e.g. ten Eikelder et al. 2023, 2024). Moreover, the use of control volumes is not essential; an equivalent modelling constraint, as discussed in § 3.2, may be derived through analogous steps at the local PDE level.*

In this paper we postulate the free energy to belong to the constitutive class

$$\Psi = \hat{\Psi}\left(\{\tilde{\rho}_\alpha\}_{\alpha=1,\ldots,N}, \{\nabla\tilde{\rho}_\alpha\}_{\alpha=1,\ldots,N}\right), \tag{3.4}$$

where we note that both $\{\tilde{\rho}_\alpha\}_{\alpha=1,\ldots,N}$ and $\{\nabla\tilde{\rho}_\alpha\}_{\alpha=1,\ldots,N}$ consist of independent variables. In addition, we introduce the constituent chemical potentials

$$\hat{\mu}_\alpha = \frac{\partial\hat{\Psi}}{\partial\tilde{\rho}_\alpha} - \operatorname{div}\frac{\partial\hat{\Psi}}{\partial\nabla\tilde{\rho}_\alpha}. \tag{3.5}$$

REMARK 3.3 *(Relation to compressible two-phase flow models). The modelling choices presented in this section distinguish our approach from conventional compressible two-phase flow models in several important ways. First, our formulation is based on the reduced set of balance laws (3.1). In contrast, compressible two-phase flow models typically include additional evolution equations for the volume fractions, which do not naturally arise from the continuum mixture theory described in § 2. Consequently, while the state variables in compressible two-phase flow models consist of specific densities $\{\rho_\alpha\}$ and volume fractions $\{\phi_\alpha\}$ (subject to the saturation constraint (2.5b)), our approach employs partial densities $\{\tilde{\rho}_\alpha\}$ instead. Finally, the constitutive class (3.4) depends on all*

https://doi.org/10.1017/jfm.2026.11366 Published online by Cambridge University Press

partial densities, thereby enabling the modelling of interaction (van der Waals) forces – an aspect that is absent in standard compressible two-phase flow models.

REMARK 3.4 *(Constitutive class free energy). In many conventional phase-field models, including those of the Cahn–Hilliard type, the free energy is expressed in terms of order parameters such as volume fractions or mass fractions (often referred to as concentrations). In contrast, the constitutive class (3.4) is formulated in terms of partial densities. We explore the relationship between these approaches in the binary case in § 6 and provide the corresponding derivation in Appendix C.*

3.2. *Modelling restriction*

We proceed with the evaluation of the evolution of the energy (3.3). By applying Reynolds transport theorem to the free energy $\hat{\Psi}$ we have

$$\frac{\mathrm{d}}{\mathrm{d}t}\int_{\mathcal{R}(t)} \hat{\Psi}\,\mathrm{d}v = \int_{\mathcal{R}(t)} \partial_t \hat{\Psi}\,\mathrm{d}v + \int_{\partial\mathcal{R}(t)} \hat{\Psi}\,\boldsymbol{v}\cdot\boldsymbol{\nu}\,\mathrm{d}a. \tag{3.6}$$

We apply the divergence theorem and expand the derivatives:

$$\frac{\mathrm{d}}{\mathrm{d}t}\int_{\mathcal{R}(t)} \hat{\Psi}\,\mathrm{d}v = \int_{\mathcal{R}(t)} \hat{\Psi}\,\mathrm{div}\boldsymbol{v} + \sum_\alpha \frac{\partial\hat{\Psi}}{\partial\tilde{\rho}_\alpha}\dot{\tilde{\rho}}_\alpha + \frac{\partial\hat{\Psi}}{\partial\nabla\tilde{\rho}_\alpha}\cdot(\nabla\tilde{\rho}_\alpha)^{\cdot}\,\mathrm{d}v. \tag{3.7}$$

Substituting the identity for the material derivative

$$(\nabla\omega)^{\cdot} = \nabla(\dot{\omega}) - (\nabla\omega)^T\nabla\boldsymbol{v} \tag{3.8}$$

with $\omega = \tilde{\rho}_\alpha$ into (3.7) yields

$$\frac{\mathrm{d}}{\mathrm{d}t}\int_{\mathcal{R}(t)} \hat{\Psi}\,\mathrm{d}v = \int_{\mathcal{R}(t)} \hat{\Psi}\,\mathrm{div}\boldsymbol{v} + \sum_\alpha \frac{\partial\hat{\Psi}}{\partial\tilde{\rho}_\alpha}\dot{\tilde{\rho}}_\alpha + \frac{\partial\hat{\Psi}}{\partial\nabla\tilde{\rho}_\alpha}\cdot\nabla\big(\dot{\tilde{\rho}}_\alpha\big) - \frac{\partial\hat{\Psi}}{\partial\nabla\tilde{\rho}_\alpha}\cdot(\nabla\tilde{\rho}_\alpha)^T\nabla\boldsymbol{v}\,\mathrm{d}v. \tag{3.9}$$

By subsequently integrating by parts, we arrive at

$$\begin{aligned}\frac{\mathrm{d}}{\mathrm{d}t}\int_{\mathcal{R}(t)} \hat{\Psi}\,\mathrm{d}v = \int_{\mathcal{R}(t)} \hat{\Psi}\,\mathrm{div}\boldsymbol{v} + \sum_\alpha \hat{\mu}_\alpha\dot{\tilde{\rho}}_\alpha - \nabla\tilde{\rho}_\alpha\otimes\frac{\partial\hat{\Psi}}{\partial\nabla\tilde{\rho}_\alpha} : \nabla\boldsymbol{v}\,\mathrm{d}v \\ + \int_{\partial\mathcal{R}(t)}\sum_\alpha \dot{\tilde{\rho}}_\alpha\frac{\partial\hat{\Psi}}{\partial\nabla\tilde{\rho}_\alpha}\cdot\boldsymbol{\nu}\,\mathrm{d}a.\end{aligned} \tag{3.10}$$

Substituting the constituent mass balance laws (2.14) and applying integration by parts leads to

$$\begin{aligned}\frac{\mathrm{d}}{\mathrm{d}t}\int_{\mathcal{R}(t)} \hat{\Psi}\,\mathrm{d}v = \int_{\mathcal{R}(t)} \hat{\Psi}\,\mathrm{div}\boldsymbol{v} - \sum_\alpha \hat{\mu}_\alpha\tilde{\rho}_\alpha\mathrm{div}\boldsymbol{v} + \sum_\alpha \nabla\hat{\mu}_\alpha\cdot\boldsymbol{H}_\alpha \\ - \sum_\alpha \nabla\tilde{\rho}_\alpha\otimes\frac{\partial\hat{\Psi}}{\partial\nabla\tilde{\rho}_\alpha} : \nabla\boldsymbol{v} + \sum_\alpha \hat{\mu}_\alpha\zeta_\alpha\,\mathrm{d}v \\ + \int_{\partial\mathcal{R}(t)}\left(\sum_\alpha \dot{\tilde{\rho}}_\alpha\frac{\partial\hat{\Psi}}{\partial\nabla\tilde{\rho}_\alpha} - \hat{\mu}_\alpha\boldsymbol{H}_\alpha\right)\cdot\boldsymbol{\nu}\,\mathrm{d}a.\end{aligned} \tag{3.11}$$

https://doi.org/10.1017/jfm.2026.11366 Published online by Cambridge University Press

Subsequently, the evolution equations for the kinetic and gravitational energies follow straightforward from (3.1*a*) and (3.1*b*) (see ten Eikelder *et al.* 2023 for details):

$$\frac{\mathrm{d}}{\mathrm{d}t}\int_{\mathcal{R}(t)} \mathscr{K}\,\mathrm{d}v = \int_{\mathcal{R}(t)} -\boldsymbol{\nabla v} : \boldsymbol{T} + \rho \boldsymbol{v}\cdot\boldsymbol{g}\,\mathrm{d}v + \int_{\partial\mathcal{R}(t)} \boldsymbol{v}\cdot\boldsymbol{T}\boldsymbol{v}\,\mathrm{d}a, \tag{3.12a}$$

$$\frac{\mathrm{d}}{\mathrm{d}t}\int_{\mathcal{R}(t)} \mathscr{G}\,\mathrm{d}v = -\int_{\mathcal{R}(t)} \rho \boldsymbol{v}\cdot\boldsymbol{g}\,\mathrm{d}v. \tag{3.12b}$$

Summing (3.11) and (3.12) yields

$$\begin{aligned}\frac{\mathrm{d}}{\mathrm{d}t}\mathscr{E} = &\int_{\partial\mathcal{R}(t)} \left(\boldsymbol{v}^T\boldsymbol{T} - \sum_\alpha \left(\hat{\mu}_\alpha \boldsymbol{H}_\alpha - \dot{\tilde{\rho}}_\alpha \frac{\partial\hat{\Psi}}{\partial\boldsymbol{\nabla}\tilde{\rho}_\alpha}\right)\right)\cdot\boldsymbol{v}\,\mathrm{d}a \\ &- \int_{\mathcal{R}(t)} \left(\boldsymbol{T} + \sum_\alpha \boldsymbol{\nabla}\tilde{\rho}_\alpha \otimes \frac{\partial\hat{\Psi}}{\partial\boldsymbol{\nabla}\tilde{\rho}_\alpha} + \left(\sum_\alpha \hat{\mu}_\alpha\tilde{\rho}_\alpha - \hat{\Psi}\right)\boldsymbol{I}\right) : \boldsymbol{\nabla v} \\ &+ \sum_\alpha \left(-\boldsymbol{\nabla}\hat{\mu}_\alpha\cdot\boldsymbol{H}_\alpha - \hat{\mu}_\alpha\zeta_\alpha\right)\mathrm{d}v,\end{aligned} \tag{3.13}$$

where we identify the rate of work and the dissipation as

$$\mathscr{W} = \int_{\partial\mathcal{R}(t)} \left(\boldsymbol{v}^T\boldsymbol{T} - \sum_\alpha \left(\hat{\mu}_\alpha \boldsymbol{H}_\alpha - \dot{\tilde{\rho}}_\alpha \frac{\partial\hat{\Psi}}{\partial\boldsymbol{\nabla}\tilde{\rho}_\alpha}\right)\right)\cdot\boldsymbol{v}\,\mathrm{d}a, \tag{3.14a}$$

$$\begin{aligned}\mathscr{D} = &\int_{\mathcal{R}(t)} \left(\boldsymbol{T} + \sum_\alpha \boldsymbol{\nabla}\tilde{\rho}_\alpha \otimes \frac{\partial\hat{\Psi}}{\partial\boldsymbol{\nabla}\tilde{\rho}_\alpha} + \left(\sum_\alpha \hat{\mu}_\alpha\tilde{\rho}_\alpha - \hat{\Psi}\right)\boldsymbol{I}\right) : \boldsymbol{\nabla v} \\ &+ \sum_\alpha \left(-\boldsymbol{\nabla}\hat{\mu}_\alpha\cdot\boldsymbol{H}_\alpha - \hat{\mu}_\alpha\zeta_\alpha\right)\mathrm{d}v.\end{aligned} \tag{3.14b}$$

Since the control volume $\mathcal{R} = \mathcal{R}(t)$ is arbitrary, the energy-dissipation law is satisfied provided that the following local inequality holds:

$$\left(\boldsymbol{T} + \sum_\alpha \boldsymbol{\nabla}\tilde{\rho}_\alpha \otimes \frac{\partial\hat{\Psi}}{\partial\boldsymbol{\nabla}\tilde{\rho}_\alpha} + \left(\sum_\alpha \hat{\mu}_\alpha\tilde{\rho}_\alpha - \hat{\Psi}\right)\boldsymbol{I}\right) : \boldsymbol{\nabla v} - \sum_\alpha \boldsymbol{H}_\alpha\cdot\boldsymbol{\nabla}\hat{\mu}_\alpha - \sum_\alpha \zeta_\alpha\hat{\mu}_\alpha \geqslant 0. \tag{3.15}$$

3.3. *Selection of constitutive models*

By means of the Colemann–Noll procedure, the inequality (3.15) permits us to restrict to mixture stress tensors $\boldsymbol{T}$, constituent diffusive fluxes $\boldsymbol{H}_\alpha$ and constituent mass fluxes ζ_α that belong to the constitutive classes:

$$\boldsymbol{T} = \hat{\boldsymbol{T}}\left(\boldsymbol{\nabla v}, \{\tilde{\rho}_\beta\}, \{\boldsymbol{\nabla}\tilde{\rho}_\beta\}, \{\hat{\mu}_\beta\}, \{\boldsymbol{\nabla}\hat{\mu}_\beta\}\right), \tag{3.16a}$$

$$\boldsymbol{H}_\alpha = \hat{\boldsymbol{H}}_\alpha\left(\{\tilde{\rho}_\beta\}, \{\boldsymbol{\nabla}\tilde{\rho}_\beta\}, \{\hat{\mu}_\beta\}, \{\boldsymbol{\nabla}\hat{\mu}_\beta\}\right), \tag{3.16b}$$

$$\zeta_\alpha = \hat{\zeta}_\alpha\left(\{\tilde{\rho}_\beta\}, \{\hat{\mu}_\beta\}\right). \tag{3.16c}$$

https://doi.org/10.1017/jfm.2026.11366 Published online by Cambridge University Press

We seek for constitutive models (3.16) that render each of the three terms in (3.15) non-negative:

$$\left(\hat{\boldsymbol{T}} + \sum_\alpha \nabla\tilde{\rho}_\alpha \otimes \frac{\partial\hat{\Psi}}{\partial\nabla\tilde{\rho}_\alpha} + \left(\sum_\alpha \hat{\mu}_\alpha\tilde{\rho}_\alpha - \hat{\Psi}\right)\boldsymbol{I}\right) : \nabla\boldsymbol{v} \geqslant 0, \tag{3.17a}$$

$$-\sum_\alpha \hat{\boldsymbol{H}}_\alpha \cdot \nabla\hat{\mu}_\alpha \geqslant 0, \tag{3.17b}$$

$$-\sum_\alpha \hat{\zeta}_\alpha\hat{\mu}_\alpha \geqslant 0. \tag{3.17c}$$

Constitutive choices: we make the following constitutive choices:

$$\hat{\boldsymbol{T}} = -\sum_\alpha \nabla\tilde{\rho}_\alpha \otimes \frac{\partial\hat{\Psi}}{\partial\nabla\tilde{\rho}_\alpha} - \left(\sum_\alpha \hat{\mu}_\alpha\tilde{\rho}_\alpha - \hat{\Psi}\right)\boldsymbol{I} + \nu\,(2\boldsymbol{D} + \lambda(\operatorname{div}\boldsymbol{v})\boldsymbol{I}), \tag{3.18a}$$

$$\hat{\boldsymbol{H}}_\alpha = -\sum_\beta \boldsymbol{M}_{\alpha\beta}\nabla\hat{\mu}_\beta, \tag{3.18b}$$

$$\hat{\zeta}_\alpha = -\sum_\beta m_{\alpha\beta}\hat{\mu}_\beta. \tag{3.18c}$$

Here $\nu \geqslant 0$ is the dynamic viscosity, $\lambda \geqslant -2/d$ (with d denoting the number of dimensions), $\boldsymbol{M}$ is a symmetric positive definite tensor, with the same dependencies as (3.16*b*), satisfying

$$\sum_\alpha \boldsymbol{M}_{\alpha\beta} = \sum_\beta \boldsymbol{M}_{\alpha\beta} = 0, \quad \boldsymbol{M}_{\alpha\beta}|_{Y_\gamma=1} = 0 \quad \text{for all } \gamma = 1, \ldots, N, \tag{3.19}$$

and m is a symmetric positive definite scalar mobility, with the same dependencies as (3.16*c*), satisfying

$$\sum_\alpha m_{\alpha\beta} = \sum_\beta m_{\alpha\beta} = 0, \quad m_{\alpha\beta}|_{Y_\gamma=1} = 0 \quad \text{for all } \gamma = 1, \ldots, N. \tag{3.20}$$

Moreover, compatibility with the angular momentum condition (3.1*c*) requires that

$$\nabla\tilde{\rho}_\alpha \otimes \frac{\partial\hat{\Psi}}{\partial\nabla\tilde{\rho}_\alpha} = \frac{\partial\hat{\Psi}}{\partial\nabla\tilde{\rho}_\alpha} \otimes \nabla\tilde{\rho}_\alpha. \tag{3.21}$$

LEMMA 3.5 *(Compatibility of constitutive choices). The choices (3.18a)–(3.18c) are compatible with the restrictions (3.17a)–(3.17c), as well as with the balance of relative gross motion (2.11) and the balance of mass supply (2.18a).*

Proof. For the stress tensor, a direct calculation yields

$$\begin{aligned}\left(\hat{\boldsymbol{T}} + \sum_\alpha \nabla\tilde{\rho}_\alpha \otimes \frac{\partial\hat{\Psi}}{\partial\nabla\tilde{\rho}_\alpha} + \Big(\sum_\alpha \hat{\mu}_\alpha\tilde{\rho}_\alpha - \hat{\Psi}\Big)\boldsymbol{I}\right) &: \nabla\boldsymbol{v} \\ = 2\nu\left(\boldsymbol{D} - \frac{1}{d}(\operatorname{div}\boldsymbol{v})\boldsymbol{I}\right) &: \left(\boldsymbol{D} - \frac{1}{d}(\operatorname{div}\boldsymbol{v})\boldsymbol{I}\right) + \nu\left(\lambda + \frac{2}{d}\right)(\operatorname{div}\boldsymbol{v})^2 \geq 0,\end{aligned} \tag{3.22}$$

which confirms compatibility with (3.17*a*). For the diffusive flux, the condition $\sum_\alpha \boldsymbol{M}_{\alpha\beta} = 0$ guarantees compatibility with the balance (2.11), while the positive semi-definiteness of $\boldsymbol{M}_{\alpha\beta}$ ensures the thermodynamical restriction (3.17*b*). Similarly, for the

https://doi.org/10.1017/jfm.2026.11366 Published online by Cambridge University Press

mass-transfer term, the properties $\sum_\alpha m_{\alpha\beta} = 0$ and the positive definiteness of $m_{\alpha\beta}$ ensure compatibility with the mass supply balance (2.18*a*) and the restriction (3.17*c*). □

REMARK 3.6 *(Mass transfer in compressible two-phase flow models). We consider the special case:*

$$m_{\alpha\beta} = \begin{cases} -\hat{m}_{\alpha\beta} & \text{if } \alpha \neq \beta, \\ \sum_{\gamma\neq\alpha} \hat{m}_{\alpha\gamma} & \text{if } \alpha = \beta. \end{cases} \tag{3.23}$$

Under this assumption, we obtain

$$\begin{aligned} \hat{\zeta}_\alpha &= -\sum_{\beta\neq\alpha} m_{\alpha\beta}\nabla\hat{\mu}_\beta - m_{\alpha\alpha}\nabla\hat{\mu}_\alpha \\ &= \sum_{\beta\neq\alpha} \hat{m}_{\alpha\beta}\nabla\hat{\mu}_\beta - \sum_{\gamma\neq\alpha} \hat{m}_{\alpha\gamma}\nabla\hat{\mu}_\alpha \\ &= -\sum_{\beta} \hat{m}_{\alpha\beta}\nabla(\hat{\mu}_\alpha - \hat{\mu}_\beta). \end{aligned} \tag{3.24}$$

This formulation is commonly used for binary flows in compressible two-phase models; see, e.g. Coquel et al. (2013), Saurel & Pantano (2018), Pelanti (2022).

This concludes the fundamental exploration of constitutive models compatible with the imposed energy-dissipative modelling restriction. Substitution provides the model

$$\partial_t(\rho\boldsymbol{v}) + \operatorname{div}(\rho\boldsymbol{v}\otimes\boldsymbol{v}) + \nabla p + \operatorname{div}\left(\sum_\beta \nabla\tilde{\rho}_\beta \otimes \frac{\partial\hat{\Psi}}{\partial\nabla\tilde{\rho}_\beta}\right) - \operatorname{div}(\nu(2\boldsymbol{D} + \lambda(\operatorname{div}\boldsymbol{v})\boldsymbol{I})) - \rho\boldsymbol{g} = 0, \tag{3.25a}$$

$$\partial_t\tilde{\rho}_\alpha + \operatorname{div}(\tilde{\rho}_\alpha\boldsymbol{v}) - \sum_\beta \operatorname{div}\left(\boldsymbol{M}_{\alpha\beta}\nabla\hat{\mu}_\beta\right) + \sum_\beta m_{\alpha\beta}\hat{\mu}_\beta = 0, \tag{3.25b}$$

$$\hat{\mu}_\alpha - \frac{\partial\Psi}{\partial\tilde{\rho}_\alpha} + \operatorname{div}\left(\frac{\partial\Psi}{\partial\nabla\tilde{\rho}_\alpha}\right) = 0, \tag{3.25c}$$

where the pressure p takes the form

$$p = \sum_\beta(\hat{\mu}_\beta\tilde{\rho}_\beta) - \hat{\Psi}. \tag{3.26}$$

REMARK 3.7 *(Relation to Cahn–Hilliard/Allen–Cahn/Korteweg models). The framework connects to Cahn–Hilliard/Allen–Cahn/Korteweg-type models by selecting* $\hat{\Psi} = \hat{\Psi}_0 + (1/2)\sum_{\beta\gamma}\lambda_{\beta\gamma}\nabla\tilde{\rho}_\beta\cdot\nabla\tilde{\rho}_\gamma$, *where* $\hat{\Psi}_0 = \hat{\Psi}_0(\{\tilde{\rho}_\beta\})$ *and where* $\lambda_{\beta\gamma}$ *are model parameters.*

REMARK 3.8 *(Alternative pressure variable). A common alternative approach is to decompose the stress tensor into its volumetric (isotropic) and deviatoric (traceless) components, which allows one to define the volumetric pressure* p^{vol}*:*

https://doi.org/10.1017/jfm.2026.11366 Published online by Cambridge University Press

$$\hat{\boldsymbol{T}} = -p^{vol}\boldsymbol{I} + \hat{\boldsymbol{T}}^{dev}, \tag{3.27a}$$

$$p^{vol} = \sum_{\beta}\left(\hat{\mu}_\beta\tilde{\rho}_\beta - \frac{1}{d}\nabla\tilde{\rho}_\beta\cdot\frac{\partial\hat{\Psi}}{\partial\nabla\tilde{\rho}_\beta}\right) - \hat{\Psi} - \nu\left(\lambda+\frac{2}{d}\right)div\boldsymbol{v}, \tag{3.27b}$$

$$\hat{\boldsymbol{T}}^{dev} = \sum_{\beta}\left(\nabla\tilde{\rho}_\beta\otimes\frac{\partial\hat{\Psi}}{\partial\nabla\tilde{\rho}_\beta} - \frac{1}{d}\nabla\tilde{\rho}_\beta\cdot\frac{\partial\hat{\Psi}}{\partial\nabla\tilde{\rho}_\beta}\boldsymbol{I}\right) + 2\nu\left(\boldsymbol{D} - \frac{1}{d}(div\boldsymbol{v})\boldsymbol{I}\right). \tag{3.27c}$$

We explicitly state the compatibility with the energy-dissipation condition.

THEOREM 3.9 *(Compatibility energy dissipation). The model (3.25) is compatible with the energy-dissipation condition (3.2).*

Proof. This follows from Lemma 3.5, in particular we have

$$\mathscr{D} = \int_{\mathcal{R}(t)} 2\nu\left(\boldsymbol{D} - \frac{1}{d}(\mathrm{div}\boldsymbol{v})\boldsymbol{I}\right) : \left(\boldsymbol{D} - \frac{1}{d}(\mathrm{div}\boldsymbol{v})\boldsymbol{I}\right) + \nu\left(\lambda+\frac{2}{d}\right)(\mathrm{div}\boldsymbol{v})^2 + \sum_{\alpha,\beta} M_{\alpha\beta}\nabla\hat{\mu}_\alpha\cdot\nabla\hat{\mu}_\beta + \sum_{\alpha,\beta} m_{\alpha\beta}\hat{\mu}_\alpha\hat{\mu}_\beta \,\mathrm{d}v \geqslant 0. \tag{3.28}$$

□

4. Properties

We first discuss compact formulations in § 4.1. Next, we discuss the decomposition of the free energy in § 4.2. Finally, in § 4.3 we present the equilibrium conditions of the model.

4.1. *Compact formulations*

Simplification of the model (3.25) can be achieved by employing the following identity.

LEMMA 4.1 *(Identity Korteweg stresses). We have the following identity for the pressure and Korteweg stresses:*

$$\nabla p + div\left(\sum_{\alpha}\nabla\tilde{\rho}_\alpha\otimes\frac{\partial\hat{\Psi}}{\partial\nabla\tilde{\rho}_\alpha}\right) = \sum_{\alpha}\tilde{\rho}_\alpha\nabla\hat{\mu}_\alpha. \tag{4.1}$$

Proof. See Lemma A.1. □

REMARK 4.2. *The identity in Lemma 4.1 represents the multicomponent extension of the well-known identity for the Korteweg stress.*

Applying Lemma 4.1 we find the more compact form

$$\partial_t(\rho\boldsymbol{v}) + \mathrm{div}\,(\rho\boldsymbol{v}\otimes\boldsymbol{v}) + \sum_{\beta}\tilde{\rho}_\beta\nabla\hat{\mu}_\beta - \mathrm{div}\,(\nu(2\boldsymbol{D} + \lambda(\mathrm{div}\boldsymbol{v})\boldsymbol{I})) - \rho\boldsymbol{g} = 0, \tag{4.2a}$$

$$\partial_t\tilde{\rho}_\alpha + \mathrm{div}(\tilde{\rho}_\alpha\boldsymbol{v}) - \sum_{\beta}\mathrm{div}\left(M_{\alpha\beta}\nabla\hat{\mu}_\beta\right) + \sum_{\beta} m_{\alpha\beta}\hat{\mu}_\beta = 0, \tag{4.2b}$$

for $\alpha = 1, \ldots, N$. Furthermore, we note that the model may alternatively be written in a form that more closely links to existing phase-field models, i.e.

https://doi.org/10.1017/jfm.2026.11366 Published online by Cambridge University Press

$$\partial_t(\rho \boldsymbol{v}) + \operatorname{div}(\rho \boldsymbol{v} \otimes \boldsymbol{v}) + \rho \sum_\beta Y_\beta \nabla \hat{\mu}_\beta - \operatorname{div}(\nu(2\boldsymbol{D} + \lambda(\operatorname{div}\boldsymbol{v})\boldsymbol{I})) - \rho \boldsymbol{g} = 0, \quad (4.3a)$$

$$\partial_t \rho + \operatorname{div}(\rho \boldsymbol{v}) = 0, \quad (4.3b)$$

$$\partial_t(\rho Y_\alpha) + \operatorname{div}(\rho Y_\alpha \boldsymbol{v}) - \sum_\beta \operatorname{div}\left(M_{\alpha\beta} \nabla \hat{\mu}_\beta\right) + \sum_\beta m_{\alpha\beta} \hat{\mu}_\beta = 0, \quad (4.3c)$$

for $\alpha = 1, \ldots, N-1$. We note that the combination of the mixture mass balance (4.3*b*) and the $N-1$ constituent balance laws (4.3*c*) are equivalent to the N balance laws (4.2*b*) or N balance laws (4.3*c*).

We observe that, in the single-fluid regime, the model simplifies to the compressible Navier–Stokes equations.

PROPOSITION 4.3 *(Reduction to compressible Navier–Stokes). If the chemical potentials $\hat{\mu}_\alpha$ are well defined for $\tilde{\rho}_\alpha = 0$ ($\alpha = 1, \ldots, N$), the multiconstituent system (4.3) reduces to the compressible Navier–Stokes equations in the single constituent regime ($Y_\beta = 1$), i.e.*

$$\partial_t(\rho \boldsymbol{v}) + div(\rho \boldsymbol{v} \otimes \boldsymbol{v}) + \nabla p - div(\nu(2\boldsymbol{D} + \lambda div \boldsymbol{v})) - \rho \boldsymbol{b} = 0, \quad (4.4a)$$

$$\partial_t \rho + div(\rho \boldsymbol{v}) = 0, \quad (4.4b)$$

with $\rho_\beta = \tilde{\rho}_\beta = \rho$ and $p = p(\rho)$.

4.2. *Decomposition of the free energy*

We proceed with decomposing the free energy into its components; in agreement with the first metaphysical principle of continuum mixture theory we have

$$\hat{\Psi}\left(\{\tilde{\rho}_\alpha\}_{\alpha=1,\ldots,N}, \{\nabla \tilde{\rho}_\alpha\}_{\alpha=1,\ldots,N}\right) = \sum_\beta \hat{\Psi}_\beta\left(\{\tilde{\rho}_\alpha\}_{\alpha=1,\ldots,N}, \{\nabla \tilde{\rho}_\alpha\}_{\alpha=1,\ldots,N}\right), \quad (4.5)$$

where $\hat{\Psi}_\beta$ is the volume-measure constituent free energy. The split of the free energy, (4.5), highlights that the constituent free energies may depend on quantities of other constituents ($\tilde{\rho}_\alpha$ and $\nabla \tilde{\rho}_\alpha$ for all $\alpha = 1, \ldots, N$), allowing for the incorporation of, for example, attraction/repelling forces.

Next, we associate constituent chemical potentials and constituent partial pressures with each $\hat{\Psi}_\beta$ in the sense:

$$\hat{\mu}_{\beta\alpha} := \frac{\partial \hat{\Psi}_\beta}{\partial \tilde{\rho}_\alpha} - \operatorname{div} \frac{\partial \hat{\Psi}_\beta}{\partial \nabla \tilde{\rho}_\alpha}, \quad (4.6a)$$

$$p_\beta = \left(\sum_\alpha \hat{\mu}_{\beta\alpha} \tilde{\rho}_\alpha\right) - \hat{\Psi}_\beta. \quad (4.6b)$$

The constituent partial pressures p_α are an extension of the classical partial pressure that includes gradient contributions essential to modelling surface tension effects. These constituent quantities satisfy the properties

$$\hat{\mu}_\alpha = \sum_\beta \hat{\mu}_{\beta\alpha}, \quad (4.7a)$$

$$p = \sum_\beta p_\beta. \quad (4.7b)$$

https://doi.org/10.1017/jfm.2026.11366 Published online by Cambridge University Press

The latter may be referred to as Dalton's law. As such, the split (4.5) reveals that the system may be written as

$$\sum_\beta \left(\partial_t(\tilde\rho_\beta \boldsymbol{v}) + \operatorname{div}\left(\tilde\rho_\beta \boldsymbol{v}\otimes\boldsymbol{v}\right) + \nabla p_\beta + \operatorname{div}\left(\sum_\alpha \nabla\tilde\rho_\alpha \otimes \frac{\partial\hat\Psi_\beta}{\partial\nabla\tilde\rho_\alpha}\right) - \tilde\rho_\beta \boldsymbol{g}\right)$$
$$-\operatorname{div}\left(\nu(2\boldsymbol{D}+\lambda(\operatorname{div}\boldsymbol{v})\boldsymbol{I})\right) = 0, \quad (4.8a)$$

$$\partial_t\tilde\rho_\alpha + \operatorname{div}(\tilde\rho_\alpha\boldsymbol{v}) - \sum_\beta \operatorname{div}\left(M_{\alpha\beta}\nabla\hat\mu_\beta\right) + \sum_\beta m_{\alpha\beta}\hat\mu_\beta = 0. \quad (4.8b)$$

REMARK 4.4 *(Absence of interaction forces). When interaction forces are absent, i.e.* $\hat\Psi_\beta = \hat\Psi_\beta(\tilde\rho_\beta, \nabla\tilde\rho_\beta)$*, we have*

$$\hat\mu_{\beta\alpha} = \hat\mu_\alpha\delta_{\alpha\beta}, \quad (4.9a)$$

$$p_\beta = \hat\mu_\beta\tilde\rho_\beta - \hat\Psi_\beta, \quad (4.9b)$$

so that

$$\sum_\alpha \nabla\tilde\rho_\alpha \otimes \frac{\partial\hat\Psi_\beta}{\partial\nabla\tilde\rho_\alpha} = \nabla\tilde\rho_\beta \otimes \frac{\partial\hat\Psi_\beta}{\partial\nabla\tilde\rho_\beta}. \quad (4.10)$$

REMARK 4.5 *(Pressure/temperature). We emphasise that the model is isothermal: a single (constant) temperature is assumed and the thermodynamic state of the mixture is determined by one Helmholtz free energy* $\hat\Psi(\{\tilde\rho_\beta\}, \{\nabla\tilde\rho_\beta\})$*. Consequently, despite the absence of explicit species energy equations, the model satisfies a standard mixture energy-dissipation balance derived from the second law. A single mixture pressure* p *is defined from* $\hat\Psi$*; when* $\hat\Psi = \sum_\beta \hat\Psi_\beta$*, constituent pressures* p_β *can also be introduced for interpretation, with* $p = \sum_\beta p_\beta$ *in general and* p_β *not necessarily equal.*

4.3. *Equilibrium conditions*

We characterise the equilibrium conditions of the model (4.8) by

$$\mathscr{D} = 0. \quad (4.11)$$

The identity (3.28) provides

$$2\nu^{eq}\left(\boldsymbol{D}^{eq} - \frac{1}{d}(\operatorname{div}\boldsymbol{v}^{eq})\boldsymbol{I}\right) : \left(\boldsymbol{D}^{eq} - \frac{1}{d}(\operatorname{div}\boldsymbol{v}^{eq})\boldsymbol{I}\right) = 0, \quad (4.12a)$$

$$\nu^{eq}\left(\lambda + \frac{2}{d}\right)\left(\operatorname{div}\boldsymbol{v}^{eq}\right)^2 = 0, \quad (4.12b)$$

$$\sum_{\alpha,\beta} \boldsymbol{M}^{eq}_{\alpha\beta}\nabla\hat\mu^{eq}_\alpha \cdot \nabla\hat\mu^{eq}_\beta = 0, \quad (4.12c)$$

$$\sum_{\alpha,\beta} m^{eq}_{\alpha\beta}\hat\mu^{eq}_\alpha\hat\mu^{eq}_\beta = 0, \quad (4.12d)$$

where the superscripts 'eq' denote the equilibrium of the quantity. Identities (4.12*a*) and (4.12*b*) dictate that $\boldsymbol{v}^{eq}$ are rigid motions. Since $\boldsymbol{M}_{\alpha\beta}$ is symmetric positive definite, we decompose it as $\boldsymbol{M}_{\alpha\beta,ij} = \sum_q \boldsymbol{B}_{q,\alpha,i}\boldsymbol{B}_{q,\beta,j}$ for some $\boldsymbol{B}_{q,\alpha,i}$ with the same dependencies as $\boldsymbol{M}_{\alpha\beta,ij}$. Hence, (4.12*c*) implies that $\sum_\alpha \boldsymbol{B}^{eq}_\alpha\nabla\hat\mu^{eq}_\alpha = 0$. In a similar fashion we deduce

https://doi.org/10.1017/jfm.2026.11366 Published online by Cambridge University Press

that $\sum_\alpha B^{eq}_{\alpha,q}\hat{\mu}^{eq}_\alpha = 0$ for all $q = 1, \ldots, N$, where $m_{\alpha\beta} = \sum_q B_{\alpha,q}B_{\beta,q}$. These conditions imply that $\hat{\boldsymbol{H}}^{eq}_\alpha = 0$, $\hat{\zeta}^{eq}_\alpha = 0$ for $\alpha = 1, \ldots, N$. Finally, restricting to zero velocities, $\boldsymbol{v}^{eq} = \boldsymbol{0}$, the mass balance laws imply constant in time partial densities, $\tilde{\rho}^{eq}_\alpha(\boldsymbol{x}, t) = \tilde{\rho}^{eq}_\alpha(\boldsymbol{x})$, while the momentum balance dictates that $\sum_\alpha Y^{eq}_\alpha \nabla\hat{\mu}^{eq}_\alpha = \boldsymbol{g}$. Summarising, we have the equilibrium conditions

$$\boldsymbol{v}^{eq} = \boldsymbol{0}, \tag{4.13a}$$

$$\tilde{\rho}^{eq}_\alpha = \text{const} \ \ (\text{in time}), \tag{4.13b}$$

$$\sum_\alpha b^{eq}_\alpha \hat{\mu}^{eq}_\alpha = 0, \tag{4.13c}$$

$$\sum_\alpha \boldsymbol{B}^{eq}_\alpha \nabla\hat{\mu}^{eq}_\alpha = 0, \tag{4.13d}$$

$$\sum_\alpha Y^{eq}_\alpha \nabla\hat{\mu}^{eq}_\alpha = \boldsymbol{g}. \tag{4.13e}$$

REMARK 4.6 *(No equilibrium conditions pressure). If the free energy Ψ does not depend on $\{\nabla\tilde{\rho}_\alpha\}$, the condition (4.13e) converts into $\nabla p = \rho\boldsymbol{g}$ (see Lemma 4.1). Thus, there is no equilibrium condition on the partial pressures $p_\alpha, \alpha = 1, \ldots, N$. This is in contrast to some compressible two-phase models in which pressure equilibrium is assumed; see, e.g. Kapila et al. (2001), Murrone & Guillard (2005), Daude et al. (2023) (and § 7.1).*

5. Analysis of the first-order system

In this section we examine the first-order system associated with (3.25). Beyond presenting the formulation, our aim is to clarify its structural properties and to check its consistency with established principles of fluid dynamics. We first introduce the system in § 5.1, then analyse its potential hyperbolic structure in § 5.2 to determine whether the dynamics admit finite-speed propagation and, finally, derive the Riemann invariants and jump conditions in § 5.3 to verify compatibility with classical interfacial balance laws.

5.1. *First-order system*

We study the first-order system associated with (3.25) in the absence of mass transfer ($\hat{\zeta}_\alpha = 0$) and body forces ($\boldsymbol{b} = 0$):

$$\partial_t(\rho\boldsymbol{v}) + \text{div}\,(\rho\boldsymbol{v}\otimes\boldsymbol{v}) + \nabla p = 0, \tag{5.1a}$$

$$\partial_t\tilde{\rho}_\alpha + \text{div}(\tilde{\rho}_\alpha\boldsymbol{v}) = 0. \tag{5.1b}$$

The system satisfies the energy law (3.2) with $\mathscr{D} = 0$. This may be written in the local form

$$\partial_t\left(\Psi + \overline{\mathscr{K}}\right) + \text{div}\left(\left(\Psi + \overline{\mathscr{K}}\right)\boldsymbol{v}\right) = 0. \tag{5.2}$$

REMARK 5.1 *(Derivation energy law). The energy law (5.2) follows directly from (5.1) by multiplying with the appropriate weights. In this regard, we note the following identities:*

$$\sum_\alpha \frac{\partial\Psi}{\partial\tilde{\rho}_\alpha}\left(\partial_t\tilde{\rho}_\alpha + div(\tilde{\rho}_\alpha\boldsymbol{v})\right) = \partial_t\Psi + div(\Psi\boldsymbol{v}) + pdiv\boldsymbol{v}, \tag{5.3a}$$

https://doi.org/10.1017/jfm.2026.11366 Published online by Cambridge University Press

$$\sum_\alpha \left(-\frac{1}{2}|\boldsymbol{v}|^2 \left(\partial_t \tilde{\rho}_\alpha + div(\tilde{\rho}_\alpha \boldsymbol{v})\right)\right) = -\frac{1}{2}|\boldsymbol{v}|^2 \left(\partial_t \rho + div(\rho \boldsymbol{v})\right), \tag{5.3b}$$

$$\boldsymbol{v} \cdot \left(\partial_t(\rho \boldsymbol{v}) + div(\rho \boldsymbol{v} \otimes \boldsymbol{v}) + \nabla p\right) = \partial_t \overline{\mathscr{K}} + div(\overline{\mathscr{K}} \boldsymbol{v}) + \boldsymbol{v} \cdot \nabla p + \frac{1}{2}|\boldsymbol{v}|^2 \left(\partial_t \rho + div(\rho \boldsymbol{v})\right). \tag{5.3c}$$

REMARK 5.2 *(Energy law for non-smooth solutions). In case of shocks or other regularities the stability condition takes the form*

$$\partial_t \left(\Psi + \overline{\mathscr{K}}\right) + div\left(\left(\Psi + \overline{\mathscr{K}} + p\right)\boldsymbol{v}\right) \leqslant 0. \tag{5.4}$$

which may be established using vanishing-viscosity solutions.

In order to analyse the wave speeds of the model, we deduce the evolution equations of the partial pressures from (5.1*b*), i.e.

$$\partial_t p_\alpha + \boldsymbol{v} \cdot \nabla p_\alpha + \sum_\beta \tilde{\rho}_\beta a_{\alpha\beta}^2 \mathrm{div}\boldsymbol{v} = 0, \tag{5.5a}$$

where the speed of sound quantities $a_{\alpha\beta}$ account for the interaction between constituents:

$$a_{\alpha\beta}^2 := \frac{\partial p_\alpha}{\partial \tilde{\rho}_\beta}. \tag{5.6}$$

The evolution of the classical mixture pressure results from the superposition of the constituent pressure equations

$$\partial_t p + \boldsymbol{v} \cdot \nabla p + \rho a^2 \mathrm{div}\boldsymbol{v} = 0, \tag{5.7}$$

where the mixture speed of sound a satisfies

$$\rho a^2 = \sum_\beta \tilde{\rho}_\beta a_\beta^2, \tag{5.8}$$

and the constituent speed of sound quantities are given by

$$a_\beta^2 = \frac{\partial p}{\partial \tilde{\rho}_\beta} = \sum_\alpha a_{\alpha\beta}^2. \tag{5.9}$$

REMARK 5.3 *(Speed of sound compressible two-phase models). The explicit dependence of the free energy on each constituent (see (3.4)) is reflected in the definitions of the sound speeds a_β and $a_{\alpha\beta}$. This approach contrasts with the sound speed definitions typically employed in compressible two-phase flow models (e.g. Baer & Nunziato 1986). In the absence of interaction forces (cf. Remark 4.4), the relation reduces to $a_\beta^2 = \mathrm{d}p_\beta/\mathrm{d}\tilde{\rho}_\beta$, where the standard definition in those models is $a_\beta^2 = \mathrm{d}p_\beta/\mathrm{d}\rho_\beta$.*

5.2. *Hyperbolic structure*

In the following we analyse the hyperbolic structure of the first-order model

$$\partial_t \boldsymbol{v} + \boldsymbol{v} \cdot \nabla \boldsymbol{v} + \rho^{-1} \nabla p = 0, \tag{5.10a}$$

$$\partial_t p_\alpha + \boldsymbol{v} \cdot \nabla p_\alpha + \sum_\beta \tilde{\rho}_\beta a_{\alpha\beta}^2 \mathrm{div}\boldsymbol{v} = 0, \tag{5.10b}$$

https://doi.org/10.1017/jfm.2026.11366 Published online by Cambridge University Press

where the momentum equation is a direct consequence from (5.1). In this section we consider the one-dimensional case $d = 1$ for conciseness and refer to Appendix D for dimension $d = 3$. We consider the case $a_{\alpha\beta}, a_\beta, a > 0$. We write the system (5.10) in the matrix-vector form

$$\partial_t \boldsymbol{W} + \boldsymbol{A}\partial_x \boldsymbol{W} = 0, \tag{5.11}$$

where

$$\boldsymbol{W} = \begin{bmatrix} p_1 \\ \vdots \\ p_N \\ v \end{bmatrix}, \quad \boldsymbol{A} = \begin{bmatrix} v & 0 & \dots & & 0 & \sum_\beta \tilde{\rho}_\beta a_{1\beta}^2 \\ 0 & v & 0 & \dots & 0 & \sum_\beta \tilde{\rho}_\beta a_{2\beta}^2 \\ \vdots & \ddots & \ddots & \ddots & \vdots & \vdots \\ 0 & \dots & 0 & v & 0 & \sum_\beta \tilde{\rho}_\beta a_{(N-1)\beta}^2 \\ 0 & \dots & & 0 & v & \sum_\beta \tilde{\rho}_\beta a_{N\beta}^2 \\ \rho^{-1} & & \dots & & \rho^{-1} & v \end{bmatrix}. \tag{5.12}$$

The system admits $N + 1$ eigenvalues:

$$\lambda_1 = v - a < \lambda_2 = \dots = \lambda_N = v < \lambda_{N+1} = v + a. \tag{5.13}$$

The corresponding right eigenvectors are

$$\boldsymbol{r}_1 = \begin{bmatrix} -\sum_\beta \tilde{\rho}_\beta a_{1\beta}^2 \\ \vdots \\ -\sum_\beta \tilde{\rho}_\beta a_{N\beta}^2 \\ a \end{bmatrix}, \ \boldsymbol{r}_2 = \begin{bmatrix} -1 \\ 1 \\ 0 \\ \vdots \\ 0 \end{bmatrix}, \ \boldsymbol{r}_3 = \begin{bmatrix} -1 \\ 0 \\ 1 \\ 0 \\ \vdots \\ 0 \end{bmatrix}, \dots, \ \boldsymbol{r}_N = \begin{bmatrix} -1 \\ 0 \\ \vdots \\ 0 \\ 1 \\ 0 \end{bmatrix},$$
$$\boldsymbol{r}_{N+1} = \begin{bmatrix} \sum_\beta \tilde{\rho}_\beta a_{1\beta}^2 \\ \vdots \\ \sum_\beta \tilde{\rho}_\beta a_{N\beta}^2 \\ a \end{bmatrix}, \tag{5.14}$$

and the left eigenvectors are

$$\boldsymbol{l}_1 = \begin{bmatrix} -\dfrac{1}{2\rho a^2} \\ \vdots \\ -\dfrac{1}{2\rho a^2} \\ \dfrac{1}{2a} \end{bmatrix}, \ \boldsymbol{l}_2 = \begin{bmatrix} -\dfrac{\sum_\beta \tilde{\rho}_\beta a_{2\beta}^2}{\sum_\beta \tilde{\rho}_\beta \left(a_{1\beta}^2 + a_{2\beta}^2\right)} \\ \dfrac{\sum_\beta \tilde{\rho}_\beta a_{1\beta}^2}{\sum_\beta \tilde{\rho}_\beta \left(a_{1\beta}^2 + a_{2\beta}^2\right)} \\ 0 \\ \vdots \\ 0 \end{bmatrix}, \ \boldsymbol{l}_3 = \begin{bmatrix} -\dfrac{\sum_\beta \tilde{\rho}_\beta a_{3\beta}^2}{\sum_\beta \tilde{\rho}_\beta \left(a_{1\beta}^2 + a_{3\beta}^2\right)} \\ 0 \\ \dfrac{\sum_\beta \tilde{\rho}_\beta a_{1\beta}^2}{\sum_\beta \tilde{\rho}_\beta \left(a_{1\beta}^2 + a_{3\beta}^2\right)} \\ 0 \\ \vdots \\ 0 \end{bmatrix}, \dots, \tag{5.15}$$

https://doi.org/10.1017/jfm.2026.11366 Published online by Cambridge University Press

$$\boldsymbol{l}_N = \begin{bmatrix} -\dfrac{\sum_\beta \tilde{\rho}_\beta a_{N\beta}^2}{\sum_\beta \tilde{\rho}_\beta \left(a_{1\beta}^2 + a_{N\beta}^2\right)} \\ 0 \\ \vdots \\ 0 \\ \dfrac{\sum_\beta \tilde{\rho}_\beta a_{1\beta}^2}{\sum_\beta \tilde{\rho}_\beta \left(a_{1\beta}^2 + a_{N\beta}^2\right)} \\ 0 \end{bmatrix}, \quad \boldsymbol{l}_{N+1} = \begin{bmatrix} \dfrac{1}{2\rho a^2} \\ \vdots \\ \dfrac{1}{2\rho a^2} \\ \dfrac{1}{2a} \end{bmatrix}. \tag{5.16}$$

The eigenvectors are scaled so that $\boldsymbol{r}_j \cdot \boldsymbol{l}_j = 1$ for all $j = 1, \ldots, N+1$. Both right and left eigenvectors are linearly independent and span $\mathbb{R}^{N+1}$. This implies that the system is hyperbolic if the eigenvalues are real valued, which holds when $a_{\alpha\beta}^2 > 0$ for all $\alpha, \beta = 1, \ldots, N$.

REMARK 5.4 *(Van der Waals equation of state). The van der Waals equation of state does not, in general, guarantee that $a_{\alpha\beta}^2 > 0$, and consequently, the resulting system is not hyperbolic.*

PROPOSITION 5.5 *(Structure of the waves). The characteristic fields associated with eigenvalues λ_j, $j = 2, \ldots, N$ are linearly degenerate (i.e. $\boldsymbol{r}_j \cdot \partial\lambda_j/\partial\boldsymbol{W} = 0$), and those associated with eigenvalues λ_j, $j = 1, N+1$ are genuinely nonlinear (i.e. $\boldsymbol{r}_j \cdot \partial\lambda_j/\partial\boldsymbol{W} \neq 0$).*

This means that fields associated with eigenvalues λ_j, $j = 2, \ldots, N$ correspond to contact discontinuities, whereas fields associated with eigenvalues λ_j, $j = 1, N+1$ correspond to shock or rarefaction waves, respectively.

Proof. A direct computation shows that the fields associated with eigenvalues λ_j, $j = 2, \ldots, N$ are linearly degenerate (i.e. $\boldsymbol{r}_j \cdot \partial\lambda_j/\partial\boldsymbol{W} = 0$).

Next we focus on the field associated with eigenvalues λ_j, $j = 1, N+1$. We have

$$\boldsymbol{r}_1 \cdot \partial\lambda_1/\partial\boldsymbol{W} = \boldsymbol{r}_{N+1} \cdot \partial\lambda_{N+1}/\partial\boldsymbol{W} = a + \sum_{\alpha\beta} \frac{\partial a}{\partial p_\alpha} \tilde{\rho}_\beta a_{\alpha\beta}^2. \tag{5.17}$$

Next we note that, for an arbitrary variable ω, we have

$$\frac{\partial a}{\partial \omega} = \frac{1}{2a\rho}\left(\frac{\partial(\rho a^2)}{\partial \omega} - a^2 \frac{\partial \rho}{\partial \omega}\right). \tag{5.18}$$

Applying this identity for $\omega = p_\alpha$ and substituting (5.8) and (5.9) yields

$$\begin{aligned} \frac{\partial a}{\partial p_\alpha} &= \frac{1}{2a\rho}\left(\sum_{\gamma\tau} \frac{\partial(\tilde{\rho}_\tau a_{\gamma\tau}^2)}{\partial p_\alpha} - a^2 \sum_\tau \frac{\partial \tilde{\rho}_\tau}{\partial p_\alpha}\right) \\ &= \frac{1}{2a\rho}\left(\sum_{\tau\gamma} \tilde{\rho}_\tau \frac{\partial a_{\gamma\tau}^2}{\partial p_\alpha} + \sum_{\tau\gamma} a_{\gamma\tau}^2 \left(a^2\right)_{\tau\alpha}^{-1} - a^2 \sum_\tau \left(a^2\right)_{\tau\alpha}^{-1}\right) \\ &= \frac{1}{2a\rho}\left(\sum_\tau \tilde{\rho}_\tau \frac{\partial a_\tau^2}{\partial p_\alpha} + 1 - a^2 \sum_\tau \left(a^2\right)_{\tau\alpha}^{-1}\right). \end{aligned} \tag{5.19}$$

https://doi.org/10.1017/jfm.2026.11366 Published online by Cambridge University Press

Inserting into (5.17) gives

$$\begin{aligned}\boldsymbol{r}_1 \cdot \partial\lambda_1/\partial \boldsymbol{W} &= \boldsymbol{r}_{N+1} \cdot \partial\lambda_{N+1}/\partial \boldsymbol{W} \\ &= a + \sum_{\alpha\beta} \frac{\partial a}{\partial p_\alpha} \tilde{\rho}_\beta a_{\alpha\beta}^2 \\ &= a + \frac{1}{2a\rho} \sum_{\alpha\beta} \tilde{\rho}_\beta a_{\alpha\beta}^2 \left(\sum_\tau \tilde{\rho}_\tau \frac{\partial a_\tau^2}{\partial p_\alpha} + 1 - a^2 \sum_\tau \left(a^2\right)_{\tau\alpha}^{-1} \right) \\ &= a + \frac{1}{2a\rho} \left(\sum_{\alpha\beta\tau} \tilde{\rho}_\beta a_{\alpha\beta}^2 \tilde{\rho}_\tau \frac{\partial a_\tau^2}{\partial p_\alpha} + \sum_{\alpha\beta} \tilde{\rho}_\beta a_{\alpha\beta}^2 - a^2 \sum_\tau \tilde{\rho}_\tau \right) \\ &= a + \frac{1}{2a\rho} \sum_{\alpha\beta\tau} \tilde{\rho}_\beta a_{\alpha\beta}^2 \tilde{\rho}_\tau \frac{\partial a_\tau^2}{\partial p_\alpha}, \end{aligned} \tag{5.20}$$

which is strictly positive by the aforementioned assumption $a_{\alpha\beta}, a > 0$ in combination with noting that the phase speed of sound increases with the pressure $\partial a_\tau/\partial p_\alpha > 0$ (see also Murrone & Guillard (2005) for a similar assumption). □

5.3. *Riemann invariants and jump conditions*

Next, we derive the Riemann invariants of the first-order system (5.1).

PROPOSITION 5.6. *The Riemann invariants associated with the various waves are*

$$\lambda_1: \quad \left\{ \{Y_\alpha\}_{\alpha\neq\beta}\,,\, v + \int_p \frac{1}{\rho a} dp \right\}, \tag{5.21a}$$

$$\lambda_2, \ldots, \lambda_N: \quad \{v,\, p\}\,, \tag{5.21b}$$

$$\lambda_{N+1}: \quad \left\{ \{Y_\alpha\}_{\alpha\neq\beta}\,,\, v - \int_p \frac{1}{\rho a} dp \right\}, \tag{5.21c}$$

for some fixed $\beta \in \{1, \ldots, N\}$.

Proof. To find the Riemann invariants, we seek for ω_i such that $\partial_{\boldsymbol{W}} \omega_i \cdot \boldsymbol{r}_j = 0$. Focusing on the Riemann invariants associated with λ_1, we have

$$0 = \frac{\partial \omega_i}{\partial \boldsymbol{W}} \cdot \boldsymbol{r}_1 = a \frac{\partial \omega_i}{\partial v} - \sum_\beta \tilde{\rho}_\beta a_\beta^2 \frac{\partial \omega_i}{\partial p_\beta}. \tag{5.22}$$

A direct computation reveals that $Y_\alpha = \tilde{\rho}_\alpha/\rho$ are Riemann invariants:

$$\begin{aligned}\frac{\partial Y_\alpha}{\partial \boldsymbol{W}} \cdot \boldsymbol{r}_1 &= -\sum_\beta \tilde{\rho}_\beta a_\beta^2 \frac{\partial Y_\alpha}{\partial p_\beta} \\ &= -\frac{1}{\rho} \sum_\beta \tilde{\rho}_\beta a_\beta^2 \frac{\partial \tilde{\rho}_\alpha}{\partial p_\beta} + \frac{\tilde{\rho}_\alpha}{\rho^2} \sum_\beta \tilde{\rho}_\beta a_\beta^2 \frac{\partial \rho}{\partial p_\beta} \\ &= -\frac{1}{\rho} \tilde{\rho}_\alpha + \frac{\tilde{\rho}_\alpha}{\rho^2} \sum_\beta \tilde{\rho}_\beta \\ &= 0. \end{aligned} \tag{5.23}$$

https://doi.org/10.1017/jfm.2026.11366 Published online by Cambridge University Press

Next, we verify that $v + \int_p (1/\rho a)\mathrm{d}p$ is the final Riemann invariant:

$$\begin{aligned}\frac{\partial v + \int_p \frac{1}{\rho a}\mathrm{d}p}{\partial \boldsymbol{W}} \cdot \boldsymbol{r}_1 &= a\frac{\partial v + \int_p \frac{1}{\rho a}\mathrm{d}p}{\partial v} - \sum_\alpha \tilde{\rho}_\alpha a_\alpha^2 \frac{\partial v + \int_p \frac{1}{\rho a}\mathrm{d}p}{\partial p_\alpha} \\ &= a - \sum_\alpha \tilde{\rho}_\alpha a_\alpha^2 \frac{\partial \int_p \frac{1}{\rho a}\mathrm{d}p}{\partial p_\alpha} \\ &= a - \sum_\alpha \tilde{\rho}_\alpha a_\alpha^2 \frac{1}{\rho a} \\ &= 0. \end{aligned} \tag{5.24}$$

In a similar fashion we find that the Riemann invariants associated with λ_{N+1} are Y_α, $\alpha = 1, \ldots, N$ and $v - \int_p (1/\rho a)\mathrm{d}p$. Finally, we compute the Riemann invariants associated with $\lambda_2, \ldots, \lambda_N$:

$$0 = \frac{\partial \omega_i}{\partial \boldsymbol{W}} \cdot \boldsymbol{r}_j = -\frac{\partial \omega_i}{\partial p_1} + \frac{\partial \omega_i}{\partial p_j} \quad \text{for } j = 2, \ldots, N. \tag{5.25}$$

This is equivalent to

$$\frac{\partial \omega_i}{\partial p_1} = \ldots = \frac{\partial \omega_i}{\partial p_N}. \tag{5.26}$$

It is now easy to verify that $\omega_i = v$, p solve system (5.26). □

Finally, we note that the conservative nature of the system permits us to uniquely define shock waves due to the Rankine–Hugoniot conditions, i.e.

$$\left[\tilde{\rho}_\alpha (v - \sigma)\right] = 0, \quad \alpha = 1, \ldots, N, \tag{5.27a}$$

$$\left[\rho v (v - \sigma) + p\right] = 0, \tag{5.27b}$$

with $[\phi] = \phi_R - \phi_L$ the jump between the left and right states of the shock wave and σ the speed of the shock wave.

6. Binary mixtures

In this section we restrict to binary mixtures ($\alpha = 1, 2$) for which we discuss alternative – equivalent – forms. The model (4.2) takes for binary mixtures the following form:

$$\partial_t(\rho \boldsymbol{v}) + \mathrm{div}\,(\rho \boldsymbol{v} \otimes \boldsymbol{v}) + \tilde{\rho}_1 \nabla \hat{\mu}_1 + \tilde{\rho}_2 \nabla \hat{\mu}_2 - \mathrm{div}\,(\nu(2\boldsymbol{D} + \lambda(\mathrm{div}\boldsymbol{v})\boldsymbol{I})) - \rho \boldsymbol{g} = 0, \tag{6.1a}$$

$$\partial_t \tilde{\rho}_1 + \mathrm{div}(\tilde{\rho}_1 \boldsymbol{v}) - \mathrm{div}\left(M\nabla\left(\hat{\mu}_1 - \hat{\mu}_2\right)\right) + m\left(\hat{\mu}_1 - \hat{\mu}_2\right) = 0, \tag{6.1b}$$

$$\partial_t \tilde{\rho}_2 + \mathrm{div}(\tilde{\rho}_2 \boldsymbol{v}) - \mathrm{div}\left(M\nabla\left(\hat{\mu}_2 - \hat{\mu}_1\right)\right) + m\left(\hat{\mu}_2 - \hat{\mu}_1\right) = 0. \tag{6.1c}$$

Here $M = -M_{12} = -M_{21} = M_{11} = M_{22}$ and $m = -m_{12} = -m_{21} = m_{11} = m_{22}$. By means of variable transformation, we may express the model in terms of the standard mixture quantities. The diffusive fluxes and mass-transfer terms constitute a single quantity by means of the balance conditions (2.11) and (2.18*a*):

$$\hat{\zeta} := \hat{\zeta}_1 - \hat{\zeta}_2, \qquad \hat{\zeta}_1 = \frac{1}{2}\hat{\zeta}, \qquad \hat{\zeta}_2 = -\frac{1}{2}\hat{\zeta}, \tag{6.2a}$$

$$\hat{\boldsymbol{H}} := \hat{\boldsymbol{H}}_1 - \hat{\boldsymbol{H}}_2, \qquad \hat{\boldsymbol{H}}_1 = \frac{1}{2}\hat{\boldsymbol{H}}, \qquad \hat{\boldsymbol{H}}_2 = -\frac{1}{2}\hat{\boldsymbol{H}}. \tag{6.2b}$$

https://doi.org/10.1017/jfm.2026.11366 Published online by Cambridge University Press

Additionally, we introduce a mass-fraction order parameter

$$Y := Y_1 - Y_2, \qquad Y_1 = \frac{1+Y}{2}, \qquad Y_2 = \frac{1-Y}{2}, \tag{6.3}$$

and deduce the relation for the density of the mixture ρ:

$$\frac{2}{\rho} = \frac{Y_1}{\tilde{\rho}_1} + \frac{Y_2}{\tilde{\rho}_2} = \frac{1}{\tilde{\rho}_1}\frac{1+Y}{2} + \frac{1}{\tilde{\rho}_2}\frac{1-Y}{2}, \tag{6.4a}$$

$$\tilde{\rho}_1 = \rho\frac{1+Y}{2}, \quad \tilde{\rho}_2 = \rho\frac{1-Y}{2}, \quad \rho = \tilde{\rho}_1 + \tilde{\rho}_2, \quad Y = \frac{\tilde{\rho}_1 - \tilde{\rho}_2}{\tilde{\rho}_1 + \tilde{\rho}_2}. \tag{6.4b}$$

Furthermore, expressing the model solely in terms of mixture quantities requires the conversion of the component chemical potential quantities. To this purpose, we define

$$\hat{\mu}_\rho = \frac{\partial\hat{\Psi}}{\partial\rho} - \mathrm{div}\frac{\partial\hat{\Psi}}{\partial\nabla\rho}, \tag{6.5a}$$

$$\hat{\mu}_Y = \frac{\partial\hat{\Psi}}{\partial Y} - \mathrm{div}\frac{\partial\hat{\Psi}}{\partial\nabla Y}. \tag{6.5b}$$

Additionally, we introduce the following identities.

LEMMA 6.1 *(Transformation identities). The component chemical potential quantities may be expressed in mixture quantities by means of the identities:*

$$\tilde{\rho}_1\nabla\hat{\mu}_1 + \tilde{\rho}_2\nabla\hat{\mu}_2 = \rho\nabla\hat{\mu}_\rho - \hat{\mu}_Y\nabla Y, \tag{6.6a}$$

$$\hat{\mu}_1 - \hat{\mu}_2 = 2\frac{\hat{\mu}_Y}{\rho}. \tag{6.6b}$$

Proof. See Lemma B.2. □

Applying the variable transformation (6.4) and the identities of Lemma 6.1 provides

$$\partial_t(\rho\boldsymbol{v}) + \mathrm{div}\,(\rho\boldsymbol{v}\otimes\boldsymbol{v}) + \rho\nabla\hat{\mu}_\rho - \hat{\mu}_Y\nabla Y - \mathrm{div}\,(\nu(2\boldsymbol{D} + \lambda(\mathrm{div}\boldsymbol{v})\boldsymbol{I})) - \rho\boldsymbol{g} = 0, \tag{6.7a}$$

$$\partial_t\rho + \mathrm{div}(\rho\boldsymbol{v}) = 0, \tag{6.7b}$$

$$\partial_t(\rho Y) + \mathrm{div}(\rho Y\boldsymbol{v}) - \mathrm{div}\left(\hat{M}\nabla\frac{\hat{\mu}_Y}{\rho}\right) + \hat{m}\frac{\hat{\mu}_Y}{\rho} = 0, \tag{6.7c}$$

where $\hat{M} = 4M$ and $\hat{m} = 4m$. Identifying $\hat{\Psi}(\tilde{\rho}_1, \nabla\tilde{\rho}_1, \tilde{\rho}_2, \nabla\tilde{\rho}_2) \equiv \breve{\Psi}(\rho, \nabla\rho, Y, \nabla Y)$ so that $\hat{\mu}\rho = \breve{\mu}\rho$ and $\hat{\mu}_Y = \breve{\mu}_Y$, and setting $\hat{M} = \breve{M}$, reveals that (6.7) matches with the models derived in Appendix C.

Furthermore, the model may be expressed using a mass-measured free energy $\hat{\psi} = \rho^{-1}\hat{\Psi}$. For this purpose, we introduce the chemical potentials

$$\hat{v}_\rho = \frac{\partial\hat{\psi}}{\partial\rho} - \frac{1}{\rho}\mathrm{div}\left(\rho\frac{\partial\hat{\psi}}{\partial\nabla\rho}\right), \tag{6.8a}$$

$$\hat{v}_Y = \frac{\partial\hat{\psi}}{\partial Y} - \frac{1}{\rho}\mathrm{div}\left(\rho\frac{\partial\hat{\Psi}}{\partial\nabla Y}\right), \tag{6.8b}$$

https://doi.org/10.1017/jfm.2026.11366 Published online by Cambridge University Press

which are related to (6.5) via $\hat{\mu}_\rho = \rho\hat{v}_\rho + \hat{\psi}$ and $\hat{\mu}_Y = \rho\hat{v}_Y$ (see also the proof of Proposition C.2). Inserting these provides the alternative formulation:

$$\partial_t(\rho\boldsymbol{v}) + \operatorname{div}(\rho\boldsymbol{v}\otimes\boldsymbol{v}) + \rho\nabla(\rho\hat{v}_\rho + \hat{\psi}) - \rho\hat{v}_Y\nabla Y - \operatorname{div}(\nu(2\boldsymbol{D} + \lambda(\operatorname{div}\boldsymbol{v})\boldsymbol{I})) - \rho\boldsymbol{g} = 0, \tag{6.9a}$$

$$\partial_t\rho + \operatorname{div}(\rho\boldsymbol{v}) = 0, \tag{6.9b}$$

$$\partial_t(\rho Y) + \operatorname{div}(\rho Y\boldsymbol{v}) - \operatorname{div}\left(\hat{M}\nabla\hat{v}_Y\right) + \hat{m}\hat{v}_Y = 0. \tag{6.9c}$$

This formulation aligns with the model derived in Appendix C.2 through the identification $\hat{\psi}(\tilde{\rho}_1, \nabla\tilde{\rho}_1, \tilde{\rho}_2, \nabla\tilde{\rho}_2) \equiv \breve{\psi}(\rho, \nabla\rho, Y, \nabla Y)$, which implies that $\hat{v}_\rho = \breve{\mu}_\rho$ and $\hat{v}_Y = \breve{\mu}_Y$, and additionally identifying $\hat{M} = \breve{M}$.

7. Connections to existing models

This section aims to establish connections with existing models. Driven by showing parallels between models, we primarily focus on models with the same number of equations. In § 7.1 we compare with established compressible two-phase models, in § 7.2 we examine links to phase-field models for binary fluids and in § 7.3 we highlight similarities with an N-phase incompressible model.

7.1. *Compressible multiphase models*

In this subsection we compare with compressible multiphase three-equation models in (7.1.1) and with the Baer-Nunziato model in (7.1.2). For a more complete overview of compressible multiphase models, we refer to the review paper of Saurel & Pantano (2018).

7.1.1. *Three equations models*

Motivated by revealing similarities between models, here we describe the connection of the first-order system (5.1) to existing three-equation compressible two-phase models.

The model of Dumbser (2011) describing a two-phase flow scenario with phase 1 a liquid phase and phase 2 a gas phase, is given by (the model of Dumbser (2011) contains an additional term that represents gravitational forces; in this comparison we consider the version without this term):

$$\partial_t(\rho_1\phi_1\boldsymbol{v}) + \operatorname{div}(\rho_1\phi_1\boldsymbol{v}\otimes\boldsymbol{v}) + \nabla\breve{p}_1 = 0, \tag{7.1a}$$

$$\partial_t(\rho_1\phi_1) + \operatorname{div}(\rho_1\phi_1\boldsymbol{v}) = 0, \tag{7.1b}$$

$$\partial_t\phi_1 + \boldsymbol{v}\cdot\nabla\phi_1 = 0. \tag{7.1c}$$

The unknowns are the specific density of phase 1, ρ_1, the volume fraction of phase 1, ϕ_1, the velocity $\boldsymbol{v}$ and the pressure of phase 1, p_1. This pressure is given by the equation of state of the form $\breve{p}_1 = \breve{p}_1(\rho_1)$ for which a Tait equation of state is employed. We compare this model to the binary version of the first-order system (5.1), i.e.

$$\partial_t(\rho\boldsymbol{v}) + \operatorname{div}(\rho\boldsymbol{v}\otimes\boldsymbol{v}) + \nabla p = 0, \tag{7.2a}$$

$$\partial_t\tilde{\rho}_1 + \operatorname{div}(\tilde{\rho}_1\boldsymbol{v}) = 0. \tag{7.2b}$$

$$\partial_t\tilde{\rho}_2 + \operatorname{div}(\tilde{\rho}_2\boldsymbol{v}) = 0, \tag{7.2c}$$

with unknowns $\tilde{\rho}_1$, $\tilde{\rho}_2$, $\boldsymbol{v}$ and $p = p(\tilde{\rho}_1, \tilde{\rho}_2)$. We observe the following similarities and differences between the models.

https://doi.org/10.1017/jfm.2026.11366 Published online by Cambridge University Press

(i) Structure equations: the mass balance equation of phase 1 is present in both models: (7.1*b*) and (7.2*b*). In contrast, the momentum equations differ in the sense that (7.1*a*) represents the momentum balance of phase 1, whereas (7.2*a*) describes the momentum balance of the mixture. We remark that (7.1) contains a single (specific) density (ρ_1), for which one might argue that this quantity represents the mixture density (and may be denoted as ρ). Finally, we note that (7.2*b*) may be written as

$$\partial_t \phi_1 + \boldsymbol{v} \cdot \boldsymbol{\nabla} \phi_1 = -\frac{\phi_1}{\rho_1}(\partial_t \rho_1 + \operatorname{div}(\rho_1 \boldsymbol{v})), \tag{7.3}$$

where the right-hand side is non-zero in general, showing that it is incompatible with (7.1*c*).

(ii) Symmetry: model (7.1) is not symmetric with respect to the phases in the sense that it contains mass and momentum balance equations with respect to phase 1, but not of phase 2. Of course, the evolution equation (7.1*c*) is symmetric due to the saturation constraint $\phi_1 + \phi_2 = 1$.

(iii) Conservative structure: in contrast to (7.2), the model (7.1) is of a non-conservative type due to the interface evolution equation (7.1*c*).

(iv) Energy law: model (7.2) satisfies the energy law (3.2) with $\mathscr{D} = 0$. No energy law is provided for (7.1).

(v) Equation of state: the equations of state of the models, $\breve{p}_1 = \breve{p}_1(\rho_1)$ for model (7.1) and $p = p(\tilde{\rho}_1, \tilde{\rho}_2)$ for model (7.2), differ in two key aspects:

  (a) their dependency on a single constituent density quantity versus dependency on each constituent density quantity,
  (b) the particular form of this/these density quantity/quantities, i.e. specific constituent density versus partial constituent densities.

(vi) Speed of sound: similarly as the equations of state, the constituent speed of sound of the models, $a_1^2 = \mathrm{d}_{\rho_1} \breve{p}_1$ for model (7.1) and $a_{\alpha\beta}^2 = \partial_{\tilde{\rho}_\beta} p_\alpha$ for model (7.2), differ in two key aspects:

  (a) their dependency on a single constituent density quantity versus dependency on each constituent density quantity,
  (b) the particular form of this/these density quantity/quantities, i.e. specific constituent density versus partial constituent densities.

(vii) Eigenvalues: the eigenvalues of (7.1) coincide with those of the first-order system (5.1).

(viii) Hyperbolicity: due to the adoption of the Tait equation of state in (7.1), this model is hyperbolic when $\rho_1 > 0$ and $\phi_1 > 0$, whereas the system (5.1) is hyperbolic when $a_{\alpha\beta}^2 > 0$ for all $\alpha, \beta = 1, 2$.

(ix) Riemann invariants: for model (5.1), these are given in (5.21), while for the model (7.1), these are not provided.

(x) Rankine–Hugoniot conditions: for model (5.1), these are given in (5.27), due to the non-conservative nature of model (7.1) these are not well defined.

Next, we study the similarity of model (5.1) with that of Daude *et al.* (2023), which is given by

$$\partial_t(\rho \boldsymbol{v}) + \operatorname{div}(\rho \boldsymbol{v} \otimes \boldsymbol{v}) + \boldsymbol{\nabla} \breve{p} = 0, \tag{7.4a}$$

$$\partial_t(\rho_\alpha \phi_\alpha) + \operatorname{div}(\rho_\alpha \phi_\alpha \boldsymbol{v}) = 0 \quad \text{for } \alpha = 1, 2, 3, \tag{7.4b}$$

https://doi.org/10.1017/jfm.2026.11366 Published online by Cambridge University Press

where the unknowns are $\boldsymbol{v}$, ϕ_α, ρ_α, $\alpha = 1, 2, 3$ and p. These quantities are connected through the equations of state $\breve{p}_\alpha = \breve{p}_\alpha(\rho_\alpha)$ in which the constituent pressures $\breve{p}_\alpha$ are assumed individually equal and equal to the mixture pressure $\breve{p}_1 = \breve{p}_2 = \breve{p}_3 = \breve{p}$. We compare this model to the ternary version of the first-order system (5.1), i.e.

$$\partial_t(\rho \boldsymbol{v}) + \operatorname{div}(\rho \boldsymbol{v} \otimes \boldsymbol{v}) + \nabla p = 0, \tag{7.5a}$$

$$\partial_t \tilde{\rho}_\alpha + \operatorname{div}(\tilde{\rho}_\alpha \boldsymbol{v}) = 0 \quad \text{for } \alpha = 1, 2, 3, \tag{7.5b}$$

with unknowns $\tilde{\rho}_\alpha$, $\alpha = 1, 2, 3$, $\boldsymbol{v}$ and p and the equation of state $p = p(\{\tilde{\rho}_\alpha\}_{\alpha=1,2,3})$. We observe the following similarities and differences between the models.

(i) Structure equations: through the identity $\tilde{\rho}_\alpha = \rho_\alpha \phi_\alpha$ we observe that the form of the equations of (7.4) and (7.5) is identical.

(ii) Symmetry: both model (7.4) and model (7.5) are symmetrical with respect to the phases.

(iii) Conservative structure: both model (7.4) and model (7.5) are conservative.

(iv) Energy law: for smooth solutions, model (7.4) satisfies the energy law

$$\partial_t(\rho u) + \operatorname{div}(\rho u \boldsymbol{v} + \breve{p} \boldsymbol{v}) = 0, \tag{7.6}$$

where $\rho u = \sum \tilde{\rho}_\alpha u_\alpha$, $u_\alpha = \epsilon_\alpha + |\boldsymbol{v}|^2/2$ and $\mathrm{d}\epsilon_\alpha/\mathrm{d}\rho_\alpha = p_\alpha/\rho_\alpha^2 = \breve{p}/\rho_\alpha^2$ for some constituent energy quantity ϵ_α. On the other hand, (7.2) satisfies the energy law (3.2) with $\mathscr{D} = 0$. This may be written in the local form

$$\partial_t(\rho \psi) + \operatorname{div}(\rho \psi \boldsymbol{v} + p \boldsymbol{v}) = 0. \tag{7.7}$$

(v) Equation of state: we observe the following similarities and differences regarding pressure quantities.

  (a) Both models contain constituent pressure quantities and a single mixture pressure quantity.

  (b) The constituent pressure quantities of the models, $\breve{p}_\alpha = \breve{p}_\alpha(\rho_\alpha)$ for model (7.4) and $p_\alpha(\{\tilde{\rho}_\beta\}_{\beta=1,2,3})$ for model (7.5), differ in two aspects:

    (bi) their dependency on a single constituent density quantity versus dependency on each constituent density quantity,

    (bii) the particular form of this/these density quantity/quantities, i.e. specific constituent density versus partial constituent densities.

  (c) The mixture pressure $\breve{p}$ of (7.4) assumes a mechanical equilibrium, i.e.

$$\breve{p} = \breve{p}_1 = \breve{p}_2 = \breve{p}_3, \tag{7.8}$$

  whereas the mixture pressure p of model (7.5) is given by Dalton's law:

$$p = p_1 + p_2 + p_3. \tag{7.9}$$

(vi) Speed of sound: We observe the following similarities and differences regarding speed of sound quantities.

  (a) Both models contains both constituent speed of sound quantities and a single mixture speed of sound quantity.

  (b) The constituent speed of sound quantities of the models, $\hat{a}_\alpha^2 = \mathrm{d}_{\rho_\alpha} \breve{p}_\alpha$ for model (7.4) and $a_{\alpha\beta}^2 = \partial_{\tilde{\rho}_\beta} p_\alpha$ for model (7.5), differ in two aspects:

https://doi.org/10.1017/jfm.2026.11366 Published online by Cambridge University Press

(bi) their dependency on a single constituent density quantity versus dependency on each constituent density quantity,

(bii) the particular form of this/these density quantity/quantities, i.e. specific constituent density versus partial constituent densities.

(c) The mixture speed of sound $\hat{a}$ of (7.4) satisfies the Wood formula

$$\frac{1}{\rho\hat{a}^2} = \sum_{\alpha=1,2,3} \frac{\phi_\alpha}{\rho_\alpha \hat{a}_\alpha^2}, \tag{7.10}$$

whereas the mixture speed of sound a of model (7.5) is given by

$$\rho a^2 = \sum_{\alpha,\beta=1,2,3} \tilde{\rho}_\beta a_{\alpha\beta}^2. \tag{7.11}$$

(vii) Eigenvalues: the eigenvalues of (7.4) and of (7.5) and of the same form, i.e.

$$\lambda_1 = v - \bar{a}, \quad \lambda_{2,3} = v, \quad \lambda_4 = v + \bar{a}, \tag{7.12}$$

with $\bar{a} = \hat{a}$ for (7.4) and $\bar{a} = a$ for (7.5).

(viii) Hyperbolicity: the models (7.4) and (7.5) are hyperbolic when the speeds of sound are positive.

(ix) Riemann invariants: the Riemann invariants associated with the various waves of the models (7.4) and (7.5) are of the same form, i.e.

$$\lambda_1: \quad \left\{ Y_1,\, Y_2,\, v + \int_p \frac{1}{\rho\bar{a}} \mathrm{d}p \right\}, \tag{7.13a}$$

$$\lambda_2,\, \lambda_3: \quad \{v,\, p\}, \tag{7.13b}$$

$$\lambda_4: \quad \left\{ Y_1,\, Y_2,\, v - \int_p \frac{1}{\rho\bar{a}} \mathrm{d}p \right\}, \tag{7.13c}$$

with $\bar{a} = \hat{a}$ for (7.4) and $\bar{a} = a$ for (7.5).

(x) Rankine–Hugoniot conditions: the Rankine–Hugoniot conditions of both model (7.4) and model (7.5) are well defined and match, i.e.

$$\left[\tilde{\rho}_\alpha (v - \sigma)\right] = 0, \quad \alpha = 1,\, 2,\, 3, \tag{7.14a}$$

$$\left[\rho v (v - \sigma) + \bar{p}\right] = 0, \tag{7.14b}$$

with $\bar{p} = \breve{p}$ for model (7.4) and $\bar{p} = p$ for model (7.5), where we recall the jump $[\phi] = \phi_R - \phi_L$ and the speed of the shock wave σ.

REMARK 7.1 *(Numerical difficulties Wood formula). The Wood formula (7.10) has a non-monotonic variation with volume fraction ϕ_α. In Saurel et al. (2009) it is argued that this causes numerical difficulties due to inaccuracies in wave transmission across interfaces.*

We provide an overview of the comparison in table 1.

https://doi.org/10.1017/jfm.2026.11366 Published online by Cambridge University Press

	Proposed model	Dumbser (2011)	Daude *et al.* (2023)
Number of phases	N	2	3
Symmetric w.r.t. phases	$\surd$	✗	$\surd$
Conservative model	$\surd$	✗	$\surd$
Energy law	$\surd$	✗	$\surd$
Mixture density	$\rho = \sum_\alpha \tilde{\rho}_\alpha$	Not defined	$\rho = \sum_\alpha \tilde{\rho}_\alpha$
Phase pressure	$p_\alpha = p_\alpha(\{\tilde{\rho}_\beta\})$	$p_1 = p_1(\rho_1)$	$p_\alpha = p_\alpha(\rho_\alpha)$
Mixture pressure	$p = \sum_\alpha p_\alpha$	Not defined	$\breve{p} = \breve{p}_1 = \breve{p}_2 = \breve{p}_3$
Phase speed of sound	$a_{\alpha\beta}^2 = \partial_{\tilde{\rho}_\beta} p_\alpha$	$a_1^2 = \partial_{\rho_1} p_1$	$a_\alpha^2 = \partial_{\rho_\alpha} p_\alpha$
Mixture speed of sound	$\rho a^2 = \sum_{\alpha\beta} \tilde{\rho}_\beta a_{\alpha\beta}^2$	Not defined	$(\rho a^2)^{-1} = \sum_\alpha \phi_\alpha (\rho_\alpha a_\alpha^2)^{-1}$
Eigenvalues	$v - a, v, \dots, v, v + a$	$v - \hat{a}, v, v, v + \hat{a}$	$v - \hat{a}, v, v, v + \hat{a}$
Riemann invariants	See (5.21)	Not given	See (7.13)
# mass balance laws	N	1	3
# momentum balance laws	1	1	1
# VOF type equations	0	1	0
Underlying theory/model	Continuum mixture theory	Baer-nunziato model	Not given

Table 1. Comparison of the first-order versions of the three compressible models with three equations (for binary fluids).

7.1.2. *The BN model*

Due to its importance, we consider here the seven-equation two-fluid model of Baer & Nunziato (1986) with the source terms

$$\partial_t \phi_\alpha + \boldsymbol{v}_I \cdot \nabla \phi_\alpha = \Phi_\alpha, \tag{7.15a}$$

$$\partial_t (\phi_\alpha \rho_\alpha) + \operatorname{div}(\phi_\alpha \rho_\alpha \boldsymbol{v}_\alpha) = \Gamma_\alpha, \tag{7.15b}$$

$$\partial_t (\phi_\alpha \rho_\alpha \boldsymbol{v}_\alpha) + \operatorname{div}\big(\phi_\alpha (\rho_\alpha \boldsymbol{v}_\alpha \otimes \boldsymbol{v}_\alpha + \breve{p}_\alpha \boldsymbol{I})\big) - p_I \nabla \phi_\alpha = \boldsymbol{m}_\alpha + \Gamma_\alpha \boldsymbol{v}_I, \tag{7.15c}$$

$$\partial_t (\phi_\alpha \rho_\alpha e_\alpha) + \operatorname{div}\big(\phi_\alpha (\rho_\alpha e_\alpha + \breve{p}_\alpha) \boldsymbol{v}_\alpha\big) - p_I \, \boldsymbol{v}_I \cdot \nabla \alpha_\alpha = Q_\alpha + \boldsymbol{m}_\alpha \cdot \boldsymbol{v}_I + \Gamma_\alpha H_I - p_I \Phi_\alpha, \tag{7.15d}$$

for $\alpha = 1, 2$. The right-hand side are the source terms with Φ_α the source term for the volume-fraction equation, Γ_α the mass-transfer term, $\boldsymbol{m}_\alpha$ the drag effect, Q_α the interfacial heat transfer and H_I an interfacial enthalpy variable. These source terms add up to zero: $\Phi_1 + \Phi_2 = 0$, $\Gamma_1 + \Gamma_2 = 0$, $\boldsymbol{M}_1 + \boldsymbol{M}_2 = 0$ and $Q_1 + Q_2 = 0$. We refer for alternative formulations of the source terms to Guillard & Labois (2006) and Zein, Hantke & Warnecke (2010). Furthermore, $\boldsymbol{v}_I = \boldsymbol{v}_I(\boldsymbol{v}_1, \boldsymbol{v}_2)$ and $p_I = p_I(\breve{p}_1, \breve{p}_2)$ are interfacial velocity and pressure quantities. The energies e_α are given by $e_\alpha = \epsilon_\alpha + (1/2)\|\boldsymbol{v}_\alpha\|^2$, where $\epsilon_\alpha = \epsilon_\alpha(\rho_\alpha, \breve{p}_\alpha)$ are the internal energies. The volume fractions are assumed to add up to unity, i.e. $\phi_1 + \phi_2 = 1$, and as such (7.15*a*) represents a single equation, making the total number of equations seven. The seven unknowns of this system are ϕ_1, ρ_1, ρ_2, $\breve{p}_1$, $\breve{p}_2$, $\boldsymbol{v}_1$, $\boldsymbol{v}_2$ and the internal energies then follow from the two equations of state, $\epsilon_1 = \epsilon_1(\rho_1, \breve{p}_1)$ and $\epsilon_2 = \epsilon_2(\rho_2, \breve{p}_2)$.

REMARK 7.2 *(Extensions of BN models). The BN framework admits extensions that incorporate viscous stresses and heat conduction, generalisations to N-fluid mixtures and surface tension effects; see ,e.g. Saurel & Pantano (2018). Since most formulations in the literature concern the classical inviscid two-fluid (seven-equation) system (7.15), we confine the discussion here to that setting.*

https://doi.org/10.1017/jfm.2026.11366 Published online by Cambridge University Press

We compare to the binary, first-order (inviscid) formulation of our model without gravity, but with mass transfer, i.e.

$$\partial_t(\rho \boldsymbol{v}) + \operatorname{div}(\rho \boldsymbol{v} \otimes \boldsymbol{v}) + \boldsymbol{\nabla} p = 0, \tag{7.16a}$$

$$\partial_t \tilde{\rho}_1 + \operatorname{div}(\tilde{\rho}_1 \boldsymbol{v}) = \zeta_1 = -m_{11}\hat{\mu}_1 - m_{12}\hat{\mu}_2, \tag{7.16b}$$

$$\partial_t \tilde{\rho}_2 + \operatorname{div}(\tilde{\rho}_2 \boldsymbol{v}) = \zeta_2 = -m_{21}\hat{\mu}_1 - m_{22}\hat{\mu}_2, \tag{7.16c}$$

with chemical potential $\hat{\mu}_\alpha = \partial\Psi/\partial\tilde{\rho}_\alpha$ and mixture pressure $p = p(\tilde{\rho}_1, \tilde{\rho}_2) = \sum_{\beta=1,2}(\hat{\mu}_\beta\tilde{\rho}_\beta) - \hat{\Psi}$ which reduces to $p = \sum_{\alpha=1,2,\beta=1,2}\tilde{\rho}_\alpha\tilde{\rho}_\beta(\partial\hat{\psi}_\beta/\partial\tilde{\rho}_\alpha)$ with $\hat{\Psi}_\beta = \tilde{\rho}_\beta\hat{\psi}_\beta$.

We observe the following differences and similarities:

(i) Structure equations: as is common in compressible two-phase flow models, the model of Baer & Nunziato (1986) contains an evolution equation of the volume fraction. Equation (7.15*a*) does not appear here in the proposed model (7.16), as detailed in (7.3). Next, the mass balance equations of the BN model may be written as

$$\partial_t \tilde{\rho}_1 + \operatorname{div}(\tilde{\rho}_1 \boldsymbol{v}) + \operatorname{div}(\tilde{\rho}_1 \boldsymbol{w}_1) = \Gamma_1, \tag{7.17a}$$

$$\partial_t \tilde{\rho}_2 + \operatorname{div}(\tilde{\rho}_2 \boldsymbol{v}) + \operatorname{div}(\tilde{\rho}_2 \boldsymbol{w}_2) = \Gamma_2, \tag{7.17b}$$

which reveal that the difference lies in (i) the presence of the peculiar velocity $\boldsymbol{w}_\alpha$, defined in (2.9); and (ii) possibly the mass-transfer terms. In order to compare the momentum equations, we add (7.15*c*) for $\alpha = 1, 2$ and find that

$$\partial_t(\rho \boldsymbol{v}) + \operatorname{div}(\rho \boldsymbol{v} \otimes \boldsymbol{v}) + \operatorname{div}\left(\sum_\alpha \phi_\alpha \rho_\alpha \boldsymbol{w}_\alpha \otimes \boldsymbol{w}_\alpha\right) + \boldsymbol{\nabla}\left(\sum_\alpha \phi_\alpha \breve{p}_\alpha\right) = 0. \tag{7.18}$$

The difference due of the models regarding the terms with the peculiar velocities in the mass and momentum equations is standard when comparing models with multiple momentum equations with models with a single momentum equation; see, e.g. ten Eikelder *et al.* (2023). Apart from this term, the mass balance equations and momentum equations coincide between the two models when p coincides with $\sum_\alpha \phi_\alpha \breve{p}_\alpha$. This holds for the perfect gas equation of state. In this regard we recall (4.7*b*) and refer to the discussion on the equation of state below. The absence of energy equations in the proposed model (7.16) is due to the isothermal assumption.

(ii) Symmetry: the symmetry of model (7.15) depends on the form of the source terms and the interfacial quantities $\boldsymbol{v}_I$ and p_I. Usually the source terms Φ_α, Γ_α, $\boldsymbol{m}_\alpha$ and Q_α are symmetric with respect to the phases (i.e. a renumbering does not change the model). However, this does not always hold for the interfacial quantities $\boldsymbol{v}_I$ and p_I. Namely, typical choices for these quantities include single phase values, i.e. $\boldsymbol{v}_I = \boldsymbol{v}_1$ or $\boldsymbol{v}_I = \boldsymbol{v}_2$ and $p_I = \breve{p}_1$ or $p_I = \breve{p}_2$; see Zein *et al.* (2010).

(iii) Conservative structure: we consider the systems without source terms. In contrast to the conservative model (7.2), the BN model (7.15) is of a non-conservative term in (i) to the interface evolution (7.15*a*), (ii) the momentum equation (7.15*c*), and (iii) the energy equation (7.15*d*). As mentioned in the introduction, these non-conservative terms vanish across genuinely nonlinear waves.

(iv) Energy/entropy law: the BN model (7.15) satisfies a mixture entropy law; see, e.g. Zein *et al.* (2010). The energy-dissipation law (3.2) (with $\mathscr{D} = 0$) of model (7.16) also follows from the second law of thermodynamics for isothermal mixtures with a single momentum equation.

https://doi.org/10.1017/jfm.2026.11366 Published online by Cambridge University Press

(v) Equation of state: a key distinction between the models lies in their equations of state. Clearly, the equation of state of the (7.15) model is of the form $\epsilon_\alpha = \epsilon_\alpha(\breve{p}_\alpha, \rho_\alpha)$, whereas in the (7.16) model the barotropic equation of state $p = p(\tilde{\rho}_1, \tilde{\rho}_2)$ is adopted. Other key differences are:

(a) their dependency on single constituent quantities (in the BN model (7.15)) versus dependency on quantities of each constituent (in the proposed model (7.16)),
(b) the particular form of density quantity/quantities, i.e. specific constituent density (in the BN model (7.15)) versus partial constituent densities (in the proposed model (7.16)).

To emphasise the structural parallels between the BN model (7.15) and the proposed model (7.16), we restrict attention to the case

$$\hat{\Psi}_\alpha = \hat{\Psi}_\alpha(\tilde{\rho}_\alpha), \tag{7.19}$$

which encompasses the perfect gas equation of state but excludes, for example, the van der Waals equation of state. In this setting, the constituent pressure becomes

$$p_\alpha = \tilde{\rho}_\alpha^2 \frac{\partial \hat{\psi}_\alpha}{\partial \tilde{\rho}_\alpha}. \tag{7.20}$$

Hence, this quantity is of the form $p_\alpha = \phi_\alpha \bar{p}_\alpha$, which closely resembles the pressure quantity $\phi_\alpha \breve{p}_\alpha$ in the BN model (7.15). Moreover, when the perfect gas equation of state is adopted the pressures match. For the BN model (7.15), the constituent perfect gas equation of state is represented by $\breve{p}_\alpha = R_\alpha \theta \rho_\alpha$, where the constituent perfect gas equation of state in the proposed model (7.16) is $p_\alpha = R_\alpha \theta \tilde{\rho}_\alpha$, with R_α the specific gas constant of constituent α. In this case we find that

$$p_\alpha = \phi_\alpha \breve{p}_\alpha. \tag{7.21}$$

(vi) Speed of sound: we observe the following similarities and differences regarding speed of sound quantities.

(a) Both models contain constituent speed of sound quantities, for model (7.15),

$$\breve{a}_\alpha^2 = \rho_\alpha^{-1} (\partial_{\breve{p}_\alpha} \breve{\epsilon}_\alpha)^{-1} \left(\frac{p_\alpha}{\rho_\alpha} - \rho_\alpha \partial_{\rho_\alpha} \breve{\epsilon}_\alpha \right) \tag{7.22}$$

and $a_\beta^2 = \partial_{\tilde{\rho}_\beta} p = \sum_\alpha a_{\alpha\beta}^2$, $a_{\alpha\beta}^2 = \partial_{\tilde{\rho}_\beta} p_\alpha$ for model (7.16), which differ in three aspects:

(ai) their dependency on a single constituent density quantity versus dependency on each constituent density quantity,
(aii) the particular form of this/these density quantity/quantities, i.e. specific constituent density versus partial constituent densities,
(aiii) the form of the equation due to the isothermal assumption in the proposed model (7.16).

(b) The mixture speed of sound of model (7.15) is not defined/applicable, whereas the mixture speed of sound a of model (7.16) is given by

$$\rho a^2 = \sum_{\beta=1,2} \tilde{\rho}_\beta a_\beta^2 = \sum_{\alpha,\beta=1,2} \tilde{\rho}_\beta a_{\alpha\beta}^2. \tag{7.23}$$

https://doi.org/10.1017/jfm.2026.11366 Published online by Cambridge University Press

(vii) Eigenvalues: the number of eigenvalues in one spatial dimension of the two systems is different due to the number of equations; for model (7.15), we have $\lambda_1 = v_I$, $\lambda_{2,4} = v_1 \pm c_1$, $\lambda_3 = v_1$, $\lambda_{5,7} = v_2 \pm c_2$, $\lambda_6 = v_2$, whereas those of the proposed model (7.16) are $\lambda_{1,3} = v \pm c$ and $\lambda_2 = v$.

(viii) Hyperbolicity: when the speed of sounds are positive, the proposed model (7.16) is hyperbolic and the BN model (7.15) is hyperbolic if additionally $v_I \neq v_1, v_2$. This property is sometimes called 'weakly hyperbolic'; see, e.g. Coquel *et al.* (2017).

(ix) Mass transfer: the symmetry and vanishing-sum conditions on $m_{\alpha\beta}$ yield the following mass-transfer terms:

$$\hat{\zeta}_1 = -m_{12}\,(\hat{\mu}_1 - \hat{\mu}_2), \tag{7.24}$$

$$\hat{\zeta}_2 = -m_{12}\,(\hat{\mu}_2 - \hat{\mu}_1). \tag{7.25}$$

In contrast, the BN model (7.15) typically expresses mass transfer in the form

$$\Gamma_1 = -c_{12}(\breve{g}_1 - \breve{g}_2), \tag{7.26}$$

$$\Gamma_2 = -c_{12}(\breve{g}_2 - \breve{g}_1), \tag{7.27}$$

where the quantity c has the dependency $c = c(\tilde{\rho}_1, \tilde{\rho}_2)$ and where

$$\breve{g}_\alpha = \epsilon_\alpha - \theta_\alpha \eta_\alpha + \frac{\breve{p}_\alpha}{\rho_\alpha}, \tag{7.28}$$

with θ_α the temperature and η_α the entropy of fluid α (see, e.g. Zein *et al.* 2010). These two formulations are, in general, not equivalent. Again, to highlight structural similarities between the BN model (7.15) and the proposed model (7.16), we restrict attention to the case (7.19). In this scenario we have the identities

$$\hat{\mu}_\alpha = \hat{\psi}_\alpha + \tilde{\rho}_\alpha \frac{\partial \hat{\psi}_\alpha}{\partial \tilde{\rho}_\alpha}, \tag{7.29}$$

$$\hat{p}_\alpha = \tilde{\rho}_\alpha^2 \frac{\partial \hat{\psi}_\alpha}{\partial \tilde{\rho}_\alpha}, \tag{7.30}$$

so that

$$\hat{\mu}_\alpha = \epsilon_\alpha - \theta_\alpha \eta_\alpha + \frac{p_\alpha}{\tilde{\rho}_\alpha}, \tag{7.31}$$

where we have inserted the Gibbs relation $\hat{\psi}_\alpha = \epsilon_\alpha - \theta_\alpha \eta_\alpha$. We can now identify $\hat{\mu}_\alpha$ with g_α when the constituent pressure satisfies $p_\alpha = \breve{p}_\alpha \phi_\alpha$; see (7.21). Finally, by identifying m_{12} with c_{12} one can obtain identical mass transfer in this case.

(x) Rankine–Hugoniot conditions: for model (7.16), these are given in (7.14), while for the BN model (7.15), these are

$$[\phi_\alpha] = 0, \tag{7.32a}$$

$$[\rho_\alpha (v_\alpha - \sigma)] = 0, \tag{7.32b}$$

$$\left[\rho_\alpha v_\alpha (v_\alpha - \sigma) + \breve{p}_\alpha\right] = 0, \tag{7.32c}$$

$$\left[\rho_\alpha e_\alpha (v_\alpha - \sigma) + \breve{p}_\alpha v_\alpha\right] = 0, \tag{7.32d}$$

for $\alpha = 1, 2$.

https://doi.org/10.1017/jfm.2026.11366 Published online by Cambridge University Press

7.2. *Phase-field models for binary fluids*

We show resemblance of model (6.1) with two existing binary fluid models in the literature. By using Lemma A.2, the model (6.7) converts into

$$\partial_t(\rho \boldsymbol{v}) + \operatorname{div}(\rho \boldsymbol{v} \otimes \boldsymbol{v}) + \nabla \check{p} + \operatorname{div}\left(\nabla Y \otimes \frac{\partial \check{\Psi}}{\partial \nabla Y} + \nabla \rho \otimes \frac{\partial \check{\Psi}}{\partial \nabla \rho}\right) - \operatorname{div}(\nu(2\boldsymbol{D} + \lambda(\operatorname{div}\boldsymbol{v})\boldsymbol{I})) - \rho \boldsymbol{g} = 0, \tag{7.33a}$$

$$\partial_t \rho + \operatorname{div}(\rho \boldsymbol{v}) = 0, \tag{7.33b}$$

$$\partial_t(\rho Y) + \operatorname{div}(\rho Y \boldsymbol{v}) - \operatorname{div}\left(\hat{M} \nabla \frac{\hat{\mu}_Y}{\rho}\right) + \hat{m} \frac{\hat{\mu}_Y}{\rho} = 0, \tag{7.33c}$$

with $p = \rho \hat{\mu}_\rho - \hat{\Psi}$. By setting $\hat{m} = 0$ and inserting arbitrary source terms on the right-hand side of (7.33*b*) and (7.33*c*), the model coincides with that of Mukherjee & Gomez (2024).

Next, through the identification $\hat{\Psi} = \rho \hat{\psi}$, the model (6.9) converts into

$$\partial_t(\rho \boldsymbol{v}) + \operatorname{div}(\rho \boldsymbol{v} \otimes \boldsymbol{v}) + \nabla \hat{p} + \operatorname{div}\left(\rho \nabla Y \otimes \frac{\partial \hat{\psi}}{\partial \nabla Y} + \rho \nabla \rho \otimes \frac{\partial \hat{\psi}}{\partial \nabla \rho}\right) - \operatorname{div}(\nu(2\boldsymbol{D} + \lambda(\operatorname{div}\boldsymbol{v})\boldsymbol{I})) - \rho \boldsymbol{g} = 0, \tag{7.34a}$$

$$\partial_t \rho + \operatorname{div}(\rho \boldsymbol{v}) = 0, \tag{7.34b}$$

$$\partial_t(\rho Y) + \operatorname{div}(\rho Y \boldsymbol{v}) - \operatorname{div}\left(\hat{M} \nabla \hat{\nu}_Y\right) + \hat{m} \hat{\nu}_Y = 0, \tag{7.34c}$$

with $\hat{p} = \rho \hat{\mu}_\rho - \hat{\Psi}$. By setting $\hat{m} = 0$ and taking $\psi = \psi_0(\rho, Y) + \epsilon \|\nabla Y\|^2/2$, the model converts into the compressible Navier–Stokes Cahn–Hilliard model proposed in Lowengrub & Truskinovsky (1998), i.e.

$$\partial_t(\rho \boldsymbol{v}) + \operatorname{div}(\rho \boldsymbol{v} \otimes \boldsymbol{v}) + \nabla \check{p} + \operatorname{div}(\rho \nabla Y \otimes \nabla Y) - \operatorname{div}(\nu(2\boldsymbol{D} + \lambda(\operatorname{div}\boldsymbol{v})\boldsymbol{I})) - \rho \boldsymbol{g} = 0, \tag{7.35a}$$

$$\partial_t \rho + \operatorname{div}(\rho \boldsymbol{v}) = 0, \tag{7.35b}$$

$$\partial_t(\rho Y) + \operatorname{div}(\rho Y \boldsymbol{v}) - \operatorname{div}\left(\hat{M} \nabla \left(\frac{\partial \psi_0}{\partial Y} - \frac{\epsilon}{\rho} \operatorname{div}(\rho \nabla Y)\right)\right) = 0, \tag{7.35c}$$

with $\check{p} = \rho^2 \partial \psi_0 / \partial \rho$. We emphasise here that the dependence of $\check{\check{\psi}}$ on $\nabla \rho$ is not taken into account in Lowengrub & Truskinovsky (1998). In other words, in terms of gradient dependency, in Lowengrub & Truskinovsky (1998) depends on $\nabla Y = \nabla((\tilde{\rho}_1 - \tilde{\rho}_2)/(\tilde{\rho}_1 + \tilde{\rho}_2))$, whereas in (6.9) the free energy depends on $\nabla \tilde{\rho}_1$ and $\nabla \tilde{\rho}_2$.

REMARK 7.3 *(Matching first-order systems). The corresponding first-order systems of Mukherjee & Gomez (2024) and Lowengrub & Truskinovsky (1998) have not been analysed in those papers. However, differences between model (6.1) and those models vanish for first-order systems, meaning that the properties in § 5 directly carry over.*

We sketch an overview of the comparison of the binary models in table 2. The present model shares many structural similarities with the formulations of Lowengrub & Truskinovsky (1998) and Mukherjee & Gomez (2024), particularly at the first-order level, where distinctions largely arise from higher-order terms. Depending on the specific modelling choices (e.g. mobility), in some scenarios the differences may diminish as the interface thickness tends to zero; however, they remain relevant in problems with finite

https://doi.org/10.1017/jfm.2026.11366 Published online by Cambridge University Press

	Proposed model	Lowengrub & Truskinovsky (1998)	Mukherjee & Gomez (2024)
Number of phases	N	2	2
# mass balance laws	N	2	2
# momentum balance laws	1	1	1
Underlying theory/model	Continuum mixture theory	Not given	Not given
Symmetric w.r.t. phases	$\surd$	$\surd$	$\surd$
Mass transfer	$\surd$	✗	✗
Energy law	$\surd$	$\surd$	$\surd$/✗*
Constituent quantities	See § 4.2	Not defined	Not defined
First-order systems**	See § 5	See § 5	See § 5

Table 2. Comparison binary models. *The model of Mukherjee & Gomez (2024) is equipped with an energy law when the source terms in the model are set to zero. **The first-order systems match; see Remark 7.3.

interface thickness or non-trivial fluid mixtures, where the models can yield significantly different predictions.

7.3. *Incompressible N-phase flows*

We compare model (4.2) with the incompressible N-phase model given in ten Eikelder (2025), which reads, for phases (constituents) $\alpha = 1, \dots, N$,

$$\partial_t(\rho \boldsymbol{v}) + \operatorname{div}(\rho \boldsymbol{v} \otimes \boldsymbol{v}) + \sum_\beta \tilde{\rho}_\beta \nabla g_\beta - \operatorname{div}\left(\nu(2\nabla^s \boldsymbol{v} + \bar{\lambda}(\operatorname{div}\boldsymbol{v})\boldsymbol{I})\right) - \rho \boldsymbol{b} = 0, \quad (7.36a)$$

$$\partial_t \tilde{\rho}_\alpha + \operatorname{div}(\tilde{\rho}_\alpha \boldsymbol{v}) + \operatorname{div} \breve{\boldsymbol{H}}_\alpha - \breve{\zeta}_\alpha = 0, \quad (7.36b)$$

$$\operatorname{div}\boldsymbol{v} + \sum_\beta \rho_\beta^{-1} \nabla \cdot \breve{\boldsymbol{H}}_\beta - \sum_\beta \rho_\beta^{-1} \breve{\zeta}_\beta = 0, \quad (7.36c)$$

$$\breve{\boldsymbol{H}}_\alpha + \sum_\beta \breve{\boldsymbol{M}}_{\alpha\beta} \nabla g_\beta = 0, \quad (7.36d)$$

$$\breve{\zeta}_\alpha + \sum_\beta \breve{m}_{\alpha\beta} g_\beta = 0, \quad (7.36e)$$

with the chemical potential quantities

$$g_\alpha = \frac{\hat{\mu}_\alpha^\phi + \lambda}{\rho_\alpha}, \quad (7.37a)$$

$$\hat{\mu}_\alpha^\phi = \frac{\partial \hat{\psi}}{\partial \phi_\alpha} - \operatorname{div} \frac{\partial \hat{\psi}}{\partial \nabla \phi_\alpha}. \quad (7.37b)$$

Model (7.36) is incompressible in the sense that ρ_α is constant is time and space, i.e. $\rho_\alpha(\boldsymbol{x}, t) = \rho_\alpha$. As such, directly enforcing the saturation condition (2.5*b*) reveals that $\{\tilde{\rho}_\alpha(\boldsymbol{x}, t) = \rho_\alpha \phi_\alpha(\boldsymbol{x}, t)\}_{\alpha=1,\dots,N}$ constitute $N-1$ independent variables. Instead, formulation (7.36) enforces the saturation constraint through (7.36*c*), therefore avoiding ambiguities. The set of variables is completed, analogously to a single-phase system, with Lagrange multiplier λ that enforces (7.36*c*).

Obviously, since models (3.25) and (4.2) have largely been derived in a similar fashion, they both share key features: N mass balance laws, 1 momentum balance law and similar

https://doi.org/10.1017/jfm.2026.11366 Published online by Cambridge University Press

closure models for diffusive fluxes and mass-transfer terms. The key difference lies in the presence of (7.36*c*). This manifests itself in the form of the chemical potentials, namely $g_\alpha = \hat{\mu}_\alpha + \rho_\alpha^{-1}\lambda$. The model may be written into the form

$$\partial_t(\rho\boldsymbol{v}) + \operatorname{div}(\rho\boldsymbol{v}\otimes\boldsymbol{v}) + \nabla p + \operatorname{div}\left(\sum_\alpha \nabla\tilde{\rho}_\alpha \otimes \frac{\partial\hat{\Psi}}{\partial\nabla\tilde{\rho}_\alpha}\right) - \operatorname{div}(\nu(2\boldsymbol{D} + \lambda(\operatorname{div}\boldsymbol{v})\boldsymbol{I})) - \rho\boldsymbol{g} = 0, \tag{7.38a}$$

$$\partial_t\tilde{\rho}_\alpha + \operatorname{div}(\tilde{\rho}_\alpha\boldsymbol{v}) + \operatorname{div}\breve{\boldsymbol{H}}_\alpha - \breve{\zeta}_\alpha = 0, \tag{7.38b}$$

$$\operatorname{div}\boldsymbol{v} + \sum_\beta \rho_\beta^{-1}\nabla\cdot\breve{\boldsymbol{H}}_\beta - \sum_\beta \rho_\beta^{-1}\breve{\zeta}_\beta = 0, \tag{7.38c}$$

where $p = \lambda + \sum_\alpha \tilde{\rho}_\alpha\hat{\mu}_\alpha - \hat{\Psi}$, which closely resembles (3.25). This shows that the pressure in (7.38) is the superposition of the thermodynamical pressure $\sum_\alpha \tilde{\rho}_\alpha\hat{\mu}_\alpha - \hat{\Psi}$ and the Lagrange multiplier λ.

The observed strong connection is in line with expectations (just as for single-phase flow), reflecting the natural link between compressible and incompressible models. However, this does not hold for existing compressible two-phase flow models, where establishing their incompressible counterparts is not straightforward.

8. Conclusion

In this work we have developed a thermodynamical framework for compressible, isothermal N-phase mixtures. The framework is formulated within the principles of continuum mixture theory, which serves as a fundamental basis for modelling multi-physics systems. We have established some connections with existing phase-field and compressible two-phase flow models in an effort to help bridge the gap between these fields of research. Specifically, the proposed formulation extends the NSK model to multiple fluids and adapts the Navier–Stokes-Cahn–Hilliard/Allen–Cahn (NSCH/AC) models to general N-phase compressible mixtures. A key distinction from existing compressible two-phase flow models is that reducing the complexity of those models (i.e. using fewer equations) often leads to the loss or degradation of essential thermodynamic properties. In contrast, the framework proposed in this work maintains thermodynamic consistency regardless of its level of complexity.

Several open challenges remain for future research. We highlight some key directions. First, the framework offers a foundation for studying spinodal decomposition in compressible mixtures, with potential applications in phase-change problems such as evaporation and condensation. Second, by incorporating free energies with explicit interface width parameters, one can investigate sharp-interface limits, both formally and rigorously. Other important extensions include the incorporation of chemical reactions and non-isothermal effects. Furthermore, an essential avenue for future work, beyond the scope of this paper, is the development of efficient numerical schemes that accurately capture interfacial dynamics while preserving key thermodynamic properties.

Acknowledgements. The authors thank the reviewers for their constructive comments and suggestions.

Funding. MtE acknowledges support from the German Research Foundation (Deutsche Forschungsgemeinschaft, DFG) via project EI 1210/5-1, number 566600860. DS gratefully acknowledges support from the DFG via the Emmy Noether Award SCH 1249/2-1.

Declaration of interests. The authors report no conflict of interest.

https://doi.org/10.1017/jfm.2026.11366 Published online by Cambridge University Press

Appendix A. Identities Korteweg tensors

LEMMA A.1 *(Identity Korteweg stresses). We have the following identity for the pressure and Korteweg stresses:*

$$\nabla p + div\left(\sum_\alpha \nabla\tilde{\rho}_\alpha \otimes \frac{\partial\hat{\Psi}}{\partial\nabla\tilde{\rho}_\alpha}\right) = \sum_\alpha \tilde{\rho}_\alpha \nabla\hat{\mu}_\alpha. \tag{A1}$$

Here we recall that $p = \sum_\alpha \hat{\mu}_\alpha\tilde{\rho}_\alpha - \hat{\Psi}$.

Proof. This follows from the sequence of identities

$$\begin{aligned}
&\nabla p + \mathrm{div}\left(\sum_\alpha \nabla\tilde{\rho}_\alpha \otimes \frac{\partial\hat{\Psi}}{\partial\nabla\tilde{\rho}_\alpha}\right)\\
&= \nabla\left(\sum_\alpha \hat{\mu}_\alpha\tilde{\rho}_\alpha - \hat{\Psi}\right) + \sum_\alpha\left(\nabla\tilde{\rho}_\alpha \mathrm{div}\left(\frac{\partial\hat{\Psi}}{\partial\nabla\tilde{\rho}_\alpha}\right) + (\boldsymbol{H}\tilde{\rho}_\alpha)\frac{\partial\hat{\Psi}}{\partial\nabla\tilde{\rho}_\alpha}\right)\\
&= \sum_\alpha\left(\nabla\left(\hat{\mu}_\alpha\tilde{\rho}_\alpha\right) - \frac{\partial\hat{\Psi}}{\partial\tilde{\rho}_\alpha}\nabla\tilde{\rho}_\alpha - (\boldsymbol{H}\tilde{\rho}_\alpha)\frac{\partial\hat{\Psi}}{\partial\nabla\tilde{\rho}_\alpha} + \nabla\tilde{\rho}_\alpha \mathrm{div}\left(\frac{\partial\hat{\Psi}}{\partial\nabla\tilde{\rho}_\alpha}\right) + (\boldsymbol{H}\tilde{\rho}_\alpha)\frac{\partial\hat{\Psi}}{\partial\nabla\tilde{\rho}_\alpha}\right)\\
&= \sum_\alpha \tilde{\rho}_\alpha\nabla\hat{\mu}_\alpha,
\end{aligned} \tag{A2}$$

where $\boldsymbol{H}\tilde{\rho}_\alpha$ denotes the Hessian of the partial density $\tilde{\rho}_\alpha$. □

LEMMA A.2 *(Identity Korteweg stresses – binary fluids – volume measure). The following identity holds for the pressure and Korteweg stresses in binary fluids:*

$$\nabla\check{p} + div\left(\nabla Y \otimes \frac{\partial\check{\Psi}}{\partial\nabla Y} + \nabla\rho \otimes \frac{\partial\check{\Psi}}{\partial\nabla\rho}\right) = \rho\nabla\check{\mu}_\rho - \check{\mu}_Y\nabla Y. \tag{A3}$$

Here we recall that $\check{p} = \check{\mu}_\rho\rho - \check{\Psi}$.

Proof. This follows from the sequence of identities

$$\begin{aligned}
&\nabla\check{p} + \mathrm{div}\left(\nabla Y \otimes \frac{\partial\check{\Psi}}{\partial\nabla Y} + \nabla\rho \otimes \frac{\partial\check{\Psi}}{\partial\nabla\rho}\right)\\
&= \nabla(\check{\mu}_\rho\rho) - \nabla\check{\Psi} + \nabla Y \mathrm{div}\frac{\partial\check{\Psi}}{\partial\nabla Y} + (\boldsymbol{H}Y)\frac{\partial\check{\Psi}}{\partial\nabla Y} + \nabla\rho\mathrm{div}\frac{\partial\check{\Psi}}{\partial\nabla\rho} + (\boldsymbol{H}\rho)\frac{\partial\check{\Psi}}{\partial\nabla\rho}\\
&= \nabla(\check{\mu}_\rho\rho) - \nabla Y\frac{\partial\check{\Psi}}{\partial Y} - \nabla\rho\frac{\partial\check{\Psi}}{\partial\rho} + \nabla Y\mathrm{div}\frac{\partial\check{\Psi}}{\partial\nabla Y} + \nabla\rho\mathrm{div}\frac{\partial\check{\Psi}}{\partial\nabla\rho}\\
&= \rho\nabla\check{\mu}_\rho - \check{\mu}_Y\nabla Y,
\end{aligned} \tag{A4}$$

with $\boldsymbol{H}\rho$ and $\boldsymbol{H}Y$ the Hessians ρ and Y. □

LEMMA A.3 *(Identity Korteweg stresses – binary fluids – mass measure). The following identity holds for the pressure and Korteweg stresses in binary fluids:*

$$\nabla\check{\check{p}} + div\left(\nabla Y \otimes \rho\frac{\partial\check{\check{\psi}}}{\partial\nabla Y} + \nabla\rho \otimes \rho\frac{\partial\check{\psi}}{\partial\nabla\rho}\right) = \rho\nabla\left(\rho\check{\check{\mu}}_\rho + \check{\check{\psi}}\right) - \rho\check{\check{\mu}}_Y\nabla Y. \tag{A5}$$

https://doi.org/10.1017/jfm.2026.11366 Published online by Cambridge University Press

Here we recall that $\check{\check{p}} = \rho^2 \check{\check{\mu}}_\rho$.

Proof. This follows from the sequence of identities

$$\begin{aligned}
&\nabla \check{\check{p}} + \operatorname{div}\left(\nabla Y \otimes \rho \frac{\partial \check{\check{\psi}}}{\partial \nabla Y} + \nabla\rho \otimes \rho \frac{\partial \check{\psi}}{\partial \nabla \rho}\right) \\
&= \rho^2 \nabla \check{\check{\mu}}_\rho + 2\rho \check{\check{\mu}}_\rho \nabla\rho + \nabla Y \operatorname{div}\left(\rho \frac{\partial \check{\psi}}{\partial \nabla Y}\right) + (\boldsymbol{H}Y)\rho \frac{\partial \check{\psi}}{\partial \nabla Y} + \nabla\rho \operatorname{div}\left(\rho \frac{\partial \check{\check{\psi}}}{\partial \nabla \rho}\right) \\
&\quad + (\boldsymbol{H}\rho)\rho \frac{\partial \check{\check{\psi}}}{\partial \nabla \rho} \\
&= \rho^2 \nabla \check{\check{\mu}}_\rho + 2\rho \check{\check{\mu}}_\rho \nabla\rho - \rho \check{\check{\mu}}_\rho \nabla\rho + \rho \frac{\partial \check{\check{\psi}}}{\partial \rho} + \rho \nabla \check{\check{\psi}} - \rho \frac{\partial \check{\check{\psi}}}{\partial \rho} \nabla\rho - \rho \frac{\partial \check{\check{\psi}}}{\partial Y} \nabla Y - \rho \check{\check{\mu}}_Y \nabla Y \\
&\quad + \rho \frac{\partial \check{\check{\psi}}}{\partial Y} \nabla Y \\
&= \rho \nabla \left(\rho \check{\check{\mu}}_\rho + \check{\check{\psi}}\right) - \rho \check{\check{\mu}}_Y \nabla Y. \qquad \text{(A6)}
\end{aligned}$$

□

Appendix B. Variable transformation – binary mixture

In this section we provide details on the transformation of constituent quantities to mixture quantities for a binary mixture. The variable transformations are given by

$$\tilde{\rho}_1 = \rho \frac{1+Y}{2}, \quad \tilde{\rho}_2 = \rho \frac{1-Y}{2}, \quad \rho = \tilde{\rho}_1 + \tilde{\rho}_2, \quad Y = \frac{\tilde{\rho}_1 - \tilde{\rho}_2}{\tilde{\rho}_1 + \tilde{\rho}_2}. \qquad \text{(B1)}$$

The derivatives of the scalar quantities are

$$\frac{\partial \tilde{\rho}_1}{\partial \rho} = \frac{1+Y}{2}, \quad \frac{\partial \tilde{\rho}_2}{\partial \rho} = \frac{1-Y}{2}, \qquad \text{(B2}a\text{)}$$

$$\frac{\partial \tilde{\rho}_1}{\partial Y} = \frac{\rho}{2}, \quad \frac{\partial \tilde{\rho}_2}{\partial Y} = -\frac{\rho}{2}, \qquad \text{(B2}b\text{)}$$

$$\frac{\partial \rho}{\partial \tilde{\rho}_1} = 1, \quad \frac{\partial \rho}{\partial \tilde{\rho}_2} = 1, \qquad \text{(B2}c\text{)}$$

$$\frac{\partial Y}{\partial \tilde{\rho}_1} = \frac{2\tilde{\rho}_2}{(\tilde{\rho}_1 + \tilde{\rho}_2)^2}, \quad \frac{\partial Y}{\partial \tilde{\rho}_2} = -\frac{2\tilde{\rho}_1}{(\tilde{\rho}_1 + \tilde{\rho}_2)^2}. \qquad \text{(B2}d\text{)}$$

The derivatives of the gradient quantities are

$$\frac{\partial \nabla\rho}{\partial \tilde{\rho}_1} = \frac{\partial \nabla\rho}{\partial \tilde{\rho}_2} = 0, \qquad \text{(B3}a\text{)}$$

$$\frac{\partial \nabla Y}{\partial \tilde{\rho}_1} = -4\frac{\tilde{\rho}_2}{(\tilde{\rho}_1 + \tilde{\rho}_2)^3} \nabla\tilde{\rho}_1 + 2\frac{\tilde{\rho}_1 - \tilde{\rho}_2}{(\tilde{\rho}_1 + \tilde{\rho}_2)^3} \nabla\tilde{\rho}_2, \qquad \text{(B3}b\text{)}$$

$$\frac{\partial \nabla Y}{\partial \tilde{\rho}_2} = 2\frac{\tilde{\rho}_1 - \tilde{\rho}_2}{(\tilde{\rho}_1 + \tilde{\rho}_2)^3} \nabla\tilde{\rho}_1 + 4\frac{\tilde{\rho}_1}{(\tilde{\rho}_1 + \tilde{\rho}_2)^3} \nabla\tilde{\rho}_2. \qquad \text{(B3}c\text{)}$$

https://doi.org/10.1017/jfm.2026.11366 Published online by Cambridge University Press

LEMMA B.1 *(Relation Korteweg stresses). The Korteweg stresses are related via*

$$\nabla\tilde{\rho}_1 \otimes \frac{\partial\hat{\Psi}}{\partial\nabla\tilde{\rho}_1} + \nabla\tilde{\rho}_2 \otimes \frac{\partial\hat{\Psi}}{\partial\nabla\tilde{\rho}_2} = \nabla\rho \otimes \frac{\partial\breve{\Psi}}{\partial\nabla\rho} + \nabla Y \otimes \frac{\partial\breve{\Psi}}{\partial\nabla Y}. \tag{B4}$$

Proof. The chain rule and the variable transformations (B2) provide

$$\nabla\tilde{\rho}_1 = \frac{1+Y}{2}\nabla\rho + \frac{\rho}{2}\nabla Y, \tag{B5a}$$

$$\nabla\tilde{\rho}_2 = \frac{1-Y}{2}\nabla\rho - \frac{\rho}{2}\nabla Y. \tag{B5b}$$

Next, the chain rule and the variable transformations (B3) provide

$$\frac{\partial\hat{\Psi}}{\partial\nabla\tilde{\rho}_1} = \frac{\partial\breve{\Psi}}{\partial\nabla\rho} + \frac{\partial\breve{\Psi}}{\partial\nabla Y}\frac{1-Y}{\rho}, \tag{B6a}$$

$$\frac{\partial\hat{\Psi}}{\partial\nabla\tilde{\rho}_2} = \frac{\partial\breve{\Psi}}{\partial\nabla\rho} - \frac{\partial\breve{\Psi}}{\partial\nabla Y}\frac{1+Y}{\rho}. \tag{B6b}$$

Combining the above expressions gives

$$\begin{aligned}\nabla\tilde{\rho}_1 \otimes \frac{\partial\hat{\Psi}}{\partial\nabla\tilde{\rho}_1} = {} & \frac{1+Y}{2}\nabla\rho \otimes \frac{\partial\breve{\Psi}}{\partial\nabla\rho} + \frac{1-Y}{2}\nabla Y \otimes \frac{\partial\breve{\Psi}}{\partial\nabla Y} \\ & + \frac{1-Y^2}{2\rho}\nabla\rho \otimes \frac{\partial\breve{\Psi}}{\partial\nabla Y} + \frac{\rho}{2}\nabla Y \otimes \frac{\partial\breve{\Psi}}{\partial\nabla\rho},\end{aligned} \tag{B7a}$$

$$\begin{aligned}\nabla\tilde{\rho}_2 \otimes \frac{\partial\hat{\Psi}}{\partial\nabla\tilde{\rho}_2} = {} & \frac{1-Y}{2}\nabla\rho \otimes \frac{\partial\breve{\Psi}}{\partial\nabla\rho} + \frac{1+Y}{2}\nabla Y \otimes \frac{\partial\breve{\Psi}}{\partial\nabla Y} \\ & - \frac{1-Y^2}{2\rho}\nabla\rho \otimes \frac{\partial\breve{\Psi}}{\partial\nabla Y} - \frac{\rho}{2}\nabla Y \otimes \frac{\partial\breve{\Psi}}{\partial\nabla\rho}.\end{aligned} \tag{B7b}$$

The addition of these two identities provides the result. □

LEMMA B.2 *(Relations chemical potentials). The chemical potentials are related via*

$$\hat{\mu}_1\tilde{\rho}_1 + \hat{\mu}_2\tilde{\rho}_2 = \hat{\mu}_\rho\rho, \tag{B8a}$$

$$\tilde{\rho}_1\nabla\hat{\mu}_1 + \tilde{\rho}_2\nabla\hat{\mu}_2 = \rho\nabla\hat{\mu}_\rho - \hat{\mu}_Y\nabla Y, \tag{B8b}$$

$$\hat{\mu}_1 - \hat{\mu}_2 = 2\frac{\hat{\mu}_Y}{\rho}. \tag{B8c}$$

Proof. The first and third identity follow from the chain rule:

$$\hat{\mu}_\rho = \hat{\mu}_1\frac{\partial\tilde{\rho}_1}{\partial\rho} + \hat{\mu}_2\frac{\partial\tilde{\rho}_2}{\partial\rho} = \frac{1}{\rho}(\hat{\mu}_1\tilde{\rho}_1 + \hat{\mu}_2\tilde{\rho}_2), \tag{B9a}$$

$$\hat{\mu}_Y = \hat{\mu}_1\frac{\partial\tilde{\rho}_1}{\partial Y} + \hat{\mu}_2\frac{\partial\tilde{\rho}_2}{\partial Y} = \frac{\rho}{2}(\hat{\mu}_1 - \hat{\mu}_2). \tag{B9b}$$

Taking the gradient of the first identity yields

$$\hat{\mu}_1\nabla\tilde{\rho}_1 + \hat{\mu}_2\nabla\tilde{\rho}_2 + \tilde{\rho}_1\nabla\hat{\mu}_1 + \tilde{\rho}_2\nabla\hat{\mu}_2 = \hat{\mu}_\rho\nabla\rho + \rho\nabla\hat{\mu}_\rho. \tag{B10}$$

Noting the identity

$$\nabla\hat{\Psi} = \hat{\mu}_1\nabla\tilde{\rho}_1 + \hat{\mu}_2\nabla\tilde{\rho}_2 = \hat{\mu}_\rho\nabla\rho + \hat{\mu}_Y\nabla Y \tag{B11}$$

completes the proof. □

https://doi.org/10.1017/jfm.2026.11366 Published online by Cambridge University Press

Appendix C. Constitutive modelling binary mixture

This section presents alternative derivations of the modelling framework for binary fluids. In Appendix C.1 we detail the derivation using a volume-measure-based free energy (Ψ), while Appendix C.2 covers the derivation based on a mass-measure-based free energy (ψ), which are related via $\Psi = \rho\psi$. We utilise the system of balance laws (3.1) in mixture variables, i.e.

$$\partial_t \rho + \operatorname{div}(\rho \boldsymbol{v}) = 0, \tag{C1a}$$

$$\partial_t (\rho Y) + \operatorname{div}(\rho Y \boldsymbol{v}) + \operatorname{div} \boldsymbol{H} = \zeta, \tag{C1b}$$

$$\partial_t (\rho \boldsymbol{v}) + \operatorname{div} (\rho \boldsymbol{v} \otimes \boldsymbol{v}) - \operatorname{div} \boldsymbol{T} - \rho \boldsymbol{b} = 0, \tag{C1c}$$

$$\boldsymbol{T} - \boldsymbol{T}^T = 0, \tag{C1d}$$

with $Y = Y_1 - Y_2$, $\boldsymbol{H} = \boldsymbol{H}_1 - \boldsymbol{H}_2$ and $\zeta = \zeta_1 - \zeta_2$. In both cases we use the energy-dissipative design condition (3.2) where the energy is given in (3.3).

C.1. *Volume-measure free energy*

We postulate the free energy to pertain to the constitutive class

$$\Psi = \check{\Psi}(\rho, \nabla\rho, Y, \nabla Y), \tag{C2}$$

and introduce the chemical potentials

$$\check{\mu}_Y = \frac{\partial \check{\Psi}}{\partial Y} - \operatorname{div} \frac{\partial \check{\Psi}}{\partial \nabla Y}, \tag{C3a}$$

$$\check{\mu}_\rho = \frac{\partial \check{\Psi}}{\partial \rho} - \operatorname{div} \frac{\partial \check{\Psi}}{\partial \nabla \rho}. \tag{C3b}$$

We proceed with the evaluation of the evolution of the energy (C2). Following the same steps as in § 3.2, we apply the Reynolds transport theorem, the divergence theorem and subsequently expand the derivatives to find that

$$\frac{\mathrm{d}}{\mathrm{d}t} \int_{\mathcal{R}(t)} \check{\Psi} \,\mathrm{d}v = \int_{\mathcal{R}(t)} \frac{\partial \check{\Psi}}{\partial \rho} \dot{\rho} + \frac{\partial \check{\Psi}}{\partial \nabla \rho} \cdot \dot{\overline{\nabla \rho}} + \frac{\partial \check{\Psi}}{\partial Y} \dot{Y} + \frac{\partial \check{\Psi}}{\partial \nabla Y} \cdot \dot{\overline{\nabla Y}} + \check{\Psi} \operatorname{div} \boldsymbol{v} \,\mathrm{d}v, \tag{C4}$$

where we recall the notation

$$\dot{\overline{\nabla \omega}} := \partial_t \nabla \omega + \boldsymbol{v} \cdot \nabla (\nabla \omega) \tag{C5}$$

for the material derivative of the quantity $\nabla\omega$. By substituting the identity (3.8) for $\omega = Y$, ρ, and subsequently integrating by parts, we arrive at

$$\frac{\mathrm{d}}{\mathrm{d}t} \int_{\mathcal{R}(t)} \check{\Psi} \,\mathrm{d}v = \int_{\mathcal{R}(t)} \check{\mu}_\rho \dot{\rho} + \check{\mu}_Y \dot{Y} - \left(\nabla Y \otimes \frac{\partial \check{\Psi}}{\partial \nabla Y} + \nabla \rho \otimes \frac{\partial \check{\Psi}}{\partial \nabla \rho} \right) : \nabla \boldsymbol{v} + \check{\Psi} \operatorname{div} \boldsymbol{v} \,\mathrm{d}v$$
$$+ \int_{\partial \mathcal{R}(t)} \left(\dot{Y} \frac{\partial \check{\Psi}}{\partial \nabla Y} + \dot{\rho} \frac{\partial \check{\Psi}}{\partial \nabla \rho} \right) \cdot \boldsymbol{v} \,\mathrm{d}a. \tag{C6}$$

https://doi.org/10.1017/jfm.2026.11366 Published online by Cambridge University Press

Substituting the mass balance (C1a) and (C1b) and applying integration by parts leads to

$$\frac{\mathrm{d}}{\mathrm{d}t}\int_{\mathcal{R}(t)}\check{\Psi}\,\mathrm{d}v=\int_{\mathcal{R}(t)}-\check{\mu}_\rho\rho\mathrm{div}\boldsymbol{v}+\boldsymbol{\nabla}\left(\frac{\check{\mu}_Y}{\rho}\right)\cdot\boldsymbol{H}-\left(\boldsymbol{\nabla}\rho\otimes\frac{\partial\check{\Psi}}{\partial\boldsymbol{\nabla}\rho}+\boldsymbol{\nabla}Y\otimes\frac{\partial\check{\Psi}}{\partial\boldsymbol{\nabla}Y}\right):\boldsymbol{\nabla}\boldsymbol{v}$$
$$+\check{\Psi}\mathrm{div}\boldsymbol{v}+\left(\frac{\check{\mu}_Y}{\rho}\right)\zeta\,\mathrm{d}v+\int_{\partial\mathcal{R}(t)}\left(-\rho^{-1}\check{\mu}_Y\boldsymbol{H}+\dot{\rho}\frac{\partial\check{\Psi}}{\partial\boldsymbol{\nabla}\rho}+\dot{Y}\frac{\partial\check{\Psi}}{\partial\boldsymbol{\nabla}Y}\right)\cdot\boldsymbol{v}\mathrm{d}a. \tag{C7}$$

Taking the sum of (C7) and (3.12), we obtain

$$\frac{\mathrm{d}}{\mathrm{d}t}\mathscr{E}=\int_{\partial\mathcal{R}(t)}\left(\boldsymbol{v}^T\boldsymbol{T}-\rho^{-1}\check{\mu}_Y\boldsymbol{H}+\dot{Y}\frac{\partial\check{\Psi}}{\partial\boldsymbol{\nabla}Y}+\dot{\rho}\frac{\partial\check{\Psi}}{\partial\boldsymbol{\nabla}\rho}\right)\cdot\boldsymbol{v}\,\mathrm{d}a$$
$$-\int_{\mathcal{R}(t)}\left(\boldsymbol{T}+\check{\mu}_\rho\rho\mathrm{div}\boldsymbol{v}-\boldsymbol{\nabla}\left(\frac{\check{\mu}_Y}{\rho}\right)\cdot\boldsymbol{H}+\left(\boldsymbol{\nabla}Y\otimes\frac{\partial\check{\Psi}}{\partial\boldsymbol{\nabla}Y}+\boldsymbol{\nabla}\rho\otimes\frac{\partial\check{\Psi}}{\partial\boldsymbol{\nabla}\rho}\right):\boldsymbol{\nabla}\boldsymbol{v}\right.$$
$$\left.-\check{\Psi}\,\mathrm{div}\boldsymbol{v}-\left(\frac{\check{\mu}_Y}{\rho}\right)\zeta\right)\,\mathrm{d}v, \tag{C8}$$

in which we identify the rate of work and the dissipation as

$$\mathscr{W}=\int_{\partial\mathcal{R}(t)}\left(\boldsymbol{v}^T\boldsymbol{T}-\left(\frac{\check{\mu}_Y}{\rho}\right)\boldsymbol{H}+\dot{Y}\frac{\partial\check{\Psi}}{\partial\boldsymbol{\nabla}Y}+\dot{\rho}\frac{\partial\check{\Psi}}{\partial\boldsymbol{\nabla}\rho}\right)\cdot\boldsymbol{v}\,\mathrm{d}a, \tag{C9a}$$
$$\mathscr{D}=\int_{\mathcal{R}(t)}\left(\boldsymbol{T}+\boldsymbol{\nabla}Y\otimes\frac{\partial\check{\Psi}}{\partial\boldsymbol{\nabla}Y}+\boldsymbol{\nabla}\rho\otimes\frac{\partial\check{\Psi}}{\partial\boldsymbol{\nabla}\rho}+\left(\check{\mu}_\rho\rho-\check{\Psi}\right)\boldsymbol{I}\right):\boldsymbol{\nabla}\boldsymbol{v}$$
$$-\boldsymbol{\nabla}\left(\frac{\check{\mu}_Y}{\rho}\right)\cdot\boldsymbol{H}-\left(\frac{\check{\mu}_Y}{\rho}\right)\zeta\,\mathrm{d}v. \tag{C9b}$$

Due to the arbitrariness of the control volume, the energy-dissipation law holds when the local inequality is satisfied:

$$\left(\boldsymbol{T}+\boldsymbol{\nabla}Y\otimes\frac{\partial\check{\Psi}}{\partial\boldsymbol{\nabla}Y}+\boldsymbol{\nabla}\rho\otimes\frac{\partial\check{\Psi}}{\partial\boldsymbol{\nabla}\rho}+\left(\check{\mu}_\rho\rho-\check{\Psi}\right)\boldsymbol{I}\right):\boldsymbol{\nabla}\boldsymbol{v}-\boldsymbol{\nabla}\left(\frac{\check{\mu}_Y}{\rho}\right)\cdot\boldsymbol{H}-\left(\frac{\check{\mu}_Y}{\rho}\right)\zeta\geqslant 0. \tag{C10}$$

Based on the inequality (C10), we now restrict ourselves to stress tensors $\boldsymbol{T}$, diffusive fluxes $\boldsymbol{h}$ and mass fluxes ζ belonging to the constitutive classes:

$$\boldsymbol{T}=\check{\boldsymbol{T}}(\boldsymbol{\nabla}\boldsymbol{v},\,\rho,\,\boldsymbol{\nabla}\rho,\,Y,\,\boldsymbol{\nabla}Y,\,\check{\mu}_\rho,\,\boldsymbol{\nabla}\check{\mu}_\rho,\,\check{\mu}_Y,\,\boldsymbol{\nabla}\check{\mu}_Y), \tag{C11a}$$
$$\boldsymbol{H}=\check{\boldsymbol{H}}(\rho,\,\boldsymbol{\nabla}\rho,\,Y,\,\boldsymbol{\nabla}Y,\,\check{\mu}_\rho,\,\boldsymbol{\nabla}\check{\mu}_\rho,\,\check{\mu}_Y,\,\boldsymbol{\nabla}\check{\mu}_Y), \tag{C11b}$$
$$\zeta=\check{\zeta}(\rho,\,Y,\,\check{\mu}_\rho,\,\check{\mu}_Y). \tag{C11c}$$

https://doi.org/10.1017/jfm.2026.11366 Published online by Cambridge University Press

We select closure models that render each of the terms in (C10) separately non-negative, i.e.

$$\check{\boldsymbol{T}} = -\nabla Y \otimes \frac{\partial \check{\Psi}}{\partial \nabla Y} - \nabla \rho \otimes \frac{\partial \check{\Psi}}{\partial \nabla \rho} - \left(\check{\mu}_\rho \rho - \check{\Psi}\right) \boldsymbol{I} + \nu(2\boldsymbol{D} + \lambda(\mathrm{div}\boldsymbol{v})\boldsymbol{I}), \tag{C12a}$$

$$\check{\boldsymbol{H}} = -\check{\boldsymbol{M}} \nabla \left(\frac{\check{\mu}_Y}{\rho}\right), \tag{C12b}$$

$$\check{\zeta} = -\check{m} \left(\frac{\check{\mu}_Y}{\rho}\right), \tag{C12c}$$

a positive definite mobility tensor $\check{\boldsymbol{M}}$ with the same dependencies as (C11*b*), satisfying $\check{\boldsymbol{M}}|_{Y=0,1} = 0$, and a non-negative scalar mobility $\check{m}$ with the same dependencies as (C11*c*), also satisfying $\check{m}|_{Y=0,1} = 0$.

This completes the constitutive modelling, and the system is given by

$$\partial_t(\rho \boldsymbol{v}) + \mathrm{div}\,(\rho \boldsymbol{v} \otimes \boldsymbol{v}) + \nabla \check{p} + \mathrm{div}\left(\nabla Y \otimes \frac{\partial \check{\Psi}}{\partial \nabla Y} + \nabla \rho \otimes \frac{\partial \check{\Psi}}{\partial \nabla \rho}\right) - \mathrm{div}\,(\nu(2\boldsymbol{D} + \lambda(\mathrm{div}\boldsymbol{v})\boldsymbol{I})) - \rho \boldsymbol{g} = 0, \tag{C13a}$$

$$\partial_t \rho + \mathrm{div}(\rho \boldsymbol{v}) = 0, \tag{C13b}$$

$$\partial_t(\rho Y) + \mathrm{div}(\rho Y \boldsymbol{v}) - \mathrm{div}\left(\check{\boldsymbol{M}} \nabla \left(\frac{\check{\mu}_Y}{\rho}\right)\right) + \check{m}\left(\frac{\check{\mu}_Y}{\rho}\right) = 0, \tag{C13c}$$

$$\check{\mu}_Y - \frac{\partial \check{\Psi}}{\partial Y} + \mathrm{div}\frac{\partial \check{\Psi}}{\partial \nabla Y} = 0, \tag{C13d}$$

$$\check{\mu}_\rho - \frac{\partial \check{\Psi}}{\partial \rho} + \mathrm{div}\frac{\partial \check{\Psi}}{\partial \nabla \rho} = 0, \tag{C13e}$$

with the pressure $\check{p} = \check{\mu}_\rho \rho - \check{\Psi}$. Analogously to Lemma 4.1, the Korteweg stress and pressure contributions in the momentum equation may be expressed using the chemical potential quantities.

LEMMA C.1 *(Identity Korteweg stresses – binary fluids – volume measure). The following identity holds for the pressure and Korteweg stresses in binary fluids:*

$$\nabla \check{p} + div\left(\nabla Y \otimes \frac{\partial \check{\Psi}}{\partial \nabla Y} + \nabla \rho \otimes \frac{\partial \check{\Psi}}{\partial \nabla \rho}\right) = \rho \nabla \check{\mu}_\rho - \check{\mu}_Y \nabla Y. \tag{C14}$$

Proof. See Lemma A.2. □

Applying the lemma converts the model into the compact form:

$$\partial_t(\rho \boldsymbol{v}) + \mathrm{div}\,(\rho \boldsymbol{v} \otimes \boldsymbol{v}) + \rho \nabla \check{\mu}_\rho - \check{\mu}_Y \nabla Y - \mathrm{div}\,(\nu(2\boldsymbol{D} + \lambda(\mathrm{div}\boldsymbol{v})\boldsymbol{I})) - \rho \boldsymbol{g} = 0, \tag{C15a}$$

$$\partial_t \rho + \mathrm{div}(\rho \boldsymbol{v}) = 0, \tag{C15b}$$

$$\partial_t(\rho Y) + \mathrm{div}(\rho Y \boldsymbol{v}) - \mathrm{div}\left(\check{\boldsymbol{M}} \nabla \left(\frac{\check{\mu}_Y}{\rho}\right)\right) + \check{m}\left(\frac{\check{\mu}_Y}{\rho}\right) = 0, \tag{C15c}$$

$$\check{\mu}_Y - \frac{\partial \check{\Psi}}{\partial Y} + \mathrm{div}\frac{\partial \check{\Psi}}{\partial \nabla Y} = 0, \tag{C15d}$$

$$\check{\mu}_\rho - \frac{\partial \check{\Psi}}{\partial \rho} + \mathrm{div}\frac{\partial \check{\Psi}}{\partial \nabla \rho} = 0. \tag{C15e}$$

https://doi.org/10.1017/jfm.2026.11366 Published online by Cambridge University Press

C.2. *Mass-measure free energy*

The mass-measure free energy is postulated to belong to the class

$$\psi = \overset{\circ\circ}{\psi}(\rho, \nabla\rho, Y, \nabla Y), \tag{C16}$$

and the chemical potential quantities defined as

$$\overset{\circ\circ}{\mu}_Y = \frac{\partial \overset{\circ\circ}{\psi}}{\partial Y} - \frac{1}{\rho}\mathrm{div}\left(\rho \frac{\partial \overset{\circ\circ}{\psi}}{\partial \nabla Y}\right), \tag{C17a}$$

$$\overset{\circ\circ}{\mu}_\rho = \frac{\partial \overset{\circ\circ}{\psi}}{\partial \rho} - \frac{1}{\rho}\mathrm{div}\left(\rho \frac{\partial \overset{\circ\circ}{\psi}}{\partial \nabla \rho}\right). \tag{C17b}$$

We proceed with the evaluation of the evolution of the energy (C16) and find, via the Reynolds transport theorem and the mass balance (C1*a*), that

$$\begin{aligned}\frac{\mathrm{d}}{\mathrm{d}t}\int_{\mathcal{R}(t)} \rho \overset{\circ\circ}{\psi}\, \mathrm{d}v &= \int_{\mathcal{R}(t)} \rho \dot{\overset{\circ\circ}{\psi}}\, \mathrm{d}v \\ &= \int_{\mathcal{R}(t)} \rho \left(\frac{\partial \overset{\circ\circ}{\psi}}{\partial \rho}\dot{\rho} + \frac{\partial \overset{\circ\circ}{\psi}}{\partial \nabla \rho}\cdot\overline{\nabla\rho}^{\cdot} + \frac{\partial \overset{\circ\circ}{\psi}}{\partial Y}\dot{Y} + \frac{\partial \overset{\circ\circ}{\psi}}{\partial \nabla Y}\cdot\overline{\nabla Y}^{\cdot}\right) \mathrm{d}v.\end{aligned} \tag{C18}$$

On the account of the relation

$$\overline{\nabla\omega}^{\cdot} = \nabla(\dot{\omega}) - (\nabla\omega)^T \nabla \boldsymbol{v}, \tag{C19}$$

for $\omega = \rho, Y$, we arrive at

$$\begin{aligned}\frac{\mathrm{d}}{\mathrm{d}t}\int_{\mathcal{R}(t)} \rho \overset{\circ\circ}{\psi}\, \mathrm{d}v &= \int_{\mathcal{R}(t)} \rho \overset{\circ\circ}{\mu}_Y \dot{Y} + \rho \overset{\circ\circ}{\mu}_\rho \dot{\rho} - \left(\nabla\rho \otimes \frac{\partial \rho \overset{\circ\circ}{\psi}}{\partial \nabla \rho} + \nabla Y \otimes \frac{\partial \rho \overset{\circ\circ}{\psi}}{\partial \nabla Y}\right) : \nabla \boldsymbol{v}\, \mathrm{d}v \\ &\quad + \int_{\partial\mathcal{R}(t)} \left(\dot{\rho}\rho \frac{\partial \overset{\circ\circ}{\psi}}{\partial \nabla \rho} + \dot{Y}\rho \frac{\partial \overset{\circ\circ}{\psi}}{\partial \nabla Y}\right) \cdot \boldsymbol{v}\, \mathrm{d}a.\end{aligned} \tag{C20}$$

By substituting the mass balance laws (C1*a*) and (C1*b*) we find that

$$\begin{aligned}\frac{\mathrm{d}}{\mathrm{d}t}\int_{\mathcal{R}(t)} \rho \overset{\circ\circ}{\psi}\, \mathrm{d}v &= \int_{\mathcal{R}(t)} \nabla \overset{\circ\circ}{\mu}_Y \cdot \boldsymbol{H} - \rho^2 \overset{\circ\circ}{\mu}_\rho \mathrm{div}\boldsymbol{v} + \overset{\circ\circ}{\mu}_Y \zeta \\ &\quad - \left(\nabla\rho \otimes \frac{\partial \rho \overset{\circ\circ}{\psi}}{\partial \nabla \rho} + \nabla Y \otimes \frac{\partial \rho \overset{\circ\circ}{\psi}}{\partial \nabla Y}\right) : \nabla \boldsymbol{v}\, \mathrm{d}v \\ &\quad + \int_{\partial\mathcal{R}(t)} \left(-\overset{\circ\circ}{\mu}_Y \boldsymbol{H} + \dot{\rho}\rho \frac{\partial \overset{\circ\circ}{\psi}}{\partial \nabla \rho} + \dot{c}\rho \frac{\partial \overset{\circ\circ}{\psi}}{\partial \nabla c}\right) \cdot \boldsymbol{v}\, \mathrm{d}a.\end{aligned} \tag{C21}$$

https://doi.org/10.1017/jfm.2026.11366 Published online by Cambridge University Press

Following the same procedure as in § 3 we find that

$$\frac{\mathrm{d}}{\mathrm{d}t}\mathscr{E} = \int_{\partial\mathcal{R}(t)} \left(\boldsymbol{v}^T \check{\check{\boldsymbol{T}}} - \check{\check{\mu}}_Y \boldsymbol{H} + \dot{\rho}\rho \frac{\partial \check{\check{\psi}}}{\partial \nabla\rho} + \dot{Y}\rho \frac{\partial \check{\check{\psi}}|}{\partial \nabla Y} \right) \cdot \boldsymbol{v} \, \mathrm{d}a$$
$$- \int_{\mathcal{R}(t)} \left(\check{\check{\boldsymbol{T}}} + \rho^2 \check{\check{\mu}}_\rho \boldsymbol{I} + \rho \nabla\rho \otimes \frac{\partial \check{\check{\psi}}}{\partial \nabla\rho} + \rho \nabla Y \otimes \frac{\partial \check{\check{\psi}}}{\partial \nabla Y} \right) : \nabla \boldsymbol{v} - \nabla \check{\check{\mu}}_Y \cdot \boldsymbol{H} - \check{\check{\mu}}_Y \zeta \, \mathrm{d}v, \tag{C22}$$

where we identify the rate of work and dissipation term:

$$\mathscr{W} = \int_{\partial\mathcal{R}(t)} \left(\boldsymbol{v}^T \check{\check{\boldsymbol{T}}} - \check{\check{\mu}}_Y \boldsymbol{H} + \dot{\rho}\rho \frac{\partial \check{\check{\psi}}}{\partial \nabla\rho} + \dot{Y}\rho \frac{\partial \check{\check{\psi}}}{\partial \nabla Y} \right) \cdot \boldsymbol{v} \, \mathrm{d}a, \tag{C23a}$$

$$\mathscr{D} = \int_{\mathcal{R}(t)} \left(\check{\check{\boldsymbol{T}}} + \rho^2 \check{\check{\mu}}_\rho \boldsymbol{I} + \rho \nabla\rho \otimes \frac{\partial \check{\check{\psi}}}{\partial \nabla\rho} + \rho \nabla Y \otimes \frac{\partial \check{\check{\psi}}}{\partial \nabla Y} \right) : \nabla \boldsymbol{v} - \nabla \check{\check{\mu}}_Y \cdot \boldsymbol{H} - \check{\check{\mu}}_Y \zeta \, \mathrm{d}v. \tag{C23b}$$

From the design condition $\mathscr{D} \geqslant 0$ we obtain the local modelling restriction:

$$\left(\check{\check{\boldsymbol{T}}} + \rho^2 \check{\check{\mu}}_\rho \boldsymbol{I} + \rho \nabla\rho \otimes \frac{\partial \check{\check{\psi}}}{\partial \nabla\rho} + \nabla Y \otimes \rho \frac{\partial \check{\check{\psi}}}{\partial \nabla Y} \right) : \nabla \boldsymbol{v} - \nabla \check{\check{\mu}}_Y \cdot \boldsymbol{H} - \check{\check{\mu}}_Y \zeta \geqslant 0. \tag{C24}$$

Based on the modelling restriction (C24) we introduce with the constitutive classes:

$$\boldsymbol{T} = \check{\check{\boldsymbol{T}}}(\nabla \boldsymbol{v}, \rho, \nabla\rho, Y, \nabla Y, \check{\check{\mu}}_\rho, \nabla \check{\check{\mu}}_\rho, \check{\check{\mu}}_Y, \nabla \check{\check{\mu}}_Y), \tag{C25a}$$

$$\boldsymbol{H} = \check{\check{\boldsymbol{H}}}(\rho, \nabla\rho, Y, \nabla Y, \check{\check{\mu}}_\rho, \nabla \check{\check{\mu}}_\rho, \check{\check{\mu}}_Y, \nabla \check{\check{\mu}}_Y), \tag{C25b}$$

$$\zeta = \check{\check{\zeta}}(\rho, Y, \check{\check{\mu}}_\rho, \check{\check{\mu}}_Y). \tag{C25c}$$

We choose closure models that ensure each term in (C10) remains separately non-negative:

$$\check{\boldsymbol{T}} = -\rho \nabla Y \otimes \frac{\partial \check{\check{\psi}}}{\partial \nabla Y} - \rho \nabla\rho \otimes \frac{\partial \check{\check{\psi}}}{\partial \nabla\rho} - \rho^2 \check{\check{\mu}}_\rho \boldsymbol{I} + \nu(2\boldsymbol{D} + \lambda(\mathrm{div}\boldsymbol{v})\boldsymbol{I}), \tag{C26a}$$

$$\check{\boldsymbol{H}} = -\check{\check{\boldsymbol{M}}} \nabla \check{\check{\mu}}_Y, \tag{C26b}$$

$$\check{\zeta} = -\check{\check{m}} \check{\check{\mu}}_Y. \tag{C26c}$$

Here the mobility tensor $\check{\check{\boldsymbol{M}}}$ is positive definite, depends on the same variables as (C25*b*) and satisfies $\check{\check{\boldsymbol{M}}}|_{Y=0,1} = 0$. The scalar mobility $\check{\check{m}} \geqslant 0$ shares the same dependencies as (C25*c*) and satisfies $\check{\check{m}}|_{Y=0,1} = 0$.

This concludes the constitutive modelling, with the system given by

$$\partial_t(\rho \boldsymbol{v}) + \mathrm{div}\,(\rho \boldsymbol{v} \otimes \boldsymbol{v}) + \nabla \check{\check{p}} + \mathrm{div} \left(\nabla\rho \otimes \rho \frac{\partial \check{\check{\psi}}}{\partial \nabla\rho} + \nabla Y \otimes \rho \frac{\partial \check{\check{\psi}}}{\partial \nabla Y} \right)$$
$$- \mathrm{div}\,(\nu(2\boldsymbol{D} + \lambda(\mathrm{div}\boldsymbol{v})\boldsymbol{I})) - \rho \boldsymbol{g} = 0, \tag{C27a}$$

$$\partial_t \rho + \mathrm{div}(\rho \boldsymbol{v}) = 0, \tag{C27b}$$

https://doi.org/10.1017/jfm.2026.11366 Published online by Cambridge University Press

$$\partial_t(\rho Y) + \operatorname{div}(\rho Y \boldsymbol{v}) - \operatorname{div}\left(\overset{\breve{\breve{}}}{\boldsymbol{M}} \boldsymbol{\nabla} \overset{\breve{\breve{}}}{\mu}_Y\right) + \overset{\breve{\breve{}}}{m} \overset{\breve{\breve{}}}{\mu}_Y = 0, \tag{C27c}$$

$$\overset{\breve{\breve{}}}{\mu}_Y - \frac{\partial \overset{\breve{\breve{}}}{\psi}}{\partial Y} + \frac{1}{\rho}\operatorname{div}\left(\rho \frac{\partial \overset{\breve{\breve{}}}{\psi}}{\partial \boldsymbol{\nabla} Y}\right) = 0, \tag{C27d}$$

$$\overset{\breve{\breve{}}}{\mu}_\rho - \frac{\partial \overset{\breve{\breve{}}}{\psi}}{\partial \rho} + \frac{1}{\rho}\operatorname{div}\left(\rho \frac{\partial \overset{\breve{\breve{}}}{\psi}}{\partial \boldsymbol{\nabla} \rho}\right) = 0, \tag{C27e}$$

with the pressure $\overset{\breve{\breve{}}}{p} = \rho^2 \overset{\breve{\breve{}}}{\mu}_\rho$.

PROPOSITION C.2 *(Equivalence binary mixture models). The mixture models (C15) and (C27) are equivalent.*

Proof. This follows from identifying $\breve{\Psi} = \rho \overset{\breve{\breve{}}}{\psi}$, $\breve{\boldsymbol{M}} = \overset{\breve{\breve{}}}{\boldsymbol{M}}$ and $\breve{m} = \overset{\breve{\breve{}}}{m}$. In particular, the first identification provides $\breve{\mu}_Y = \rho \overset{\breve{\breve{}}}{\mu}_Y$ and the identification of the pressure follows from

$$\breve{p} = \rho \breve{\mu}_\rho - \breve{\Psi} = \rho(\rho \overset{\breve{\breve{}}}{\mu}_\rho + \overset{\breve{\breve{}}}{\psi}) - \rho \overset{\breve{\breve{}}}{\psi} = \rho^2 \overset{\breve{\breve{}}}{\mu}_\rho = \overset{\breve{\breve{}}}{p}, \tag{C28}$$

with $\breve{\mu}_\rho = \rho \overset{\breve{\breve{}}}{\mu}_\rho + \overset{\breve{\breve{}}}{\psi}$. □

Finally, utilising Lemma A.3 the model may be written in the compact form:

$$\begin{aligned}\partial_t(\rho \boldsymbol{v}) + \operatorname{div}(\rho \boldsymbol{v} \otimes \boldsymbol{v}) + \rho \boldsymbol{\nabla}(\rho \overset{\breve{\breve{}}}{\mu}_\rho + \overset{\breve{\breve{}}}{\psi}) - \rho \overset{\breve{\breve{}}}{\mu}_Y \boldsymbol{\nabla} Y \\ -\operatorname{div}(\nu(2\boldsymbol{D} + \lambda(\operatorname{div}\boldsymbol{v})\boldsymbol{I})) - \rho \boldsymbol{g} = 0, \qquad \text{(C29a)}\\ \partial_t \rho + \operatorname{div}(\rho \boldsymbol{v}) = 0, \qquad \text{(C29b)}\\ \partial_t(\rho Y) + \operatorname{div}(\rho Y \boldsymbol{v}) - \operatorname{div}\left(\overset{\breve{\breve{}}}{M} \boldsymbol{\nabla} \overset{\breve{\breve{}}}{\mu}_Y\right) + \overset{\breve{\breve{}}}{m} \overset{\breve{\breve{}}}{\mu}_Y = 0. \qquad \text{(C29c)}\end{aligned}$$

Appendix D. Hyperbolicity in d dimensions

We write the system in the matrix-vector form

$$\partial_t \boldsymbol{W} + \boldsymbol{A}_{x_1}\partial_{x_1}\boldsymbol{W} + \boldsymbol{A}_{x_2}\partial_{x_2}\boldsymbol{W} + \boldsymbol{A}_{x_3}\partial_{x_3}\boldsymbol{W} = 0, \tag{D1}$$

where

$$\boldsymbol{W} = \begin{bmatrix} p_1 \\ \vdots \\ p_N \\ v_{x_1} \\ v_{x_2} \\ v_{x_3} \end{bmatrix}, \quad \boldsymbol{A}_{x_1} = \begin{bmatrix} v_{x_1} & 0 & \dots & & 0 & \sum_\beta \tilde{\rho}_\beta a_{1\beta}^2 & 0 & 0 \\ 0 & v_{x_1} & 0 & \dots & 0 & \sum_\beta \tilde{\rho}_\beta a_{2\beta}^2 & 0 & 0 \\ \vdots & \ddots & \ddots & \ddots & \vdots & \vdots & 0 & 0 \\ 0 & \dots & 0 & v_{x_1} & 0 & \sum_\beta \tilde{\rho}_\beta a_{(N-1)\beta}^2 & 0 & 0 \\ 0 & \dots & & 0 & v_{x_1} & \sum_\beta \tilde{\rho}_\beta a_{N\beta}^2 & 0 & 0 \\ \rho^{-1} & & \dots & & \rho^{-1} & v_{x_1} & 0 & 0 \\ 0 & & & & \dots & 0 & v_{x_1} & 0 \\ 0 & & & & \dots & & 0 & v_{x_1} \end{bmatrix},$$

https://doi.org/10.1017/jfm.2026.11366 Published online by Cambridge University Press

$$\boldsymbol{A}_{x_2} = \begin{bmatrix} v_{x_2} & 0 & \dots & & 0 & 0 & \sum_\beta \tilde{\rho}_\beta a_{1\beta}^2 & 0 \\ 0 & v_{x_2} & 0 & \dots & 0 & 0 & \sum_\beta \tilde{\rho}_\beta a_{2\beta}^2 & 0 \\ \vdots & \ddots & \ddots & \ddots & \vdots & 0 & \vdots & 0 \\ 0 & \dots & 0 & v_{x_2} & 0 & 0 & \sum_\beta \tilde{\rho}_\beta a_{(N-1)\beta}^2 & 0 \\ 0 & \dots & & 0 & v_{x_2} & 0 & \sum_\beta \tilde{\rho}_\beta a_{N\beta}^2 & 0 \\ 0 & & \dots & & 0 & v_{x_2} & 0 & 0 \\ \rho^{-1} & & \dots & & \rho^{-1} & 0 & v_{x_2} & 0 \\ 0 & & & & \dots & & 0 & v_{x_2} \end{bmatrix},$$

$$\boldsymbol{A}_{x_3} = \begin{bmatrix} v_{x_3} & 0 & \dots & & 0 & 0 & 0 & \sum_\beta \tilde{\rho}_\beta a_{1\beta}^2 \\ 0 & v_{x_3} & 0 & \dots & 0 & 0 & 0 & \sum_\beta \tilde{\rho}_\beta a_{2\beta}^2 \\ \vdots & \ddots & \ddots & \ddots & \vdots & 0 & 0 & \vdots \\ 0 & \dots & 0 & v_{x_3} & 0 & 0 & 0 & \sum_\beta \tilde{\rho}_\beta a_{(N-1)\beta}^2 \\ 0 & \dots & & 0 & v_{x_3} & 0 & 0 & \sum_\beta \tilde{\rho}_\beta a_{N\beta}^2 \\ 0 & & \dots & & 0 & v_{x_3} & 0 & 0 \\ 0 & & & \dots & & 0 & v_{x_3} & 0 \\ \rho^{-1} & & \dots & & \rho^{-1} & 0 & 0 & v_{x_3} \end{bmatrix}. \tag{D2}$$

The matrices $\boldsymbol{A}_{x_i}$, $i = 1, 2, 3$ have $N + d$ eigenvalues:

$$\lambda_{i,1} = v_i - a < \lambda_{i,2} = \dots = \lambda_{i,N+d-1} = v_i < \lambda_{i,N+d} = v_i + a. \tag{D3}$$

The corresponding right eigenvectors are

$$\boldsymbol{r}_{x_1,1} = \begin{bmatrix} -\sum_\beta \tilde{\rho}_\beta a_{1\beta}^2 \\ \vdots \\ -\sum_\beta \tilde{\rho}_\beta a_{N\beta}^2 \\ a \\ 0 \\ 0 \end{bmatrix}, \quad \boldsymbol{r}_{x_1,2} = \begin{bmatrix} -1 \\ 1 \\ 0 \\ \vdots \\ 0 \end{bmatrix}, \quad \boldsymbol{r}_{x_1,3} = \begin{bmatrix} -1 \\ 0 \\ 1 \\ 0 \\ \vdots \\ 0 \end{bmatrix}, \dots, \quad \boldsymbol{r}_{x_1,N} = \begin{bmatrix} -1 \\ 0 \\ \vdots \\ 0 \\ 1 \\ 0 \\ 0 \\ 0 \end{bmatrix},$$

$$\boldsymbol{r}_{x_1,N+1} = \begin{bmatrix} 0 \\ \vdots \\ 0 \\ 1 \\ 0 \end{bmatrix}, \quad \boldsymbol{r}_{x_1,N+2} = \begin{bmatrix} 0 \\ \vdots \\ 0 \\ 0 \\ 1 \end{bmatrix}, \quad \boldsymbol{r}_{x_1,N+3} = \begin{bmatrix} \sum_\beta \tilde{\rho}_\beta a_{1\beta}^2 \\ \vdots \\ \sum_\beta \tilde{\rho}_\beta a_{N\beta}^2 \\ a \\ 0 \\ 0 \end{bmatrix}, \tag{D4a}$$

https://doi.org/10.1017/jfm.2026.11366 Published online by Cambridge University Press

$$\boldsymbol{r}_{x_2,1}=\begin{bmatrix}-\sum_\beta \tilde{\rho}_\beta a_{1\beta}^2\\ \vdots\\ -\sum_\beta \tilde{\rho}_\beta a_{N\beta}^2\\ 0\\ a\\ 0\end{bmatrix},\ \boldsymbol{r}_{x_2,2}=\begin{bmatrix}-1\\ 1\\ 0\\ \vdots\\ 0\end{bmatrix},\ \boldsymbol{r}_{x_2,3}=\begin{bmatrix}-1\\ 0\\ 1\\ 0\\ \vdots\\ 0\end{bmatrix},\ \ldots,\ \boldsymbol{r}_{x_2,N}=\begin{bmatrix}-1\\ 0\\ \vdots\\ 0\\ 1\\ 0\\ 0\\ 0\end{bmatrix},$$

$$\boldsymbol{r}_{x_2,N+1}=\begin{bmatrix}0\\ \vdots\\ 1\\ 0\\ 0\end{bmatrix},\ \boldsymbol{r}_{x_2,N+2}=\begin{bmatrix}0\\ \vdots\\ 0\\ 0\\ 1\end{bmatrix},\ \boldsymbol{r}_{x_2,N+3}=\begin{bmatrix}\sum_\beta \tilde{\rho}_\beta a_{1\beta}^2\\ \vdots\\ \sum_\beta \tilde{\rho}_\beta a_{N\beta}^2\\ 0\\ a\\ 0\end{bmatrix}, \tag{D4b}$$

$$\boldsymbol{r}_{x_3,1}=\begin{bmatrix}-\sum_\beta \tilde{\rho}_\beta a_{1\beta}^2\\ \vdots\\ -\sum_\beta \tilde{\rho}_\beta a_{N\beta}^2\\ 0\\ 0\\ a\end{bmatrix},\ \boldsymbol{r}_{x_3,2}=\begin{bmatrix}-1\\ 1\\ 0\\ \vdots\\ 0\end{bmatrix},\ \boldsymbol{r}_{x_3,3}=\begin{bmatrix}-1\\ 0\\ 1\\ 0\\ \vdots\\ 0\end{bmatrix},\ \ldots,\ \boldsymbol{r}_{x_3,N}=\begin{bmatrix}-1\\ 0\\ \vdots\\ 0\\ 1\\ 0\\ 0\\ 0\end{bmatrix},$$

$$\boldsymbol{r}_{x_3,N+1}=\begin{bmatrix}0\\ \vdots\\ 1\\ 0\\ 0\end{bmatrix},\ \boldsymbol{r}_{x_3,N+2}=\begin{bmatrix}0\\ \vdots\\ 0\\ 1\\ 0\end{bmatrix},\ \boldsymbol{r}_{x_3,N+3}=\begin{bmatrix}\sum_\beta \tilde{\rho}_\beta a_{1\beta}^2\\ \vdots\\ \sum_\beta \tilde{\rho}_\beta a_{N\beta}^2\\ 0\\ 0\\ a\end{bmatrix}, \tag{D4c}$$

and the left eigenvectors are

$$\boldsymbol{l}_{x_1,1}=\begin{bmatrix}-\dfrac{1}{2\rho a^2}\\ \vdots\\ -\dfrac{1}{2\rho a^2}\\ \dfrac{1}{2a}\\ 0\\ 0\end{bmatrix},\ \boldsymbol{l}_{x_1,2}=\begin{bmatrix}-\dfrac{\sum_\beta \tilde{\rho}_\beta a_{2\beta}^2}{\sum_\beta \tilde{\rho}_\beta\left(a_{1\beta}^2+a_{2\beta}^2\right)}\\ \dfrac{\sum_\beta \tilde{\rho}_\beta a_{1\beta}^2}{\sum_\beta \tilde{\rho}_\beta\left(a_{1\beta}^2+a_{2\beta}^2\right)}\\ 0\\ \vdots\\ 0\end{bmatrix},\ \boldsymbol{l}_{x_1,3}=\begin{bmatrix}-\dfrac{\sum_\beta \tilde{\rho}_\beta a_{3\beta}^2}{\sum_\beta \tilde{\rho}_\beta\left(a_{1\beta}^2+a_{3\beta}^2\right)}\\ 0\\ \dfrac{\sum_\beta \tilde{\rho}_\beta a_{1\beta}^2}{\sum_\beta \tilde{\rho}_\beta\left(a_{1\beta}^2+a_{3\beta}^2\right)}\\ 0\\ \vdots\\ 0\end{bmatrix},\ \ldots,$$

https://doi.org/10.1017/jfm.2026.11366 Published online by Cambridge University Press

$$\boldsymbol{l}_{x_1,N} = \begin{bmatrix} -\dfrac{\sum_\beta \tilde{\rho}_\beta a_{N\beta}^2}{\sum_\beta \tilde{\rho}_\beta \left(a_{1\beta}^2 + a_{N\beta}^2\right)} \\ 0 \\ \vdots \\ 0 \\ \dfrac{\sum_\beta \tilde{\rho}_\beta a_{1\beta}^2}{\sum_\beta \tilde{\rho}_\beta \left(a_{1\beta}^2 + a_{N\beta}^2\right)} \\ 0 \\ 0 \\ 0 \end{bmatrix}, \quad \boldsymbol{l}_{x_1,N+1} = \begin{bmatrix} 0 \\ \vdots \\ 0 \\ 1 \\ 0 \end{bmatrix}, \quad \boldsymbol{l}_{x_1,N+2} = \begin{bmatrix} 0 \\ \vdots \\ 0 \\ 0 \\ 1 \end{bmatrix}, \quad \boldsymbol{l}_{x_1,N+3} = \begin{bmatrix} \dfrac{1}{2\rho a^2} \\ \vdots \\ \dfrac{1}{2\rho a^2} \\ \dfrac{1}{2a} \\ 0 \\ 0 \end{bmatrix},$$

(D5*a*)

$$\boldsymbol{l}_{x_2,1} = \begin{bmatrix} -\dfrac{1}{2\rho a^2} \\ \vdots \\ -\dfrac{1}{2\rho a^2} \\ 0 \\ \dfrac{1}{2a} \\ 0 \end{bmatrix}, \quad \boldsymbol{l}_{x_2,2} = \begin{bmatrix} -\dfrac{\sum_\beta \tilde{\rho}_\beta a_{2\beta}^2}{\sum_\beta \tilde{\rho}_\beta \left(a_{1\beta}^2 + a_{2\beta}^2\right)} \\ \dfrac{\sum_\beta \tilde{\rho}_\beta a_{1\beta}^2}{\sum_\beta \tilde{\rho}_\beta \left(a_{1\beta}^2 + a_{2\beta}^2\right)} \\ 0 \\ \vdots \\ 0 \end{bmatrix}, \quad \boldsymbol{l}_{x_2,3} = \begin{bmatrix} -\dfrac{\sum_\beta \tilde{\rho}_\beta a_{3\beta}^2}{\sum_\beta \tilde{\rho}_\beta \left(a_{1\beta}^2 + a_{3\beta}^2\right)} \\ 0 \\ \dfrac{\sum_\beta \tilde{\rho}_\beta a_{1\beta}^2}{\sum_\beta \tilde{\rho}_\beta \left(a_{1\beta}^2 + a_{3\beta}^2\right)} \\ 0 \\ \vdots \\ 0 \end{bmatrix}, \ldots,$$

$$\boldsymbol{l}_{x_2,N} = \begin{bmatrix} -\dfrac{\sum_\beta \tilde{\rho}_\beta a_{N\beta}^2}{\sum_\beta \tilde{\rho}_\beta \left(a_{1\beta}^2 + a_{N\beta}^2\right)} \\ 0 \\ \vdots \\ 0 \\ \dfrac{\sum_\beta \tilde{\rho}_\beta a_{1\beta}^2}{\sum_\beta \tilde{\rho}_\beta \left(a_{1\beta}^2 + a_{N\beta}^2\right)} \\ 0 \\ 0 \\ 0 \end{bmatrix}, \quad \boldsymbol{l}_{x_2,N+1} = \begin{bmatrix} 0 \\ \vdots \\ 1 \\ 0 \\ 0 \end{bmatrix}, \quad \boldsymbol{l}_{x_2,N+2} = \begin{bmatrix} 0 \\ \vdots \\ 0 \\ 0 \\ 1 \end{bmatrix}, \quad \boldsymbol{l}_{x_2,N+3} = \begin{bmatrix} \dfrac{1}{2\rho a^2} \\ \vdots \\ \dfrac{1}{2\rho a^2} \\ 0 \\ \dfrac{1}{2a} \\ 0 \end{bmatrix},$$

(D5*b*)

https://doi.org/10.1017/jfm.2026.11366 Published online by Cambridge University Press

$$\boldsymbol{l}_{x_3,1} = \begin{bmatrix} -\dfrac{1}{2\rho a^2} \\ \vdots \\ -\dfrac{1}{2\rho a^2} \\ 0 \\ 0 \\ \dfrac{1}{2a} \end{bmatrix}, \; \boldsymbol{l}_{x_3,2} = \begin{bmatrix} -\dfrac{\sum_\beta \tilde{\rho}_\beta a_{2\beta}^2}{\sum_\beta \tilde{\rho}_\beta \left(a_{1\beta}^2 + a_{2\beta}^2\right)} \\ \dfrac{\sum_\beta \tilde{\rho}_\beta a_{1\beta}^2}{\sum_\beta \tilde{\rho}_\beta \left(a_{1\beta}^2 + a_{2\beta}^2\right)} \\ 0 \\ \vdots \\ 0 \end{bmatrix}, \; \boldsymbol{l}_{x_3,3} = \begin{bmatrix} -\dfrac{\sum_\beta \tilde{\rho}_\beta a_{3\beta}^2}{\sum_\beta \tilde{\rho}_\beta \left(a_{1\beta}^2 + a_{3\beta}^2\right)} \\ 0 \\ \dfrac{\sum_\beta \tilde{\rho}_\beta a_{1\beta}^2}{\sum_\beta \tilde{\rho}_\beta \left(a_{1\beta}^2 + a_{3\beta}^2\right)} \\ 0 \\ \vdots \\ 0 \end{bmatrix}, \ldots,$$

$$\boldsymbol{l}_{x_3,N} = \begin{bmatrix} -\dfrac{\sum_\beta \tilde{\rho}_\beta a_{N\beta}^2}{\sum_\beta \tilde{\rho}_\beta \left(a_{1\beta}^2 + a_{N\beta}^2\right)} \\ 0 \\ \vdots \\ 0 \\ \dfrac{\sum_\beta \tilde{\rho}_\beta a_{1\beta}^2}{\sum_\beta \tilde{\rho}_\beta \left(a_{1\beta}^2 + a_{N\beta}^2\right)} \\ 0 \\ 0 \\ 0 \end{bmatrix}, \; \boldsymbol{l}_{x_3,N+1} = \begin{bmatrix} 0 \\ \vdots \\ 1 \\ 0 \\ 0 \end{bmatrix}, \; \boldsymbol{l}_{x_3,N+2} = \begin{bmatrix} 0 \\ \vdots \\ 0 \\ 1 \\ 0 \end{bmatrix}, \; \boldsymbol{l}_{x_3,N+3} = \begin{bmatrix} \dfrac{1}{2\rho a^2} \\ \vdots \\ \dfrac{1}{2\rho a^2} \\ 0 \\ 0 \\ \dfrac{1}{2a} \end{bmatrix}. \tag{D5c}$$

The eigenvectors are scaled so that $\boldsymbol{r}_j \cdot \boldsymbol{l}_j = 1$ for all $j = 1, \ldots, N+1$. Both right and left eigenvectors are linearly independent and span $\mathbb{R}^{N+d}$. This implies that the system is hyperbolic if the eigenvalues are real valued, which holds when $a_{\alpha\beta}^2 = \mathrm{d}p_\alpha / \mathrm{d}\tilde{\rho}_\beta > 0$. Similar to the one-dimensional case, fields associated with $\lambda_2, \ldots, \lambda_{N+2}$ correspond to contact discontinuities and those associated with λ_1, λ_{N+3} correspond to shock or rarefaction waves, respectively.

References

Abels, H., Garcke, H. & Grün, G. 2012 Thermodynamically consistent, frame indifferent diffuse interface models for incompressible two-phase flows with different densities. *Math. Models Meth. Appl. Sci.* **22**, 1150013.

Aki, G.L., Dreyer, W., Giesselmann, J. & Kraus, C. 2014 A quasi-incompressible diffuse interface model with phase transition. *Math. Models Meth. Appl. Sci.* **24**, 827–861.

Aland, S. & Mokbel, D. 2021 A unified numerical model for wetting of soft substrates. *Intl J. Numer. Meth. Engng* **122**, 903–918.

Anderson, D.M., McFadden, G.B. & Wheeler, A.A. 1998 Diffuse-interface methods in fluid mechanics. *Annu. Rev. Fluid Mech.* **30**, 139–165.

Andrianov, N. & Warnecke, G. 2004 The Riemann problem for the Baer–Nunziato two-phase flow model. *J. Comput. Phys.* **195**, 434–464.

Baer, M.R. & Nunziato, J.W. 1986 A two-phase mixture theory for the deflagration-to-detonation transition (DDT) in reactive granular materials. *Intl J. Multiphase Flow* **12**, 861–889.

Bhopalam, S.R., Bueno, J. & Gomez, H. 2022 Elasto-capillary fluid–structure interaction with compound droplets. *Comput. Meth. Appl. Mech. Engng* **400**, 115507.

Boyer, F. 2002 A theoretical and numerical model for the study of incompressible mixture flows. *Comput. Fluids* **31**, 41–68.

Bresch, D., Gisclon, M. & Lacroix-Violet, I. 2019 On Navier–Stokes–Korteweg and Euler–Korteweg systems: application to quantum fluids models. *Arch. Ration. Mech. Anal.* **233**, 975–1025.

https://doi.org/10.1017/jfm.2026.11366 Published online by Cambridge University Press

BRUNK, A. & TEN EIKELDER, M.F.P. 2025 A simple, fully-discrete, unconditionally energy-stable method for the two-phase Navier-Stokes Cahn-Hilliard model with arbitrary density ratios. *J. Comput. Phys.* 114558.

COLEMAN, B.D. & NOLL, W. 1974 *The Thermodynamics of Elastic Materials with Heat Conduction and Viscosity*, pp. 145–156. Springer.

COQUEL, F., GALLOUËT, T., HELLUY, P., HÉRARD, J.-M., HURISSE, O. & SEGUIN, N. 2013 Modelling compressible multiphase flows. In *ESAIM: Proceedings*, vol. 40, pp. 34–50. EDP Sciences.

COQUEL, F., HÉRARD, J.-M. & SALEH, K. 2017 A positive and entropy-satisfying finite volume scheme for the Baer–Nunziato model. *J. Comput. Phys.* **330**, 401–435.

CROUZET, F., DAUDE, F., GALON, P., HELLUY, P., HÉRARD, J.-M., HURISSE, O. & LIU, Y. 2013 Approximate solutions of the Baer-Nunziato model. In *ESAIM: Proceedings*, vol. 40, pp. 63–82. EDP Sciences.

DAUDE, F., GALON, P., POTAPOV, S., BECCANTINI, A. & MIANNÉ, G. 2023 A hyperbolic conservative one-velocity one-pressure barotropic three-component model for fast-transient fluid-structure interaction problems. *Appl. Math. Comput.* **447**, 127919.

DEMONT, T.H.B., STOTER, S.K.F., DIDDENS, C. & VAN BRUMMELEN, E.H. 2024 On the consistency of dynamic wetting boundary conditions for the Navier–Stokes Cahn-Hilliard equations. arxiv.org 2407.06049.

DING, H., SPELT, P.D.M. & SHU, C. 2007 Diffuse interface model for incompressible two-phase flows with large density ratios. *J. Comput. Phys.* **226**, 2078–2095.

DUMBSER, M. 2011 A simple two-phase method for the simulation of complex free surface flows. *Comput. Meth. Appl. Mech. Engng* **200**, 1204–1219.

TEN EIKELDER, M.F.P. 2025 A unified framework for N-phase Navier–Stokes Cahn–Hilliard Allen–Cahn mixture models with non-matching densities. *J. Fluid Mech.* **1013**, A26.

TEN EIKELDER, M.F.P. & AKKERMAN, I. 2021 A novel diffuse-interface model and a fully-discrete maximum-principle-preserving energy-stable method for two-phase flow with surface tension and non-matching densities. *Comput. Meth. Appl. Mech. Engng* **379**, 113751.

TEN EIKELDER, M.F.P. & SCHILLINGER, D. 2024 The divergence-free velocity formulation of the consistent Navier–Stokes Cahn-Hilliard model with non-matching densities, divergence-conforming discretization, and benchmarks. *J. Comput. Phys.* **513**, 113148.

TEN EIKELDER, M.F.P., VAN DER ZEE, K.G. & SCHILLINGER, D. 2024 Thermodynamically consistent diffuse-interface mixture models of incompressible multicomponent fluids. *J. Fluid Mech.* **990**, A8.

TEN EIKELDER, M.F.P., VAN DER ZEE, K.G., AKKERMAN, I. & SCHILLINGER, D. 2023 A unified framework for Navier–Stokes Cahn-Hilliard models with non-matching densities. *Math. Models Meth. Appl. Sci.* **33**, 175–221.

FREISTÜHLER, H. & KOTSCHOTE, M. 2017 Phase-field and Korteweg-type models for the time-dependent flow of compressible two-phase fluids. *Arch. Ration. Mech. Anal.* **224**, 1–20.

GHIAS, R., MITTAL, R. & DONG, H. 2007 A sharp interface immersed boundary method for compressible viscous flows. *J. Comput. Phys.* **225**, 528–553.

GOMEZ, H., HUGHES, T.J.R., NOGUEIRA, X. & CALO, V.M. 2010 Isogeometric analysis of the isothermal Navier–Stokes-Korteweg equations. *Comput. Meth. Appl. Mech. Engng* **199**, 1828–1840.

GOMEZ, H. & VAN DER ZEE, K.G. 2018 Computational phase-field modeling. In *Encyclopedia of Computational Mechanics Second Edition*, pp. 1–35.

GUILLARD, H. & LABOIS, M. 2006 Numerical modelling of compressible two-phase flows. In *European Conference on Computational Fluid Dynamics (ECCOMAS CFD)* (ed. P. Wesseling, E. Oñate & J. Périaux). TU Delft.

HILLAIRET, M. 2019 On Baer-Nunziato multiphase flow models. *ESAIM: Proc. Surveys* **66**, 61–83.

HOHENBERG, P.C. & HALPERIN, B.I. 1977 Theory of dynamic critical phenomena. *Rev. Mod. Phys.* **49**, 435.

HUANG, Z. & JOHNSEN, E. 2023 A consistent and conservative phase-field method for compressible multiphase flows with shocks. *J. Comput. Phys.* **488**, 112195.

HUANG, Z. & JOHNSEN, E. 2024 A consistent and conservative phase-field method for compressible N-phase flows: consistent limiter and multiphase reduction-consistent formulation. *J. Comput. Phys.* **501**, 112801.

KAPILA, A.K., MENIKOFF, R., BDZIL, J.B., SON, S.F. & STEWART, D.S. 2001 Two-phase modeling of deflagration-to-detonation transition in granular materials: reduced equations. *Phys. Fluids* **13**, 3002–3024.

LOWENGRUB, J. & TRUSKINOVSKY, L. 1998 Quasi–incompressible Cahn–Hilliard fluids and topological transitions. *Proc. R. Soc. A* **454**, 2617–2654.

MÁLEK, J. & RAJAGOPAL, K.R. 2008 A thermodynamic framework for a mixture of two liquids. *Nonlinear Anal. Real World Appl.* **9**, 1649–1660.

MUKHERJEE, S. & GOMEZ, H. 2024 Mixtures of phase transforming fluids and gases: phase field model and stabilized isogeometric discretization. *Comput. Fluids* **271**, 106176.

MÜLLER, S., HANTKE, M. & RICHTER, P. 2016 Closure conditions for non-equilibrium multi-component models. *Continuum Mech. Thermodyn.* **28**, 1157–1189.

https://doi.org/10.1017/jfm.2026.11366 Published online by Cambridge University Press

MURRONE, A. & GUILLARD, H. 2005 A five equation reduced model for compressible two phase flow problems. *J. Comput. Phys.* **202**, 664–698.
PELANTI, M. 2022 Arbitrary-rate relaxation techniques for the numerical modeling of compressible two-phase flows with heat and mass transfer. *Intl J. Multiphase Flow* **153**, 104097.
PERRIER, V. & GUTIÉRREZ, E. 2021 Derivation and closure of Baer and Nunziato type multiphase models by averaging a simple stochastic model. *Multiscale Model. Sim.* **19**, 401–439.
SALEH, K. & SEGUIN, N. 2020 Some mathematical properties of a barotropic multiphase flow model. *ESAIM: Proc. Surveys* **69**, 70–78.
SAUREL, R. & ABGRALL, R. 1999 A multiphase Godunov method for compressible multifluid and multiphase flows. *J. Comput. Phys.* **150**, 425–467.
SAUREL, R. & PANTANO, C. 2018 Diffuse-interface capturing methods for compressible two-phase flows. *Annu. Rev. Fluid Mech.* **50**, 105–130.
SAUREL, R., PETITPAS, F. & BERRY, R.A. 2009 Simple and efficient relaxation methods for interfaces separating compressible fluids, cavitating flows and shocks in multiphase mixtures. *J. Comput. Phys.* **228**, 1678–1712.
SETHIAN, J.A. 1999 *Level Set Methods and Fast Marching Methods: Evolving Interfaces in Computational Geometry, Fluid Mechanics, Computer Vision, and Materials Science*, vol. 3. Cambridge University Press.
SHEN, J., YANG, X. & WANG, Q. 2013 Mass and volume conservation in phase field models for binary fluids. *Commun. Comput. Phys.* **13**, 1045–1065.
SHEN, Y., REN, Y. & DING, H. 2020 A 3D conservative sharp interface method for simulation of compressible two-phase flows. *J. Comput. Phys.* **403**, 109107.
SIRIANNI, G., RE, B. & ABGRALL, R. 2025 Mixture-conservative temperature-based Baer–Nunziato solver for efficient full-disequilibrium simulations of real fluids. *Comput. Fluids* **300**, 106761.
SUSSMAN, M., SMEREKA, P. & OSHER, S. 1994 A level set approach for computing solutions to incompressible two-phase flow. *J. Comput. Phys.* **114**, 146–159.
TOKAREVA, S.A. & TORO, E.F. 2010 HLLC-type Riemann solver for the Baer–Nunziato equations of compressible two-phase flow. *J. Comput. Phys.* **229**, 3573–3604.
TRUESDELL, C. 1984 *Historical Introit the Origins of Rational Thermodynamics*. Springer.
TRUESDELL, C. & TOUPIN, R. 1960 *The Classical Field Theories*, pp. 226–858. Springer.
VAN DER WAALS, J.D. 1894 The thermodynamic theory of capillarity under the hypothesis of a continuous variation of density. *Z. Phys. Chem. Stöchiom. Verwandtschaftsl* **13**, 657.
ZEIN, A., HANTKE, M. & WARNECKE, G. 2010 Modeling phase transition for compressible two-phase flows applied to metastable liquids. *J. Comput. Phys.* **229** (8), 2964–2998.

https://doi.org/10.1017/jfm.2026.11366 Published online by Cambridge University Press